HYDROCRACKING OF COAL S. A. Qader, E. A. Everett, A. Basu and W. H. Wiser, Department of Mining, Metallurgical and Fuels Engineering, University of Utah, Salt Lake City, Utah 84112.

A subbituminous coal was hydrocracked with and without catalysts in the temperature range 450°-550°C under 1000-4000 psi hydrogen pressure. In the thermal hydrocracking experiments, conversion increased with reaction temperature and a coal conversion of about 40% was obtained at 10 minutes residence time. Hydrogen pressure did not effect the conversion to any significant extent. In the catalytic hydrocracking experiments, physical mixtures of coal and catalysts were heated under hydrogen pressure at residence times of up to 10 minutes. Reaction temperature and pressure increased the conversion and a coal conversion of about 90% was obtained at a temperature of 550°C under 4000 psi hydrogen pressure. Catalytic activity varied in the order CoS > WS_2 > FeS. Thermal and catalytic coal hydrocracking data were evaluated by first order kinetics and apparent activation energies of 13-15 K calories/gram mole were obtained in the noncatalytic hydrotreatment of coal in the pressure range 2000-4000 psi. But in catalytic hydrotreatment, activation energies varied significantly with pressure. At 2000 psi, only an activation energy of about 5 K cal/gram mole was obtained whereas at 3000 and 4000 psi, activation energies were found to be about 26 and 27 K cal/gram mole respectively. Some data on hydrocracking of coal in a fluid bed reactor were also presented.

COAL TAR AUTOXIDATION - KINETIC STUDIES BY VISCOMETRIC AND REFRACTOMETRIC METHODS

by

Yung-Yi Lin, L. L. Anderson and W. H. Wiser

Department of Mining, Metallurgical and Fuels Engineering
College of Mines and Mineral Industries
University of Utah
Salt Lake City, Utah 84112

INTRODUCTION

Coal tar is a complex mixture of hydrocarbons and organic compounds containing sulfur, oxygen and nitrogen. Some of these compounds are easily attacked by oxygen when they are exposed to air. This attack always results in the formation of high-molecular-weight compounds, thus reducing the value of the tar. The ability of coal tar to resist the changes in its composition and properties is referred to as its stability. In attempting to evaluate the stability, it was necessary to investigate the kinetics of coal-tar autoxidation. Because of the complexity of the coal-tar composition, it was very difficult to apply conventional methods to this kinetic study. The measurement of viscosity and refractive-index change were regarded as the most convenient ways to determine the extent of coal-tar autoxidation; hence, both of these methods were used in this study. Present-day theory of autoxidation is employed to explain the different mechanisms involved in the autoxidation of whole tar, neutral oils, tar acids, and tar bases respectively, under ambient storage conditions.

EXPERIMENTAL PROCEDURES

Sample Material

The coal tars used in this study were obtained from two processes: hydrogenation (at 650°C reactor temperature), and carbonization (at 700°C). The distillate boiling in the range of 110 to 300°C was used as the sample. Neutral oils, tar acids, and tar bases were chemically separated from this distillate. Samples of Hiawatha, and Spencer coals were selected for hydrogenation, and carbonization. Both coals are

bituminous coals and analyses for them are given in Table 1.

TABLE 1

Analyses of coals (% by weight, as received) which were used to produce coal tar.

	Hiawatha	Spencer
Volatile matter (DAF)	48.6	45.4
Fixed carbon (DAF)	51.4	54.6
Moisture	3.20	5.16
Ash	5.51	4.42
Sulfur	0.80	0.53

Oxidation of Tar Sample

50 ml of tar sample was stored and exposed to air (20°C) in a 100 ml beaker which was covered with a plastic sheet to prevent the evaporation of tar sample. The number of samples used in each different experimental run was 4 or 5, except tar acids, and tar bases, which were difficult to collect. After the sample had been oxidized for the desired period, it was taken from the beaker for measurements or analyses.

Measurement of Viscosity

The viscosity of the tar samples was measured with a Haake falling-ball viscometer. The measuring temperature was controlled by a constant temperature circulator at 25.0 $\pm$ 0.1°C.

Measurement of Refractive Index

A Bausch & Lomb Model ABBE-3L refractometer was used to measure the

refractive index of tar samples at 25°C. The refractive index could be read to the fourth decimal place.

Determination of Iodine Number

The Hanus method was employed in this study to determine the iodine number of tar samples.

Analysis of Oxygen Content

Oxygen analyses were obtained from Gailbraith Laboratories, Inc. of Knoxville, Tennessee. Duplicate samples were run on the tars as prepared fresh by hydrogenation of Spencer coal.

Infrared Absorption Spectrum Analysis

The infrared absorption spectra were measured with a Beckman Model IR 20 Spectrometer over the wave-length interval 25 to 40 microns. In this study, a routine scan was selected, and the time required to scan the region was 30 minutes. After the tar sample had been stirred mildly, a liquid film of coal tar, approximately 0.015 mm thick, was spread on a KBr sample holder, and the spectrum was observed immediately.

Auxiliary Experiments

In order to understand the kinetics of the coal-tar autoxidation, some auxiliary experiments were carried out to determine the following:

a. effect of stirring
b. effect of oxygen pressure
c. effect of temperature
d. effect of light irradiation

RESULTS AND DISCUSSION

Viscosity

The viscosity-change behavior of the whole-tar samples oxidized in air is shown in Figures 1 and 2. It is apparent that the viscosity increases linearly with the reaction time. This indicates that a particular mechanism is involved in the whole tar autoxidation.

In the process of coal-tar autoxidation, some high-molecular-weight compounds are believed to be formed in the liquid, so the viscosity of coal tar increases continuously. The relations between the viscosity of tar sample, the concentration of new compounds, and the time of reaction is shown in Figure 3. In some small interval of reaction time, say, Δt, the viscosity of the tar sample increases from η to $\eta + \Delta\eta$, and the concentration of new compounds increases from C to $C + \Delta C$. If the tar sample with viscosity η at time t is considered as the solvent of new compounds formed from time t to time $t + \Delta t$, then, at the end of the time interval Δt, the relative viscosity is written as

$$\eta_r = \frac{\eta + \Delta\eta}{\eta}$$

and the specific viscosity becomes

$$\eta_{sp} = \eta_r - 1 = \frac{\eta + \Delta\eta}{\eta} - 1 = \frac{\Delta\eta}{\eta}$$

Also, according to definition, the intrinsic viscosity can be expressed as

$$[\eta] = \left(\frac{\eta_{sp}}{\Delta C}\right)_{\Delta C \to 0} = \left(\frac{\Delta\eta/\eta}{\Delta C}\right)_{\Delta C \to 0}$$

Substitution of the Mark-Houwink equation (1), which is applicable to a mixture, into the latter equation gives

$$\left(\frac{\Delta\eta/\eta}{\Delta c}\right)_{\Delta c \to 0} = K\bar{M}v^{a}$$

in which K and a are constants, $\bar{M}v$ represents the viscosity average molecular weight of the high-molecular-weight compounds. It is true that as Δt approaches 0, Δc also approaches 0, so does $\Delta\eta$; hence, division of both the numerator and the denominator by Δt at the left-hand side and taking the limit as Δt goes to 0 yields

$$\frac{d\ln\eta/dt}{dc/dt} = K\bar{M}v^{a}$$

After rearrangement, it becomes

$$\frac{d\ln\eta}{dt} = K\bar{M}v^{a}\frac{dc}{dt} \qquad (I)$$

This kinetic equation relates the viscosity-change rate with the chemical-reaction rate. Most products of coal-tar autoxidation are dimers, which can be considered roughly as a rigid spherical particle, so that the interaction between different new compounds is negligible, and the characteric constants K and a can be assumed to be constant during reaction (2).

The mechanism of the chain oxidation of hydrocarbons can be represented in the following way (3):

$RH \xrightarrow{O_2} R\cdot$	(0)	(origin of the chains)
$R\cdot + O_2 \rightarrow RO_2\cdot$	(1)	(propagation of the chains)
$RO_2\cdot + RH \rightarrow ROOH + R\cdot$	(2)	
$ROOH \rightarrow RO\cdot + OH\cdot$	(3)	(degenerate branching)
$R\cdot + R\cdot \rightarrow R - R$	(4)	
$RO_2\cdot + R\cdot \rightarrow ROOR$	(5)	(termination of the chains)
$RO_2\cdot + RO_2\cdot \rightarrow ROH + R_1COR_2 + O_2$	(6)	

Usually reaction 1 is believed to be a very fast reaction (4). However, in the process of the whole-tar autoxidation, the free radical $R^{\cdot}$ reacts not only with oxygen, but also with the antioxidants such as phenols (belonging to tar acids), amines (belonging to tar bases), and sulfur-containing compounds. At the same time, the peroxy radical $RO_2^{\cdot}$ is easily arrested by these antioxidants too. Thus, the concentration of free radicals is kept at such a low level that the propagation of free radicals fails to proceed eventually, and reaction 1 becomes a rate-determining step. For this study the tar sample was stored in a static container (cf. Figure 4), before collision with free radical R·, the oxygen molecule had to diffuse from air through some media of the tar sample to meet the reactant; the overall reaction was therefore a diffusion-controlled reaction, which has been substantiated by the data shown in Figure 5. Thus, in accordance with Smoluchowski theory (5,6), the rate of the diffusion-controlled reaction can be written as

$$W = \frac{4\pi N_0 \sigma_{12} D}{1000} [R\cdot][O_2]$$

where $[R\cdot]$ and $[O_2]$ are the concentration of free radical $R^{\cdot}$ and oxygen respectively, D is the diffusion coefficient, N_0 is Avogadro's number, and σ_{12} is the reaction radius, (the distance between the centers of the particles when they are reacted). For simplicity, the rate equation can be expressed as

$$W = \alpha D[O_2] \qquad (II)$$

in which

$$\alpha = \frac{4\pi N_0 \sigma_{12}[R\cdot]}{1000} = \text{constant}$$

The autoxidation system used in this study and the oxygen profile in the coal-tar sample are also shown in Figure 4. Here A represents the oxygen in air, B represents the coal-tar sample to be oxidized, Z represents the depth of the sample, C_A is the concentration of oxygen and N_{AZ} is the molar flux of oxygen in the Z-direction. As gas A diffuses into liquid B and undergoes an irreversible reaction: $A + B\cdot \rightarrow AB\cdot$, the mass balance (input - output + production = 0) takes the form (7)

$$N_{AZ}|_Z S - N_{AZ}|_{Z+\Delta Z} S - D\alpha C_A S\Delta Z = 0$$

in which S is the cross-sectional area of the liquid. The quantity αDC_A represents the moles of oxygen disappearing per unit volume per unit time. Division of both sides by $S\Delta Z$ and taking the limit as ΔZ goes to zero gives

$$\frac{dN_{AZ}}{dz} + D\alpha C_A = 0$$

Since A and $AB\cdot$ are present in small concentrations, the following approximation (Fick's first law) can be established:

$$N_{AZ} = -D \frac{dC_A}{dz}$$

Substitution of this relation into the preceding equation and division of both sides by D gives

$$-\frac{d^2C_A}{dz^2} + \alpha C_A = 0$$

This is to be solved with the boundary conditions:

$$\text{at } z = 0, \qquad C_A = C_{Ao}$$

$$\text{at } z = L, \qquad N_{AZ} = 0 \quad \text{or} \quad \frac{dC_A}{dz} = 0$$

Thus, the concentration profile of oxygen is obtained and expressed as

$$C_A = \frac{\text{COSh } b[1 - (Z/L)]}{\text{COSh } b} C_{Ao}$$

in which $b = L\sqrt{\alpha}$

and the rate of oxygen consumption is

$$\frac{dQ_A}{dt} = N_{AZ}|_{Z=o} S$$

$$= -D \frac{dC_A}{dz}|_{Z=o} S$$

$$= DS\sqrt{\alpha}\, C_{Ao} \tanh b \qquad \text{(III)}$$

The rate of generation of high-molecular-weight compounds in this diffusion-controlled reaction is proportional to the consumption rate of oxygen. Therefore, substitution of the consumption rate of oxygen (III) into the preceding kinetic equation (I) gives

$$\frac{d\ln\eta}{dt} = K'K\bar{M}v^a DS\sqrt{\alpha}\, C_{Ao} \tanh b/(SL)$$

in which K' is a proportionality constant and SL is the volume of the sample. For simplicity, this can be written as

$$\frac{d\ln\eta}{dt} = \beta DC_{Ao}$$

where

$$\beta = K'K\bar{M}v^a\sqrt{\alpha} \tanh b/L$$

It may be noted that an approximate equation for the diffusion coefficient of a spherical molecule of radius σ is

$$D = \frac{RT}{6\pi N_o \sigma\eta}$$

in which η is the viscosity of the medium, R is the gas law constant, T is the absolute temperature and N_o is Avogadro's number (5). Sub-

stitution of the relation into the preceding equation yields

$$\frac{d\eta/\eta}{dt} = \beta\left(\frac{RT}{6\pi N_o \sigma \eta}\right) C_{Ao}$$

Because η is different from zero, multiplication of both sides by η gives

$$\frac{d\eta}{dt} = \beta\left(\frac{RT}{6\pi N_o \sigma}\right) C_{Ao} = \gamma$$

Under constant pressure and temperature, β and C_{Ao} are assumed to be constant, therefore so is γ. Thus

$$\frac{d\eta}{dt} = \gamma = \text{constant}$$

After integration, it becomes

$$\eta = \eta_o + \gamma t \qquad \text{(IV)}$$

where η_o is a constant of integration. This accounts for the linear relation between viscosity and time as shown in Figures 1 and 2.

The total amount of oxygen which diffuses into the coal-tar sample from air during reaction, can be calculated by introducing the relation above (IV) into the rate equation of oxygen consumption (III), that is

$$\frac{dQ_A}{dt} = DS\sqrt{\alpha}\, C_{Ao} \tanh b$$

$$= \frac{RT}{6\pi N_o \sigma (\eta_o + \gamma t)} S\sqrt{\alpha}\, C_{Ao} \tanh b$$

$$= \frac{\delta}{\eta_o + \gamma t}$$

where

$$\delta = \frac{RT}{6\pi N_o \sigma} S\sqrt{\alpha}\, C_{Ao} \tanh b = \text{constant}$$

Integration gives

$$\int_o^{Q_A} dQ_A = \int_o^t \frac{\delta dt}{\eta_o + \gamma t}$$

$$Q_A = \frac{\delta}{\gamma} \ln(\eta_o + \gamma t)\Big|_o^t$$

$$= \frac{\delta}{\gamma} \ln\left(\frac{\eta_o + \gamma t}{\eta_o}\right) \qquad (V)$$

When neutral oils are chemically separated from coal tar and oxidized in air, its viscosity-change behavior (Figure 6) is different from that of the whole tars. For neutral oils, olefins are usually regarded as the compounds which most easily react with the oxygen in air. Because most of the tar acids and the tar bases are absent in the neutral oils, few antioxidants compete with oxygen to consume the free radicals during autoxidation; thus the propagation reaction can be self-sustained, and the overall reaction becomes a long chain reaction. At relatively high pressure (> 100 mm) and high-chain length during autoxidation at the steady state the integrated equation is found to be:

$$-\ln(\ln\eta_\infty - \ln\eta) = K_\infty t + \text{constant}$$

in which η_∞ is the viscosity of neutral oil as time approaches infinity.

When the quantity $\ln(\ln\eta_\infty - \ln\eta)$ is plotted against the reaction time t, a straight line is obtained as shown in Figure 7. The slope of the linear plot represents the rate constant of the overall autoxidation reaction. The rate constant thus obtained for the neutral oil from Hiawatha coal by carbonization is 4.56×10^{-2}/hr., and that for the neutral oil from hydrogenation is 2.62×10^{-2}/hr. The reason for this difference is perhaps that the neutral oil from carbonization contains more diolefins than that from hydrogenation because the unsaturation of coal tar is reduced in the hydrogenation reactions.

The viscosity-change behavior of tar acids and tar bases during autoxidation are shown in Figures 8 and 9. Although these are quite

similar to that of neutral oils, both autoxidation mechanisms of tar acids and tar bases are somewhat different. Some workers reported that inhibitors (AH) may react directly with oxygen (8) in the following way:

$$AH + O_2 \rightarrow A\cdot + HO_2\cdot \qquad (7)$$

Tar acids contain a large amount of phenols, and tar bases contain various amines. Both phenols and amines are generally used as inhibitors for hydrocarbon autoxidation. Hence, reaction (7) must be the main reaction involved in the autoxidation of tar acids and tar bases. In the absence of other hydrocarbon radicals, the following reaction is also believed to take place in the tar acids and tar bases (8):

$$AH + HO_2\cdot \rightarrow A\cdot + H_2O_2 \qquad (8)$$

Finally the reaction may be terminated by dimerization of A· radicals:

$$2\ A\cdot \rightarrow A\text{-}A \qquad (9)$$

Hence, assuming steady state, the rate equation can be expressed as

$$\frac{-d[AH]}{dt} = 2K_7[O_2][AH]$$

Here the concentration of oxygen ($[O_2]$) can be considered as constant because tar acids and tar bases are oxidized in air. Thus, the autoxidations of tar acids and tar bases become a pseudo-first reaction, which is similar to the rate equation of the neutral oil autoxidation. The linear plots for $-\ln(\ln n_\infty - \ln n)$ vs. time are shown in Figures 10 and 11. The apparent rate constant of tar-acid autoxidation is 2.88×10^{-2}/hr for samples from both carbonization and hydrogenation and that for tar bases from both processes is 3.75×10^{-2}/hr. It

is evident that the composition of active compounds contained in either tar acids or tar bases is independent of the coal liquefaction process.

The dependence of the viscosity-change rate for the whole-tar autoxidation on the partial pressure of oxygen is shown in Figure 12. It can be seen that at oxygen pressures greater than 50 mm Hg, the rate of oxidation is independent of the oxygen partial pressure. This corresponds with the inhibited oxidation theory (9).

The temperature effect on the viscosity-change behavior for the whole-tar autoxidation is shown in Figure 13. At higher reaction temperatures the viscosity changes faster. If the slopes of these curves near zero time are taken as the apparent rate constants for the initial reaction period, a linear plot for the Arrhenius equation (Figure 14) gives an activation energy of 9.07 kcal/mole. Usually, the activation energy of a physical-process-controlled reaction is less than this value; therefore, the autoxidation of whole tar is probably not a purely physical-process-controlled reaction.

The effect of light on the viscosity-change behavior during the autoxidation of whole tar is shown in Figure 15. The viscosity-change of the sample under continuous irradiation of fluorescent light is higher than that of the sample isolated from light. In photochemical oxidation, the rate of formation of radicals W_i is directly proportional to the density of the light (3); hence, some compounds contained in the coal tar may be subjected to photochemical oxidation.

Refraction

The refractive-index change behavior accompanying the viscosity change during the whole-tar autoxidation is shown in Figures 1 and 2. For a pure substance, the Lorenz-Lorentz refraction equation is expressed as (10)

$$\frac{n^2 - 1}{n^2 + 2} = \frac{4}{3}\pi N\tilde{\alpha}$$

in which n represents the refractive index, N represents the number of particles per unit volume and $\tilde{\alpha}$ is the polarizability of the particle. Coal tar is a complex mixture; therefore, for simplicity the assumption is made that the internal field strength is homogeneous throughout the liquid, and the polarizability of the individual particle is independent of its environment, so the Lorenz-Lorentz refraction equation for coal tar can be roughly written as

$$\frac{n^2 - 1}{n^2 + 2} = \frac{4}{3}\pi(\Sigma N_i\tilde{\alpha}_i)$$

in which N_i represents the number of particles of i per unit volume and $\tilde{\alpha}_i$ is the polarizability of particle i. Since whole-tar autoxidation appears to be a diffusion-controlled reaction, the number of reactant molecules disappearing and the number of product molecules generated are proportional to the number of oxygen molecules consumed in the reaction, which is small compared to that of whole tar; thus, substitution of equation (V) into the Lorenz-Lorentz refraction equation for coal tar the following relation is obtained:

$$\left(\frac{n^2 - 1}{n^2 + 2} \cdot \frac{1}{d}\right)_t = \left(\frac{n^2 - 1}{n^2 + 2} \cdot \frac{1}{d}\right)_o + \zeta \ln\left(\frac{n_o + \gamma t}{n_o}\right) \quad \text{(VI)}$$

in which ζ is a constant, subscript o indicates the initial state, and subscript t indicates the state at time t. According to equation (VI), if the refraction $(n^2 - 1)/[(n^2 + 2)\cdot d]$ is plotted against $\ln[(n_o + \gamma t)/n_o]$, a straight line is obtained (Figure 16). The negative slope of the linear plot is a good evidence for polymerization reaction involved in coal-tar autoxidation. The polarizability of the product is not much

larger than that of the reactant, however the difference between the number of reactant molecules which disappeared and that of the product molecules generated during the reaction is tremendously big. Thus, the net gain of the polarizability per unit volume is negative, and the value of the proportional constant ζ of equation (VI) is negative.

Oxygen Content

The oxygen content of the whole tar during autoxidation is shown in Figure 17. The continuous increase of oxygen content indicates that autoxidation is a main factor leading to deterioration of coal-tar properties.

Iodine Number

Iodine number is the common designation for the determination of unsaturation via the addition of iodine monohalides. The iodine-number change for the whole-tar autoxidation is shown in Figure 18. The decrease of iodine number with reaction time indicates that olefins in the coal tar are attacked by oxygen and saturated by polymerization reactions and therefore play an important part in coal-tar autoxidation.

Infrared Absorption Spectra (numbers in parentheses indicate wave numbers where infrared absorption takes place)

For the whole tar autoxidation, the oxygen-containing groups such as phenols (3200-3600 cm^{-1}), hydroperoxides (3400 cm^{-1}), carboxylic acids (1960-1760 cm^{-1}), and esters (1250 cm^{-1}) increase; however, the double bonds (3020-3080 cm^{-1}) diminish (Figures 19 and 20). This corresponds very well with the decrease of iodine number, indicating

that the unsaturated hydrocarbons become saturated during oxidation. Furthermore, the reduction of amines (1474 cm^{-1}) indicates that they take part in the whole-tar autoxidation. Finally, the decrease of monosubstituted aromatic compounds (690-710, 730-770 cm^{-1}) and the increase of m-disubstituted aromatic compounds (750-810 cm^{-1}) indicate that some aromatic molecules enlarge by addition or polymerization reactions.

CONCLUSION

Coal tars are easily attacked by oxygen when they are exposed to air. The ease and extent of this attack are determined by a number of factors, among which are the composition of the coal tar, the reaction temperature and the oxygen pressure.

According to the viscosity-change behavior, it is believed that the whole-tar autoxidation is a diffusion-controlled reaction; the autoxidation of neutral oils is a long-chain, radical reaction, the rate of which is proportional to the concentration of hydrocarbon reactants; the oxidation of tar acids, and tar bases is a second-order reaction, the rate of which is proportional to the concentration of tar acids or tar bases, and the partial pressure of oxygen.

The decrease of refraction of coal tars as reaction with oxygen proceeds indicates that some polymerization reactions are involved in coal-tar autoxidation.

The decrease of iodine number with reaction time reveals that the olefins play an important part in coal-tar autoxidation. The same conclusion is drawn from the results of the infrared absorption analyses.

To prevent deterioration of coal-tar properties, coal tars should be isolated from oxygen and light; otherwise significant quantities of

good oxidation inhibitors are required for stability.

Acknowledgement is made to the Office of Coal Research, U. S. Department of the Interior and the University of Utah who supported the research reported here.

REFERENCES

1. Flory, P. J., Principles of Polymer Chemistry, pp. 308-314, Cornell University Press, Ithaca, New York, 1953.

2. Flory, P. J., Principles of Polymer Chemistry, pp. 595-639, Cornell University Press, Ithaca, New York, 1953.

3. Emanuel, N. M., E. T. Denisov, and Z. K. Maizus, Liquid-phase Oxidation of Hydrocarbons, pp. 9-14, Plenum Press, New York, 1967.

4. Frost, A. A. and R. G. Pearson, Kinetics and Mechanism, pp. 249, John Wiley & Sons, Inc., New York, 1961.

5. Frost, A. A. and R. G. Pearson, Kinetics and Mechanism, pp. 268-272, John Wiley & Sons, Inc., New York, 1961.

6. Daniels, F. and R. A. Alberty, Physical Chemistry, pp. 362-363, John Wiley & Sons, Inc., New York, 1966.

7. Bird, R. B., W. E. Stewart, and E. N. Lightfoot, Transport Phenomena, pp. 532-533, John Wiley & Sons, Inc., New York, 1960.

8. Reich L. and S. S. Stivala, Autoxidation of Hydrocarbons and Polyolefins- Kinetics and Mechanisms, pp. 140-141 and 402, Marcel Dekker, Inc., New York, 1969.

9. Emanuel, N. M., E. T. Denisov, and Z. K. Maizus, Liquid-phase Oxidation of Hydrocarbons, pp. 241-243, Plenum Press, New York, 1967.

10. Batsanov, S. S., Refractometry and Chemical Structure, pp. 6-7, Consultants Bureau, New York, 1961.

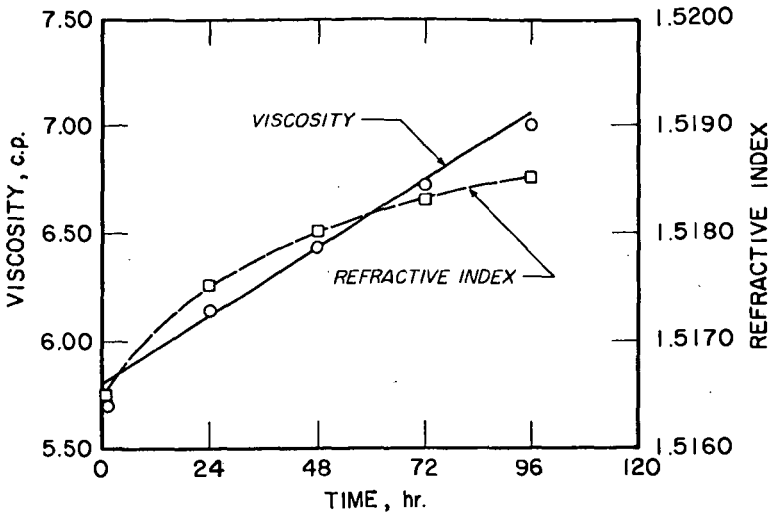

Fig. 1. Viscosity and refractive-index change as a function of time for the autoxidation (at 20°C) of whole tar obtained from Hiawatha coal by carbonization.

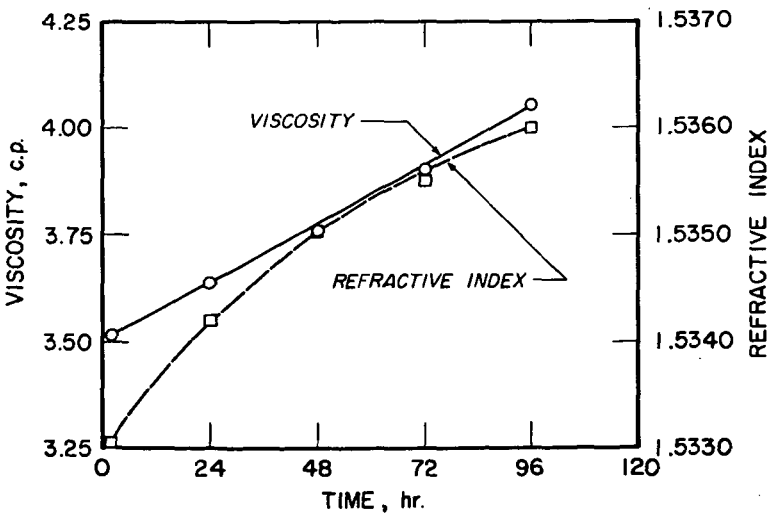

Fig. 2. Viscosity and refractive-index change as a function of time for the autoxidation (at 20°C) of whole tar obtained from Hiawatha coal by hydrogenation.

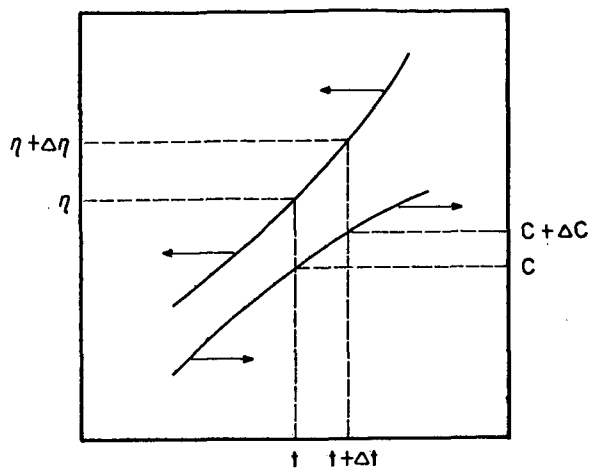

Fig. 3. Relation among viscosity, concentration and time.

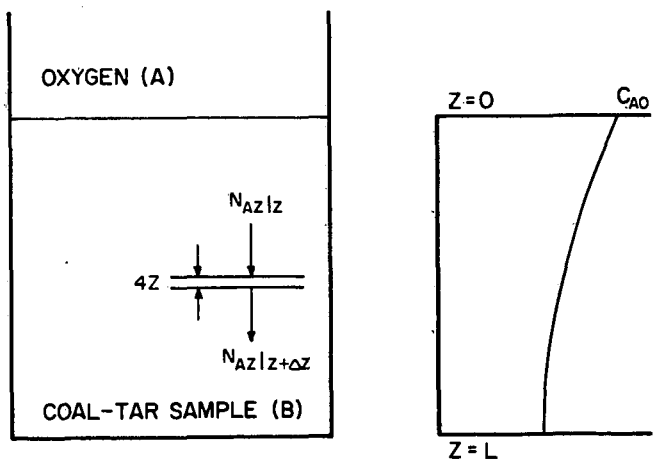

Fig. 4. Autoxidation system and oxygen profile in coal tar sample.

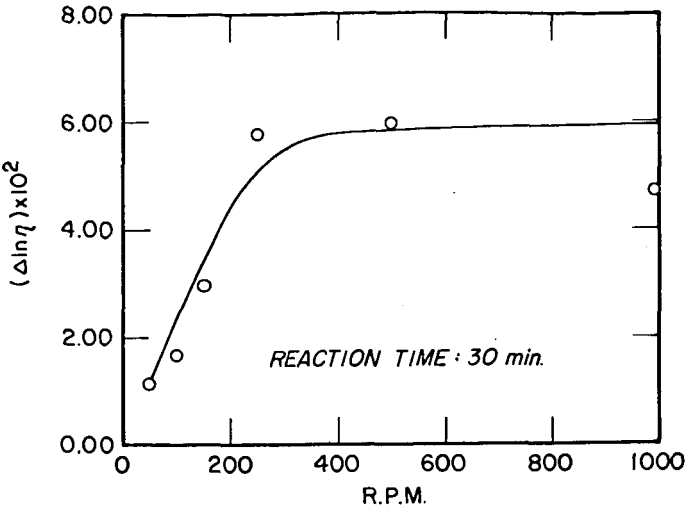

Fig. 5. Viscosity increase as a function of stirring speed for the autoxidation (at 20°C) of whole tar obtained from Hiawatha coal by carbonization.

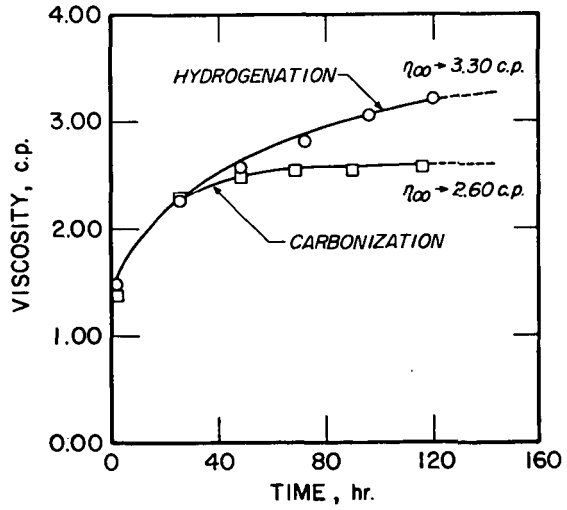

Fig. 6. Viscosity change as a function of time for the autoxidation (at 25°C) of neutral oils from Hiawatha coal.

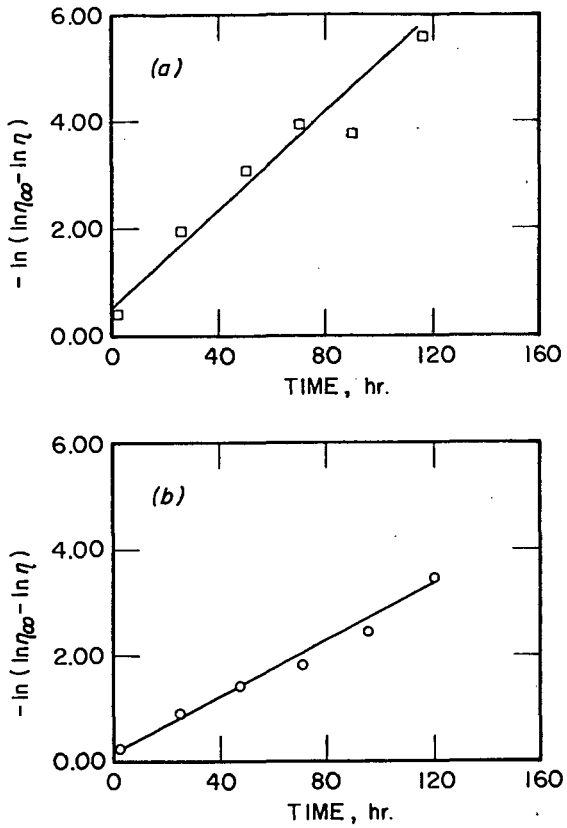

Fig. 7. Linear plot for a first-order autoxidation reaction of neutral oils obtained from Hiawatha coal by (a) carbonization and (b) hydrogenation.

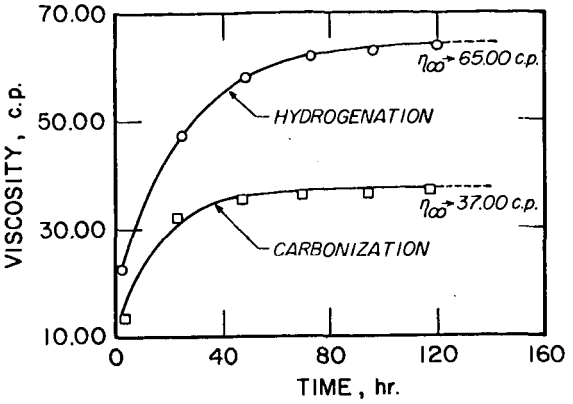

Fig. 8. Viscosity change as a function of time for the autoxidation (at 25°C) of tar acids from Hiawatha coal.

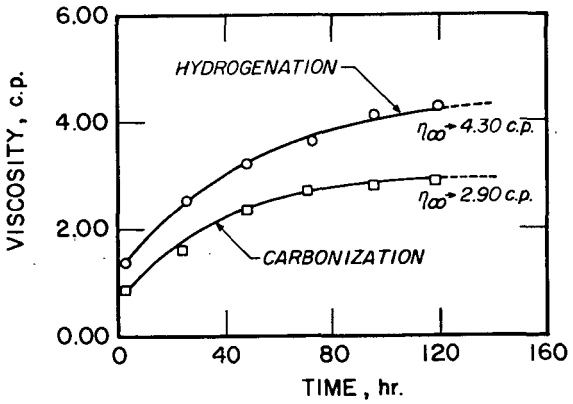

Fig. 9. Viscosity change as a function of time for the autoxidation (at 25°C) of tar bases from Hiawatha coal.

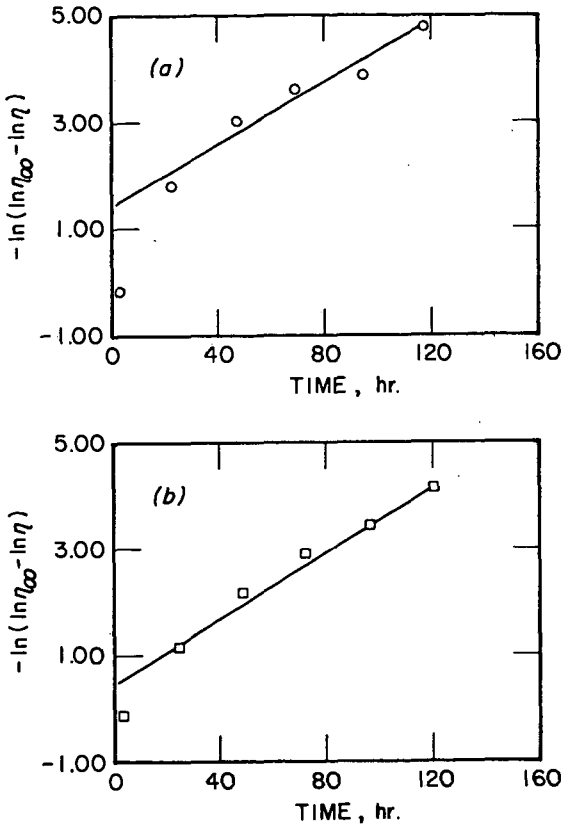

Fig. 10. Linear plot for a pseudo-first-order autoxidation reaction of tar acids from Hiawatha coal by (a) carbonization and (b) hydrogenation.

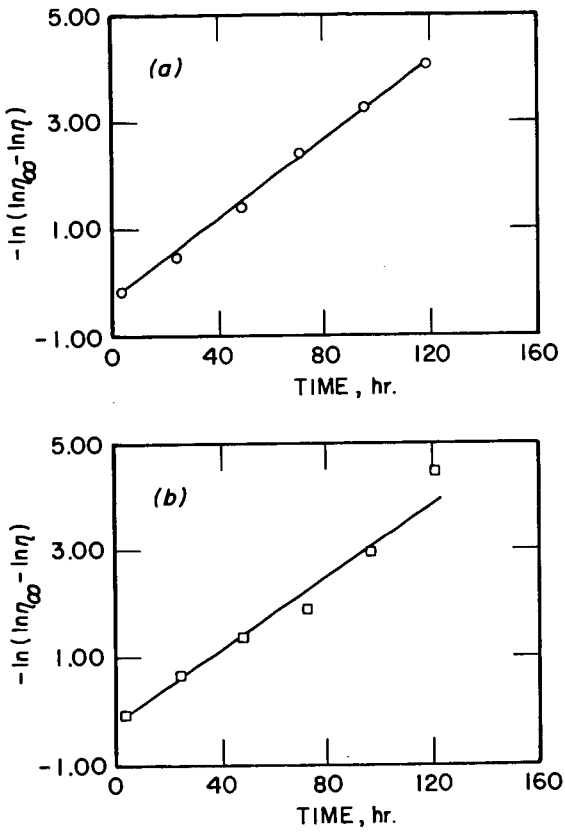

Fig. 11. Linear plot for a pseudo-first-order autoxidation reaction of tar bases obtained from Hiawatha coal by (a) carbonization and (b) hydrogenation.

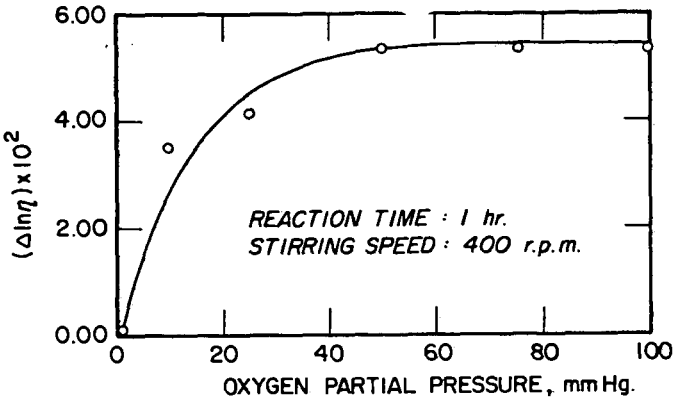

Fig. 12. Dependence of the viscosity-change rate on the oxygen partial pressure for the autoxidation (at 20°C) of whole tar obtained from Hiawatha coal by hydrogenation.

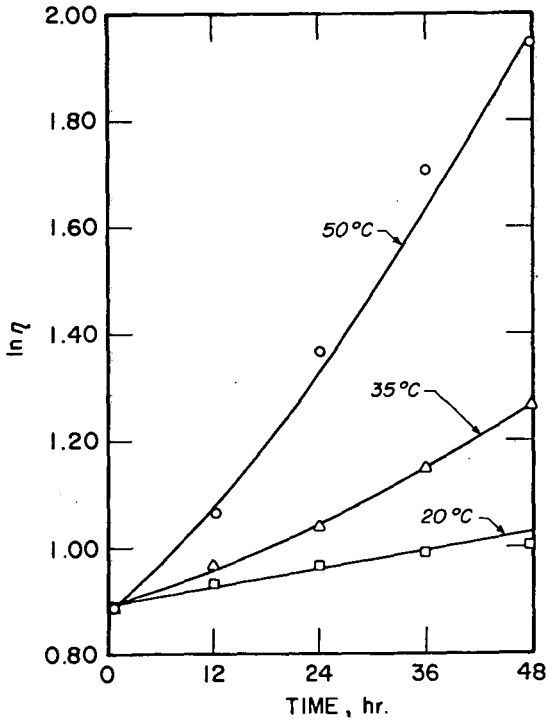

Fig. 13. Logarithm of viscosity vs. reaction time for the whole-tar autoxidation at various temperatures. (Sample obtained from Hiawatha coal by hydrogenation)

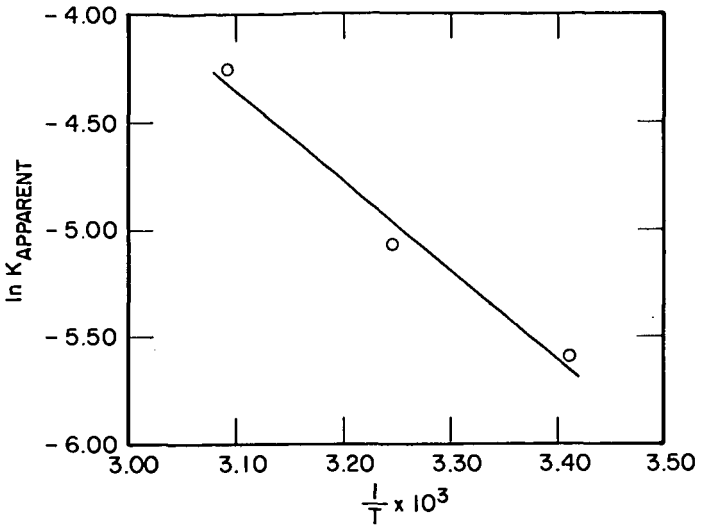

Fig. 14. Linear plot of Arrhenius equation for evaluation of activation energy for initial reaction of whole tar with air.

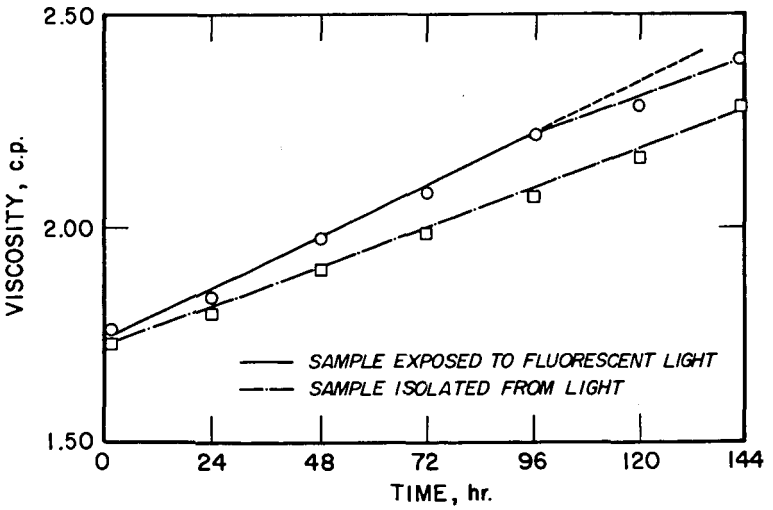

Fig. 15. Fluorescent light effect on viscosity change for the autoxidation (at 20°C) of whole tar obtained from Spencer coal by hydrogenation.

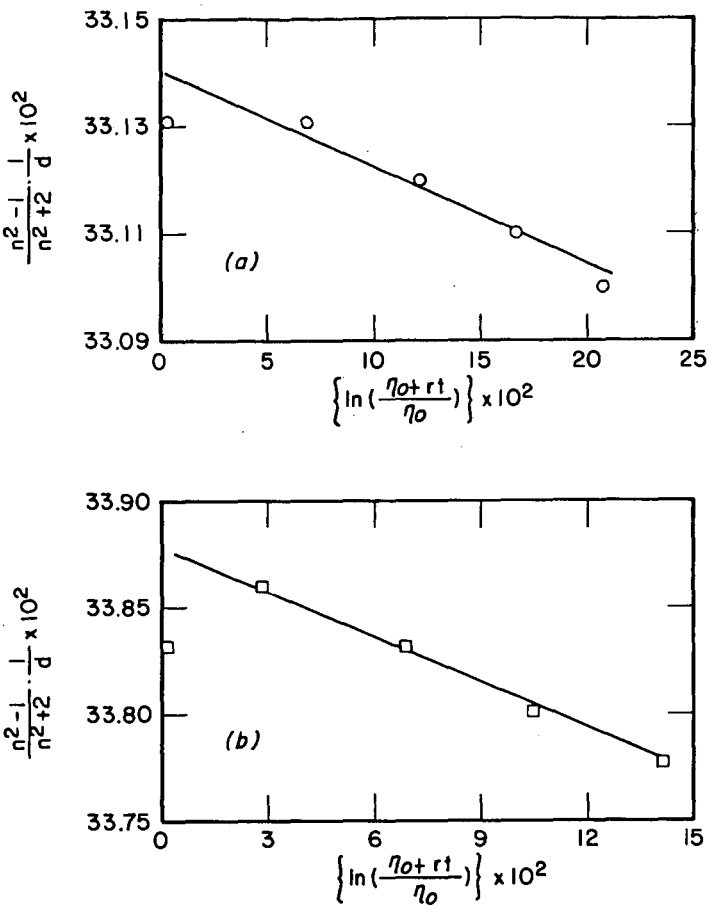

Fig. 16. Refraction as a function of time for the autoxidation (at 20°C) of whole tars obtained from Hiawatha coal by (a) carbonization and (b) hydrogenation.

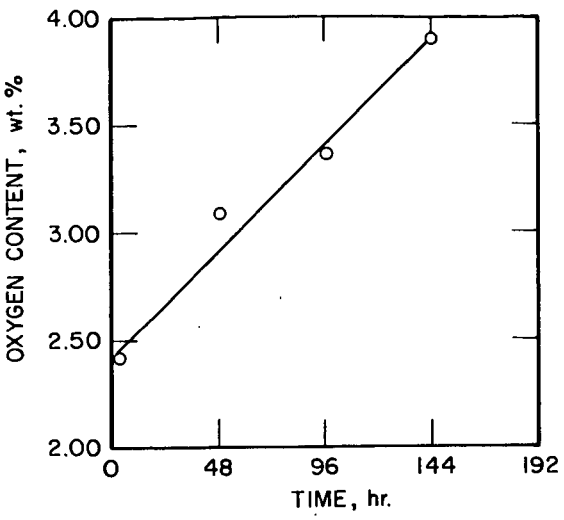

Fig. 17. Oxygen content as a function of time for the autoxidation (at 20°C) of whole tar obtained from Spencer coal by hydrogenation.

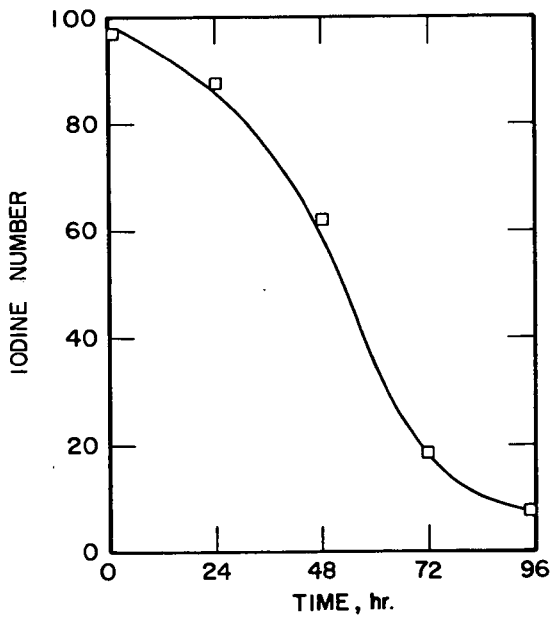

Fig. 18. Iodine number vs. time for the autoxidation (at 50°C) of whole tar obtained from Spencer coal by hydrogenation.

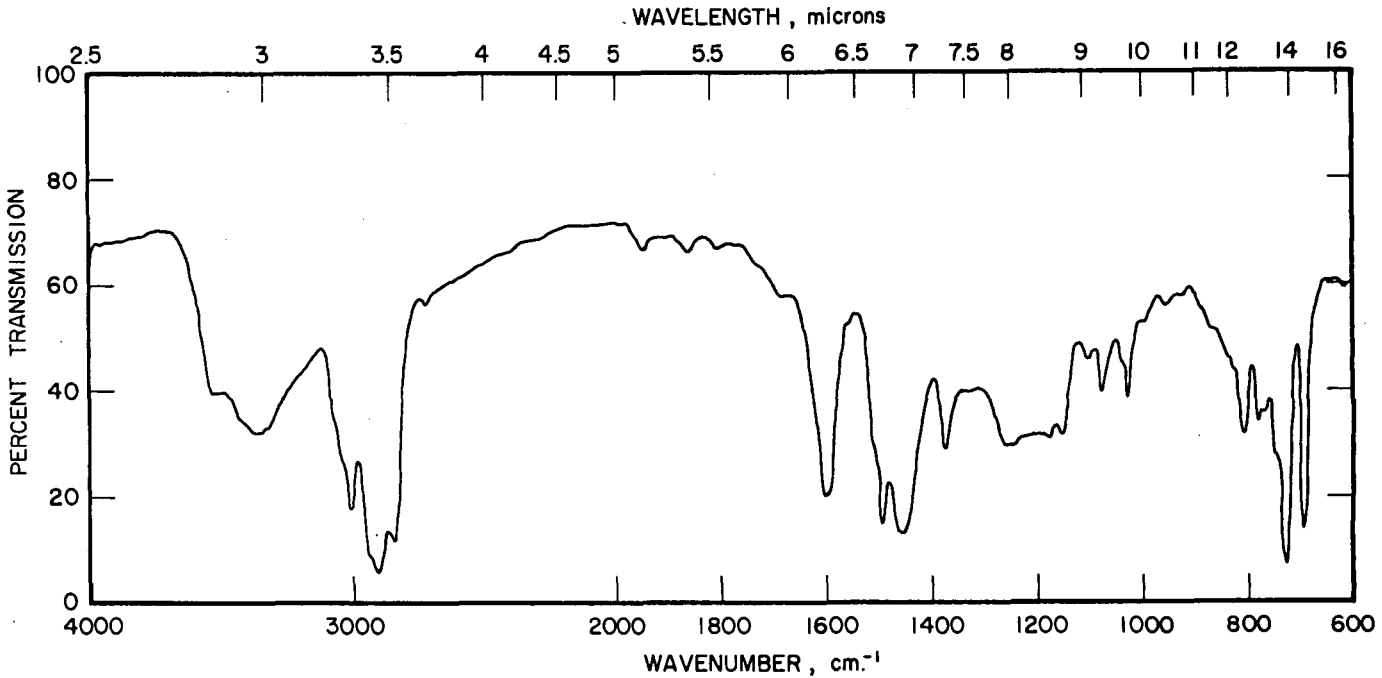

Fig. 19. Infrared absorption spectrum of whole tar before oxidation (Sample obtained from Hiawatha coal by hydrogenation)

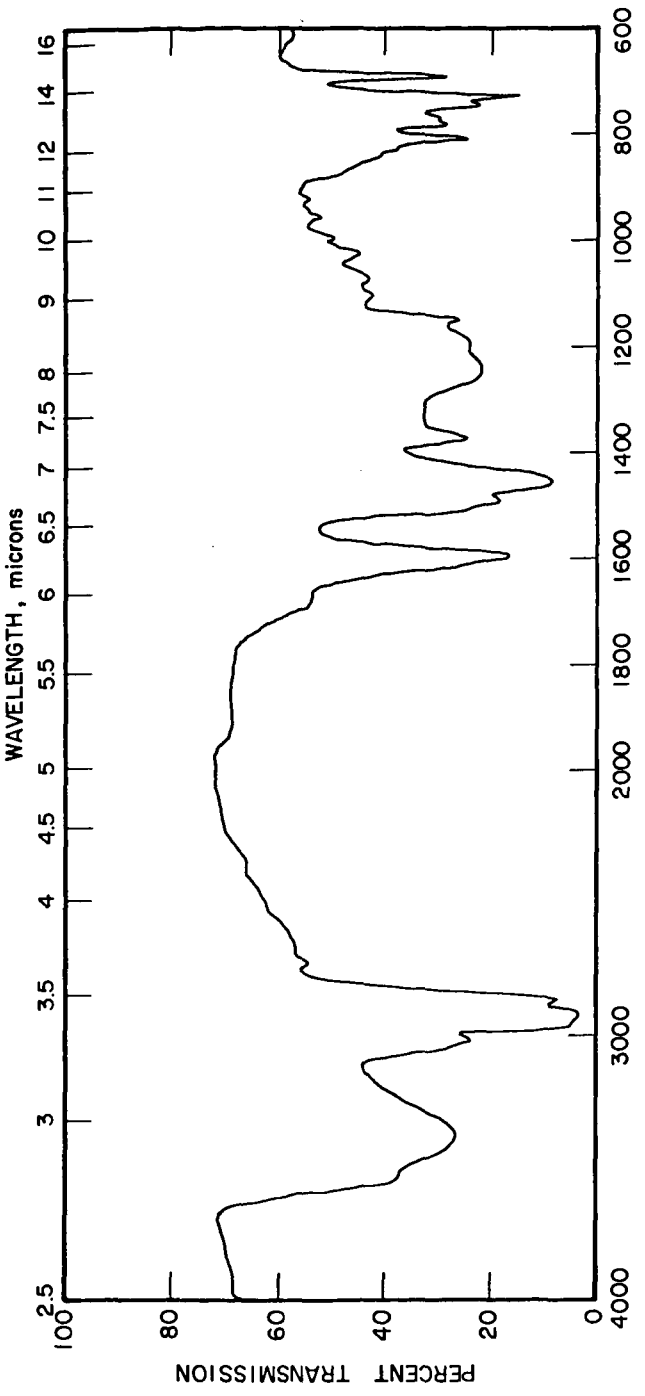

Fig. 20. Infrared absorption spectrum of whole tar oxidized (at 50°C) for 48 hr. (Sample obtained from Hiawatha coal by hydrogenation)

THE DIRECT PRODUCTION OF METHANE FROM HEAVY HYDROCARBONS AND STEAM

N. J. KERTAMUS AND G. D. WOOLBERT

THE BABCOCK & WILCOX COMPANY
ALLIANCE RESEARCH CENTER
ALLIANCE, OHIO

1.0 INTRODUCTION

During the past several years, much concern and interest has been focused on the so-called single-reactor concept for making substitute natural gas (SNG) from coal. In principle, this concept proposes to charge coal and steam as well as catalysts, if necessary, into a single reactor to generate a gas that contains methane as the primary combustible constituent. Diluents such as acid gases could be removed during the process to yield a product gas of high methane concentration that would not require external methanation. This single-reactor concept is generally referred to as The Direct Production of Hydrocarbons (Methane) from Coal-Steam Systems method or, more simply, as the "Wyoming Concept."

The initial concept was developed at the University of Wyoming and has been supported by the Office of Coal Research (OCR) at the University of Wyoming under Contract 14-01-0001-1196.

About 1 year ago our Process Engineering Group developed process flowsheets and approximate costs for erecting and operating equivalent sized plants using different technologies to produce medium (300-500) and high (1000) Btu gas. The results of this study suggested that, if coal could be gasified to methane directly by using steam in the process, such a concept would have a definite economic advantage over other gasification technologies presently being developed.

To substantiate our Process Engineering calculations, a limited experimental program was initiated to assess the technical feasibility of the concept. This paper summarizes the results of that program.

2.0 BACKGROUND

As a company, Babcock and Wilcox has been interested in coal gasification for over 20 years. Our accomplishments range from the construction of an oxygen-blown gasifier for the DuPont Company in the mid 1950's to the current construction of the BIGAS gasifier that will be built at Homer City, Pennsylvania.

So that the reader will understand our rating of product gas quality, we will identify a low Btu gas as one that produces 80-150 Btu/scf, a medium Btu gas as one that produces 300-500 Btu/scf, and a high Btu gas as one that could serve as a pipeline gas (i.e., ~1000 Btu/scf). The difference between low and medium Btu gas stems from the use of air or oxygen as the blowing medium. The major difference is that nitrogen is present as a diluent in the low Btu gas. Nitrogen, of course, is not readily removed from the product gas.

Medium Btu gas, after the removal of acid gases, consists primarily of hydrogen (H_2) and carbon monoxide (CO) with a heating value of 320 Btu/scf. In addition, depending on the specific gasification process, a medium Btu gas may contain a low concentration of higher hydrocarbon gases for a heating value in excess of 320 Btu/scf.

In the production of high Btu gas, methane is generated in several ways. Two important routes for its production are as follows:

- During the gasification step by pyrolysis of the coal and/or hydrogasification of the volatile matter.
- By reaction of the H_2 and CO externally on the surface of the catalyst to form CH_4 (methanation).

In terms of gasification efficiency (i.e., Btu content of coal converted to Btu's as methane), the first route is preferred. For example, if char is first gasified to CO and H_2 and then reacted to form methane via the second path, the gasification efficiency is 69%, assuming cold reactants and an end point theoretical temperature in the gasifier of 1500°F. If, on the other hand, methane can be coupled to the gasification process so that $2.453\ C + 2H_2O + 0.453\ O_2 = CH_4 + 1.453\ CO_2$ (also starting with cold reactants and winding up at 1500°F), then the theoretical gasification efficiency is close to 90%.

2.1 PREVIOUS WORK

Development effort on the direct methanation process reported in the literature consisted primarily of batch-type tests at the bench scale level. The published results suggest that the following experimental procedure would provide the best approach to the problem (see references).

Coal was first mixed with caustic (K_2CO_3), then charged to the upstream part of a small (~1/2-inch ID) reactor 6 feet in length. A nickel methanation catalyst was either placed downstream or intimately mixed with the coal and caustic. After electrical resistance heaters heated the system to test temperature, water (or steam) was fed to react or gasify the coal. Off gas volume was measured and periodically analyzed. Typical test conditions were as follows:

Temperature, °F	1200 – 1400
Pressure, psig	Atmospheric – 800
Coal Weight, gm	125
K_2CO_3 Weight, gm	15
Ni Methanation Catalyst Weight, gm	50 – 100
H_2O Rate, ml/hr	4 – 8

2.2 LIMITATIONS

During the review of published results on gasification and the methanation catalyst state-of-the-art conducted before initiating our experimental program, we identified several potential limitations that could severely limit successful application of the concept. These limitations are discussed below.

2.2.1 Methanation Catalyst Life

Major concern centers on the anticipated "life" of the expensive nickel methanation catalyst. This catalyst sells for about $3.00 per pound. Scaling the previous batch tests, that is, gasifying 125 pounds of carbon consuming 100 pounds of catalyst, indicates a projected catalyst cost of about $150 per 1000 scf of methane produced. If we assume repeated 7-1/2 hour cycles intermittently charging fresh char, the nickel catalyst must last for 15 months to drive catalyst cost down to $.10 per 1000 scf of methane produced.

The environment surrounding the nickel methanation catalyst is extremely harsh. Operation at 1200°F represents a temperature significantly higher than that normally used in methanating H_2 and CO. In addition, the possible effects of the sulfur, ash,

and coke forming entities on the life expectancy of the nickel catalyst are not currently known. Our concern for the life of the catalyst therefore relates to the following areas:

- Sintering of the catalyst at high temperatures
- Sulfur poisoning
- Deactivation by coking and ash

2.2.2 Low Throughput – Batch

Using the published results as a basis for estimating coal throughput per unit of catalyst, the low weight hourly space velocity (WHSV) – WHSV = 125 lb coal/100 lb Ni catalyst/7.4 hrs = 0.17 – may limit application of the concept, even with a durable long-life catalyst.

The concept, as tested, involves batch operation with intermittent charging of the coal catalyst mix. Scaling up the batch operation to plants with capacities of 250 x 10^6 scf-SNG per day seems unrealistic. Demonstration of continuous operation (continuous charging of hydrocarbon) is paramount to the success of the concept.

The low coal throughput rate may be due to the fact that the endothermic carbon-steam reaction to CO and H_2 does not occur at a rapid rate, even catalyzed with K_2CO_3 at 1200 to 1400°F. On the other hand, a temperature of 1200°F represents a higher than optimum temperature for methanation. The overall concept settles for a tradeoff at temperatures below that desirable for rapid gasification but higher than that desired for good methanation.

3.0 OBJECTIVE

The focal point of the experiments was the demonstration of long methanation catalyst "life" in the direct production of methane from coal (or coal-like hydrocarbons) with steam in a continuous reactor. Pursuant to our major aim, catalysts were also surveyed at 1200°F to find the "best" catalyst to methanate CO and H_2 – some in the presence of sulfur.

4.0 EXPERIMENTAL EQUIPMENT – PROCEDURE

4.1 METHANATION CATALYSTS – 1200°F

The apparatus used to test methanation catalysts at 1200°F is sketched in Figure 1. The reaction consisted of a 1-inch ID Vycor tube filled, normally, with 4 inches of catalyst. Space velocities ranged from 250 to 2000, while the H_2 to CO ratio was also varied from 4:1 to 1.6:1. Hydrogen sulfide, when used, ranged from 0.5 to 2.0 volume percent.

Existing gases were dried and passed through a Fisher Gas Partitioner, which is capable of analyzing H_2, O_2, N_2, CH_4, CO and CO_2. The methane yield was determined from a chromatograph by using the peak height technique. Calibration samples were run periodically to check for shifts in peak height.

4.2 DIRECT PRODUCTION OF METHANE

The apparatus used in this phase is shown in Figures 2 and 3. Two Lapp pumps were used to force the feedstock and/or water at elevated pressures into the reactor. The reactor shown in Figure 3 is 4 feet long and has a 1-inch ID. It is designed to withstand temperatures of 1500°F and pressures of 1000 psig. The catalyst bed is placed in the middle of the reactor and heated to the desired temperature by a Lindberg

furnace. The temperature is monitored by three thermocouples located in the thermowell inside the reactor. The product gas passes through a motor valve which allows the pressure to be controlled.

The pressure is recorded and controlled by a Taylor Fulscope Recorder Controller. Provisions have also been made to introduce gases under pressure with controlled flow. The product gas from the reactor is sampled periodically from a water trap and passed through a Fisher Gas Partitioner which determines the methane yield. The remainder of the product gas, less the small amount used for the chromatograph, passes through a wet test meter which measures the amount of gas produced.

Several fail-safe devices are incorporated into the system. If the temperature within the reactor rises above a predetermined level, the complete system shuts down. Sensors monitor reactor pressure so that either too high an upstream pressure or too low a downstream pressure shuts down the complete system. This system is designed for a one-man operation with the possibility of unattended, continuous operation, if necessary.

4.3 FEEDSTOCKS

During the direct production of methane phase of the testing, a number of different feedstocks were tried. Direct injection of coal under pressure was not considered feasible in our small laboratory reactor, so further batch tests were conducted using char. During these tests samples of char were mixed with catalysts, placed in the reactor and steamed at specific temperatures and pressures.

To evaluate the feasibility of continuous operation, feedstocks were chosen that could be continuously injected into the reactor. Four feedstocks that could be continuously added with steam to the reactor were coal tar, benzene, No. 2 fuel oil, and anthracene oil. Anthracene oil was chosen for further testing because of its ease in handling and its similarity in composition to coal, especially its H/C ratio (see Table 1).

4.4 CATALYSTS

Of the 55 different catalysts tested, 10 were commercially available methanation catalysts and 45 were laboratory-prepared catalysts using accepted catalyst preparation techniques. Catalysts were prepared by impregnation, ion exchange, and decomposition. Many different promoters and combinations of promoters were examined. All prepared catalysts were calcined at 1200°F and activated using the standard activation procedure. Commercial catalysts were activated using the manufacturers' recommended procedure (see 5.0).

5.0 RESULTS

5.1 METHANATION CATALYST SURVEY

Table 2 provides a selected list of catalysts tested and their methane yields at a H_2 to CO ratio of 3 to 1 under varying conditions of space velocity and H_2S. We observed that the nickel (Ni) promoted catalysts lost activity as the catalyst bed was sulfided. Other metal catalysts were tried; however, except for platinum (Pt), each was poisoned by the H_2S in the gas feedstock. Moreover, as the space velocity was increased, the methane yield decreased for these other catalysts.

All tests were run at atmospheric conditions, and most were short-term tests ranging from 6 to 8 hours. The platinum catalysts showed no decrease in reactivity as a function of time and H_2S concentration, but all the other catalysts decreased as

the time of the test with H_2S was extended. The Norton, low surface area support is very resistant to high temperatures and should be considered an excellent support for high temperature-high pressure work.

5.2 DIRECT PRODUCTION OF METHANE

A data sheet of selected results is provided in Table 3. The temperatures, pressures, feedstock, catalyst, product gas produced, and weight of methane produced are tabulated. Our yield data was evaluated by integrating under the curve. An example of one of our curves appears in Figure 4. The first four tests were run so that we could determine the base for each feedstock and better understand the catalyst performance. These tests ranged in length from 1 to 30 hours, although a number of the tests were terminated because plugs formed in the reactor.

One problem was to determine the best way to introduce the alkali material needed to enhance gasification. In previous experiments, 200 grams of lignite coal with and without K_2CO_3 were steamed at a water rate of 65 ml/hr. Assuming the stoichiometry to be $2C + 3H_2O = 3H_2 + CO + CO_2$, the theoretical yield would be 35 scf gas/lb H_2O. In the experiments without K_2CO_3, 7.1 scf gas/lb H_2O was produced for a 20% theoretical yield, whereas 25 grams of K_2CO_3 gave 25.0 scf gas/lb H_2O, or a 71% theoretical yield. Therefore, K_2CO_3 is obviously needed to accelerate the gasification reaction. Three methods for introducing K_2CO_3 were tried in our continuous testing program. One method involved the direct addition of K_2CO_3 to the feedstock before injection into the reactor. A second method tried the direct impregnation of K_2CO_3 into the catalyst used for methanation. The last method added activated alumina impregnated with K_2CO_3 to the methanation catalyst bed. The first method proved to be the best procedure.

From the results in Table 4, several general conclusions were drawn. In all experiments, the feedstock conversion decreased as a function of time; therefore, the gas production decreased. The catalyst activity also decreased as a function of time; therefore, the methane yield decreased (Figure 4). A number of the catalysts used were found to be regenerable after an oxidation and reduction scheme, but the decreases in feedstock conversion and methane yield were again observed.

Two possible explanations for the decrease in methane yield have been suggested. One is that the metallic nickel surface, which forms the active site for methane production, has been deactivated by the formation of nickel carbide (Ni_3C). The second possibility is that amorphous carbon formed during the reaction plugs the catalyst surface and prevents the H_2 and CO gas mixture from making contact with the active nickel. With the low sulfur feeds no detection of sulfur poisoning of the nickel catalyst has been observed at the conditions established in our tests.

6.0 CONCLUSIONS

6.1 METHANATION CATALYST SURVEY AT 1200°F

Of the 55 catalysts examined, the nickel (Ni) promoted catalyst provided the best activity for the production of methane from a hydrogen and carbon monoxide gas mixture. We also found that all nickel-promoted catalysts were deactivated when a gas containing H_2S was passed over the bed. Other metal-promoted catalysts were examined and, except for platinum (Pt), each was poisoned by the H_2S in the gas feedstock. The major drawback to using the platinum-promoted catalyst is its high cost. It is our opinion that the conventional methanation catalysts are not suitable for operation at these conditions (1200°F and H_2S) and that further catalyst development in this area is needed.

6.2 DIRECT PRODUCTION OF METHANE

In the direct conversion of hydrocarbon feedstocks to methane, we have observed, in all cases, a decrease in both gas production and methane yield as the test continued.

This decrease was attributed to catalyst instability at the established operating conditions. We tried a number of different hydrocarbon feedstocks, except coal, and all our data have revealed the same results. A number of different catalysts were tried, and all showed that carbon deposition (Ni_3C) on the active surface deactivated the catalyst. We feel that the heart of this concept is the catalyst. Before successful operation on a continuous basis is achieved, a better catalyst system must be developed.

REFERENCES

1. Hoffman, E. J., Preprints, Div. of Pet. Chem., ACS, 16, No. 2, C20 (1971).

2. Hoffman, E. J., Cox, J. L., Hoffman, R. W., Roberts, J. A., and Willson, W. G., Preprints, Div. of Fuel Chem., 16, No. 2, 64-67 (1972).

3. Willson, W. G., Sealock, L. J., Jr., Hoodmaker, F. C., Hoffman, R. W., Cox, J. L., and Stinson, D. L., Preprints, Div. of Fuel Chem., 18, No. 2, 29-41, (1973).

4. Cox, J. L., Sealock, L. J., Jr., and Hoodmaker, F. C., Preprints, Div. of Fuel Chem., 19, No. 1, 64-77, (1974).

TABLE 1

FEEDSTOCK COMPOSITIONS

	Coal Tar	#2 Fuel Oil	Benzene	Anthracene Oil	Char
BTU	16,340	19,400	17,986	16,680	13,960
H	5.5	12.7	7.7	6.0	1.0
C	90.9	86.7	92.3	91.6	80.0
N	0.83	--	--	.54	--
S	0.7	.4	--	.5	.4
Ash	.29	--	--	.02	13.9

TABLE 2

% METHANE

Temperature, °F (One Atm)	1200	1200	1200	1200
Space Velocity	250	1000	250	1000
H_2S Volume, %			2	2
Catalyst				
Katalco 41-7				3
Katalco 11-3		13	6→2	
Houdry-Topsoe		13		
Harshaw Ni-0104T	20	20	20→5	20→4
Harshaw Ni-0104T + 6% Mo			8→4	
Harshaw Ni-0104T + 5% Th			8→5	
Harshaw Zn-0308T	ND	ND	ND	ND
Harshaw Cr-0103T	3%	ND	3	1
Harshaw Al-1602T + 14% Ni, 7% Mo			8	
Harshaw Al-1602T + 14% Ni, 7% Mo + 13% K_2CO_3			4	5
Harshaw Al-0104T + 7% Ni			7	
Harshaw Al-0104T + 5% Sn			ND	
Harshaw Al-0104T + 5% Pd	10→4		<1	
Harshaw Al-0104T + 5% Co + 5% Cs			10→0	
Harshaw Al-0104T + 15% Ni			5	
Harshaw Al-0104T + Ni, 6% Mo, 5% Ba			14→2	
Harshaw Al-0104T + 7% Ni*	17→12		19→3	
Harshaw Al-0104T + 7% Ni, 6% Mo, 5% Ba*			19→2	
Harshaw Al-0104T + WO_3			<1	
Harshaw Al-0104T + 5% Pt			12→10	
Engelhard RD 150 Pt			11	3
Engelhard RD 150 Pt + 5% Ba			8	
Catalysts and Chemicals Inc. C11-2-03			<1	<1
Catalysts and Chemicals Inc. C13-4-04			<1	<1
Union Carbide 13X + Ni			11→1	
Norton Zeolon + Ni			16→ND	
Norton Zeolon + Ni + Ba			18→3	
Norton SA-101 + Ni, Al Slurry	16→14		16→1	
Norton SA-101 + Na, Al Slurry + Mo + Ba			16→2	
Norton SA-101 + WO_3			<1	

*Added H_2S after bed had reached 1200°F
ND — None Detected

TABLE 3

SELECTED DATA SHEET

Test No.	Temp. (°F)	Pressure (PSIG)	Time Of Test (Hr)	Catalyst	Feedstock	Total Grams Of Carbon In	Product Gas Vol. (Cu Ft)	Wt. Of Methane (Grams)
1A	1200	1000	5.50	Norton SA-101	#2 Fuel Oil	290	4.38	50.40
B	1200	1000	4.50	Norton SA-101	Coal Tar	280	2.45	19.00
C	1200	1000	2.50	Norton SA-101	Benzene	172	.26	.50
D	1200	1000	3.00	Norton SA-101	Anthracene Oil	181	.88	6.97
2	1200	1000	4.75	Ni-0104T	Coal Tar	340	1.68	23.20
3	1200	1000	8.75	Norton SA-101-A	Coal Tar	170	1.56	23.90
5	1200	1000	11.50	Norton SA-101-B	#2 Fuel Oil	460	15.99	163.90
6	1200	1000	6.00	Norton SA-101-B	#2 Fuel Oil	583	9.94	91.40
9	1200	1000	10.00	Ni-3210T	Anthracene Oil	212	2.11	5.16
10	1200	500	2.00	RD-150 Pt	Anthracene Oil	254	1.83	6.46
11	1200	500	2.50	C11-2-03	Anthracene Oil	170	1.61	11.37
12	1200	500	2.00	Ni-3210T	Anthracene Oil	78	2.64	28.88
18	1200	1000	5.75	Ni-3210T	Char	80	2.17	17.26
20	1200	1000	4.60	IFT Ni + Ru	Char	80	1.28	3.54
21	1200	1000	5.00	Ni-3210T	Char	80	2.00	8.42

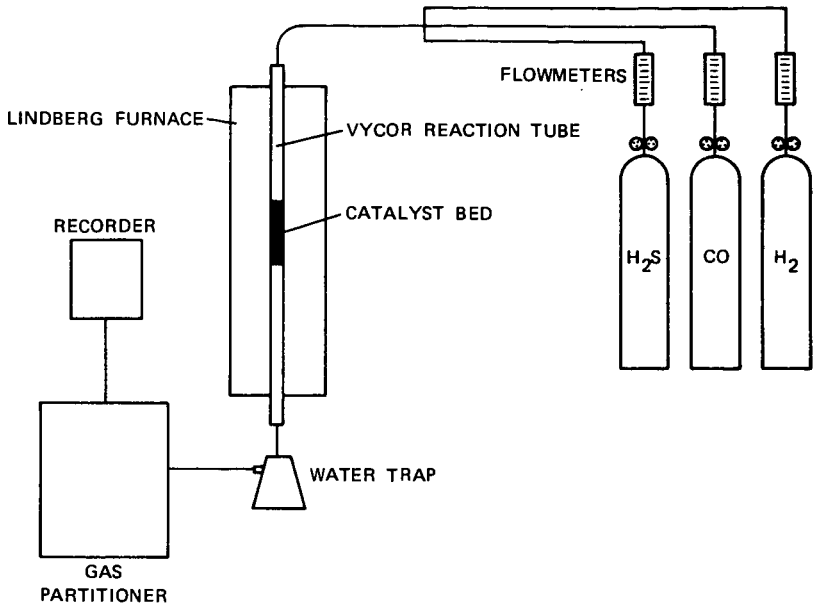

FIGURE 1 CATALYST TESTING APPARATUS

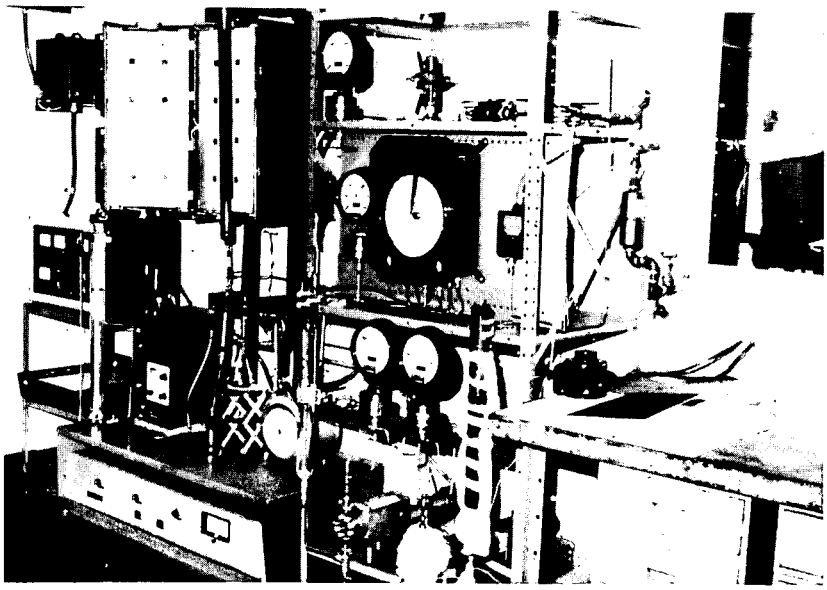

FIGURE 2 ADVANCED GASIFICATION APPARATUS

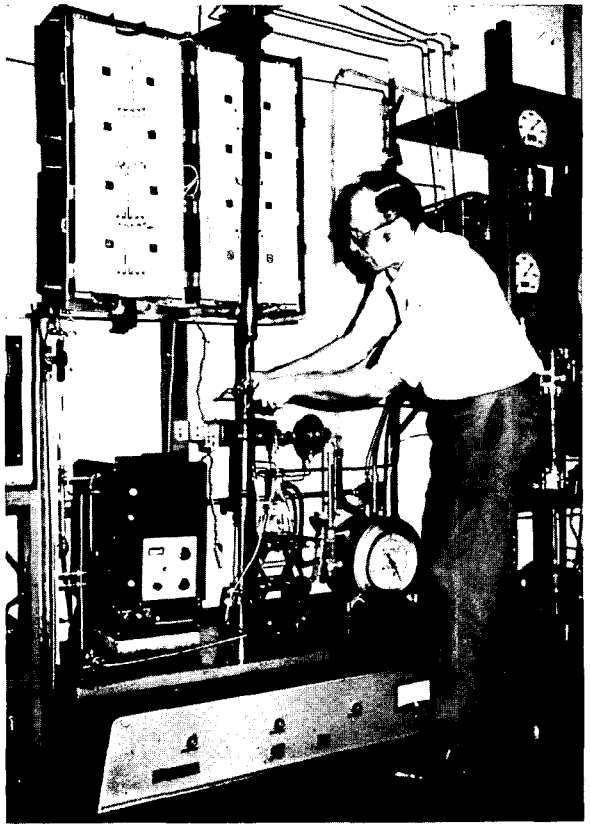

FIGURE 3 HIGH PRESSURE-HIGH TEMPERATURE REACTOR

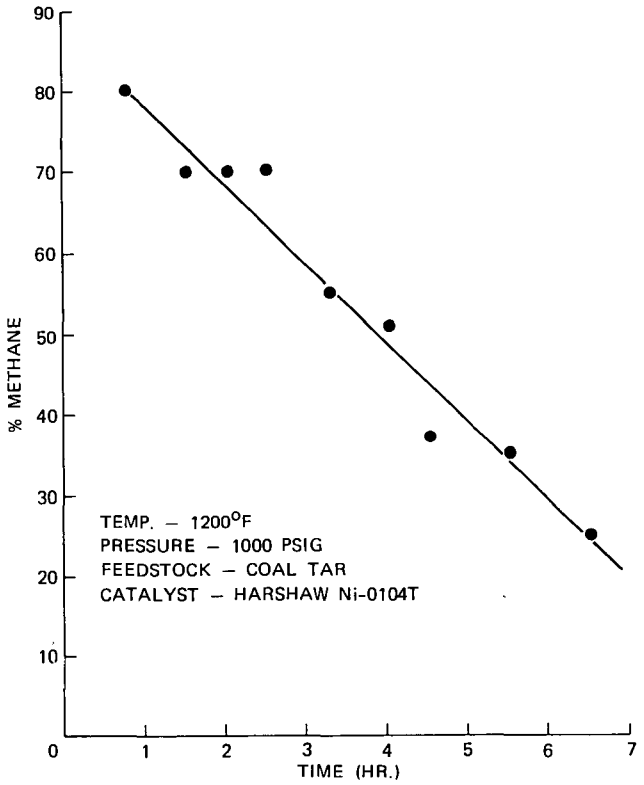

FIGURE 4 % METHANE VERSUS TIME

PRODUCTION OF HYDROGEN FROM GASIFIED COAL AND LASER FUSION ATOMIC ENERGY

Frederic H. Emery

Spectron Systems, 8003 Fairfax Road, Alexandria, Va. 22308

This paper is a presentation of the case for the immediate construction of a commercial size plant for the production of hydrogen from coal and nuclear energy. Hydrogen is the ideal source of energy for space heating and for electric power. Since hydrogen burns to water, power sources using this fuel will not pollute the atmosphere. There are important savings when energy is transmitted as hydrogen rather than as electric current. A standard cubic foot of hydrogen contains more energy than an equal volume of other gaseous fuels. The cost of transmitting hydrogen by pipe line will be low, in part due to the availability of instruments which can quickly detect infinitesimal amounts of leaking gas. It is possible to economically ship hydrogen by pipe line for at least a thousand miles.

Altho electricity can be transmitted over high voltage lines for about 500 miles, the energy losses in transmission are substantial. Hydrogen will also be preferred by environmentalists when compared to electric power. Hydrogen pipe lines will be underground, and farming operations can be carried out over them. On the other hand high voltage power lines are unsightly and cause many difficulties to families who live near them.

The ideal electric power supply will be a hydrogen air fuel cell system. (1) The D. C. power produced will be transmitted through sodium filled plastic tubes. These power conductors can be located underground. Since the electricity will be produced close to the electric power consumer, transmission line losses will be small. Replacing copper conductors with sodium conductors will result in substantial capital cost savings.

Hydrogen is now used to make ammonia and a cheaper source of hydrogen is necessary before it can be used to make electricity. The cooperative action of two sources of energy is necessary for the production of cheap hydrogen. These two sources are laser induced nuclear fusion and bituminous coal. The fusion energy plant design is to be based on a Lawrence Livermore laboratories 1000 megawatt power plant. (2) The coal energy plant design follows U.S. Steel's Clean-Char process. (3) Figure 1. Steam plus the clean fuel gas and clean char from U.S. Steel's process are the principal raw materials for the production of cheap hydrogen.

Photochemical energy for the endothermic carbon steam reaction is to be obtained from micro H bomb explosions. The radiant energy from the micro H bomb is to be absorbed by a steam fogged mixture of barium hydroxide and char as shown in Figure 2. The overall process equation is

$$BaO + C + 2\,H_2O \longrightarrow BaCO_3 + 2H_2. \qquad 1)$$

Equation 1) is similar to the CO_2 acceptor process (4), except that BaO is substituted for CaO. Using barium instead of calcium will allow complete absorption of the fusion energy. The reaction chamber will need to be large enough to absorb the x-rays produced by the micro H bomb gamma rays. In aqueous environments the principal end results of x-ray absorption is rupture of hydrogen oxygen bonds.

This photochemical process can be regarded as a first order reaction with resulting high efficiency and low cost.

As shown in Figure 3 the raw materials for the micro H bomb are deuterium, tritium and helium-3. Tritium and helium-3 can be recovered from the micro H bomb explosion out gases. Altho deuterium can be purchased it will probably be manufactured on site from river water and energy derived from burning coal. The by-product from the micro H bomb explosion is Helium-4. It can be separated from the explosion out gases by passage through an ultra centrifuge.

The cost of the hydrogen produced can be substantially reduced by the sale of by-products from U.S. Steel's Clean Char process. (3) A wide variety of by-products based on compounds derived from carbon, nitrogen or sulfur are available. There should be sufficient flexibility in the hydrogen manufacturing processes, so that the by-product mix can be varied to suit varying market conditions. Most probably the nitrogen and sulfur will go into fertilizers. Most carbon compounds will be used for fuel, but some of the hydrocarbon by-products may be upgraded and sold as raw materials for plastic production.

Substantial capital investments are necessary before heat and power can be enjoyed by consumers. Coal must be located, separated from the earth, processed and transported. Hydroelectric power also requires large investments for the production and transmission of electricity. Investments in hydroelectric power systems are considered by many, to be one of the best hedges against the inflationary erosion of the purchasing power of the dollar. Nuclear power plants are still more capital intensive that steam or hydro power plants, and also can be considered as inflation hedges.

TABLE 1 **CAPITAL COSTS**

1973 ESTIMATES; ELECTRIC POWER DELIVERED TO THE EASTERN SEABOARD

TYPE OF PLANT	DOLLARS PER KW OF POWER CAPABILITY
NO POLLUTION FUEL OIL PLANT	350
COAL FIRED PLANT	400
NO POLLUTION COAL FIRED PLANT	550
FISSION NUCLEAR PLANT	700
FUSION NUCLEAR PLANT	650

Environmental and pollution considerations importantly effect both the operating and capital costs of power plants. Table one shows that the addition of anti-pollution equipment to a coal fired electric power plant increases the capital cost by 37%. The capital costs of a fusion nuclear power plant are estimated to be slightly lower than those of a fission nuclear power plant. Capital costs for hydrogen production will run parallel to capital costs for power production. For hydrogen production, fusion energy should be cheaper than fission energy.

The input requirements of the plant shown in Figure 2 are Appalachian bituminous coal, pure water, and energy. Pure water and electricity are also required for the production of deuterium which is the principal raw material for the production of energy by atomic fusion. Pipe line hydrogen, as shown in Figure 2, is the final product of the hydrogen production process.

In the ultimate ideal situation everyone will heat his house with pipe line hydrogen, or with electricity locally generated from hydrogen. This ideal cheap fuel abundance has been called a hydrogen fuel economy. The plant investment necessary to fuel the furnaces of American with hydrogen is enormous. It will probably take 25 years to find enough money to build the plant and mining facilities necessary for the United States hydrogen fuel economy. The first commercial hydrogen plants will be forced to find markets for their product which will be more lucrative than the space heating which is required by the hydrogen economy. Examples of such markets are production of:

a. methanol for manufacture of lead free high octane gasolene
b. hydrazine for peak power, pollution free, electric fuel cells
c. methane for upgrading 500 BTU coal gas into 1000 BTU SNG
d. sulfur free fuel oils for pollution free electric plants.

All nations who have the necessary technical capabilities are diligently working on the problem of initiating nuclear fusion by concentrating intense energy from lasers. The aim is to ignite a tiny pellet of hydrogen like material so that a micro H bomb explosion will result. If the expenditure of billions of dollars guarantees success, the United States should be the winner in the world wide atomic fusion sweepstakes.

Fusion ignition energy requirements are very large. A high temperature, high pressure laser should be capable of generating the required power levels. It ought to have an efficiency of 50% and be of the Excimer type. Its output should be in a wavelength area between 2000 and 10000 Angstroms. It is probable that the successful laser will operate in the midrange or at a wavelength of approximately 300 nanometers. The output of the laser should be 10^{12} watts, and the length of the output pulse should be 10 picoseconds. Even with an output of this magnitude, it will be necessary to hit the deuterium pellet with an array of lasers fired simultaneously.

Figure 4 is a schematic diagram of a laser proposed for fusion initiation. Energy is injected into the lasing tube by a traverse electron avalanche. The power flash of the laser breaks the output mirror, thus allowing the high power pulse to leave the lasing tube.

The micro H bomb explosions will occur at 25 or less pulses per second. After each explosion a new aluminum mirror on thin plastic sheet will be positioned over the exit port. The distance between the two lasing mirrors is then adjusted by varying the gas pressure on the upper mirror sheet until correct focus is obtained. Coherent light from the laser is concentrated onto the pellet by fused silica lenses. These lenses are maintained in a vacuum by the shot chamber vacuum system. The second or lower mirror in the lasing tube is figured in a blank which can be water cooled. The optics of the lower mirro are designed to minimize damage to the mirror, and to work with the coherent light concentrating optics.

Hydrogen can be produced by the proposed photochemical process for much less than the cost of electrolytic hydrogen. In addition the break even point for gamma and neutron ray hydrogen production is an order of magnitude better than the fusion electric power break even point.

The construction of a full size AEC approved deuterium pellet factory should be initiated at once. Concurrently contracts for model production and testing of TEA UHP lasers should be let. Hydrogen plant site preparation should be included in the contract to be placed for the construction of a U.S. Steel Clean-Char coal gasification plant. In the near future, UHP lasers will be commercially available. It would then be possible to proceed without delay with the construction and operation of a laser fusion hydrogen plant.

Now is the time to proceed with the commercial production of hydrogen from gasified coal and laser fusion atomic energy. The demonstration hydrogen plant must be built close to coal deposits. Also it must be situated on the banks of a river which will supply large volumes of soft water for all 12 months of every year of the projected life of the plant.

REFERENCES

(1) Chem. & Eng. News 52 Fuel Cell Research Finally Paying Off, page 31, Jan. 7, 1974.

(2) Nuckolls, Emmett, Wood, Physics Today, 26, page 47, Aug. 1973.

(3) Chem. & Eng. News 52 Processes Lower Sulfur Content of Coal, page 28, April 8, 1974.

(4) Chem. & Eng. News. Energy: The Squeeze Begins, page 33, Nov. 13, 1972.

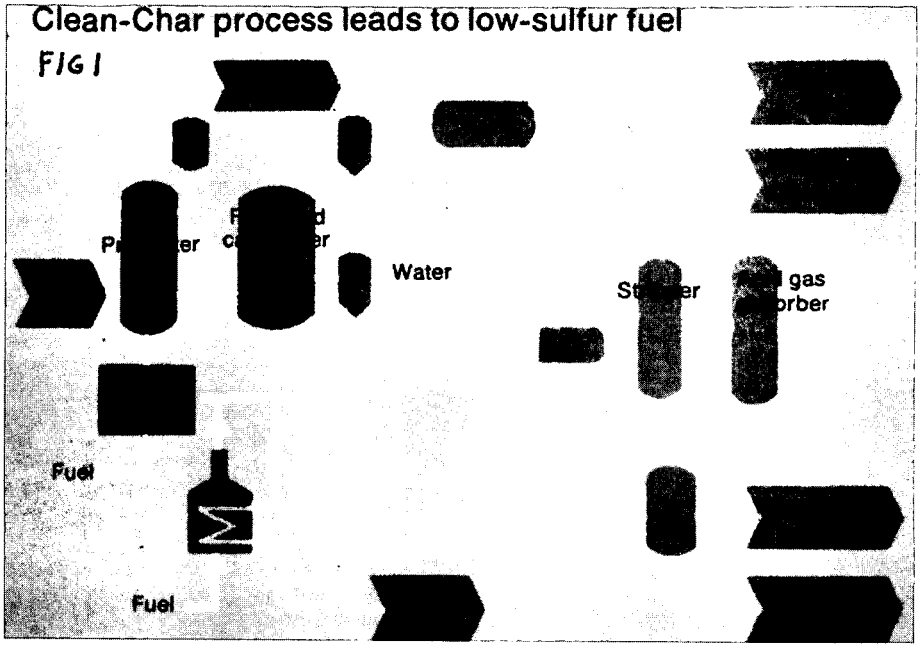
Clean-Char process leads to low-sulfur fuel
FIG 1
Water
Fuel
Fuel

FIG 2

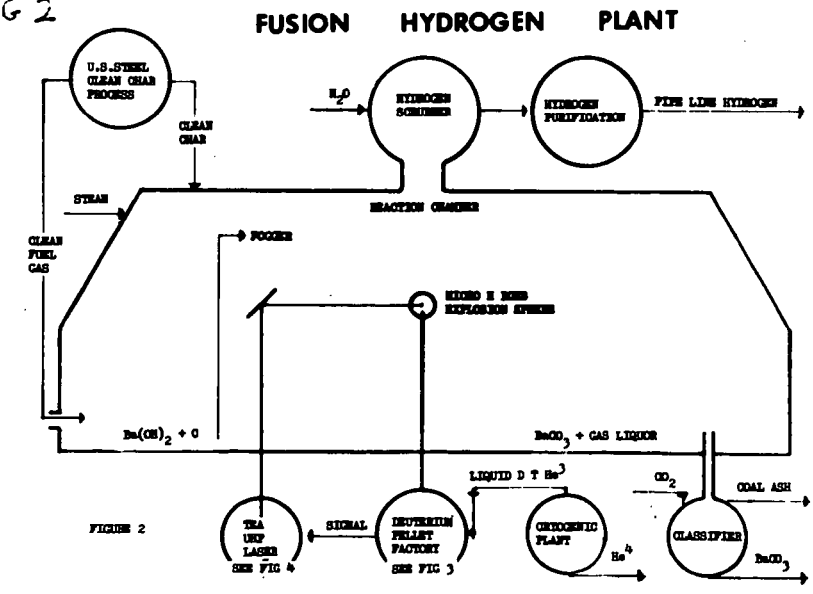
FUSION HYDROGEN PLANT
U.S.STEEL CLEAN CHAR PROCESS
CLEAN CHAR
STEAM
CLEAN FUEL GAS
REACTION CHAMBER
FOCUS
LIQUID D T He3
SIGNAL
He4
CO2
COAL ASH
FIGURE 2

FIG 3

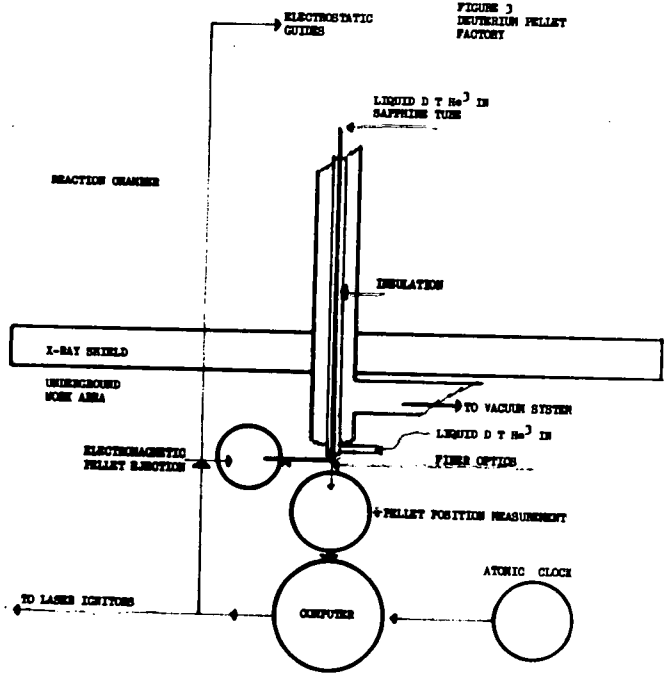

FIGURE 3
DEUTERIUM PELLET FACTORY

FIG 4

TRAVERSE ELECTRON AVALANCHE
ULTRA HIGH POWER
EXCIMER LASER

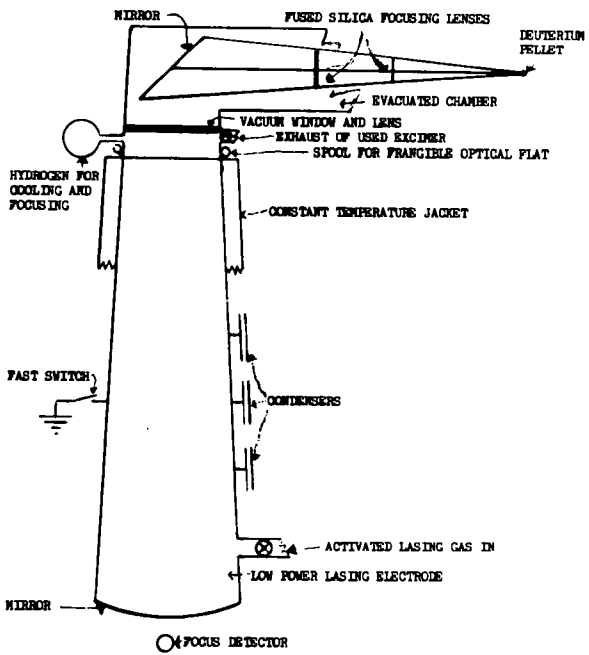

Emissions from Domestic Heating Oil Combustion

B. J. Kraus and J. F. Coburn

Exxon Research and Engineering Company
Linden, New Jersey

INTRODUCTION

During the last ten years, in which the protection of the environment and especially our air has become a major national concern, the automobile has received most attention. As federal controls limiting the emissions from the automobile have been legislated and gone into force, and federal ambient air quality standards were adopted, the diesel engine and large stationary steam generators have also come control by virtue of federal law. All combustion processes are potential sources of air pollution and all of the major fuel consuming units except one are now covered by federal emissions regulations. The one exception is the residential heating unit. Since a substantial share of all petroleum is consumed in residential use particularly in the winter, we felt it important to study this potential source of air pollutants. Previous work reported in the literature (1-7) studied effects of equipment design and operating conditions. Our own interest in this study was to look at the effect of fuel composition on emissions. This paper summarizes the more important results of this study.

EXPERIMENTAL

The pollutants measured in this study can be divided into gaseous emissions, smoke and particulates, and polynuclear aromatic hydrocarbons. Among the gaseous emissions direct measurements were made of carbon monoxide, total hydrocarbons, and nitrogen oxides. Carbon monoxide was measured with a non-dispersive infrared analyzer which on its most sensitive setting was calibrated to read in the range of 0-250 parts per million (ppm). Total hydrocarbons (HC) were measured by flame ionization. Both the analyzer and the sampling lines were heated to keep the sample temperature at no less than 270°F (135°C) to minimize losses of the higher boiling hydrocarbons. The most sensitive range of the analyzer was 0-10 ppm HC as methane. Nitrogen oxides (NO_x) were measured with a chemiluminescence analyzer. The most sensitive range of the analyzer was 0-2.5 ppm.

A parameter of long standing in the heating oil business to characterize combustion is smokiness. The Bacharach smoke spot measurement is the universally used technique for measuring the degree of smokiness. This technique was used in this study to measure smoke at steady state conditions. For continuous measurement of smoke, the Von Brand smoke meter was used. This latter is particularly useful for measuring the smoke during burner startup and shutdown. In both techniques, a sample of the flue gas is pulled through a filter paper and the resulting smoke spot or trace can be compared to a standard scale going from zero smoke to a number 9 smoke.

Mass particulate emissions were measured using the EPA technique specified for stationary sources for which emissions regulations exist. An isokinetic sample of flue gas is drawn from the breech of the furnace through a heated probe and then a filter is used to catch the solids contained in the measured volume of sample gas. The quantity of particulates trapped on the filter is determined gravimetrically.

No standardized method for sampling polynuclear aromatic hydrocarbons (PNA's) exists at present. Our approach has been to withdraw continuously a

flue gas sample from the furnace breech under isokinetic flow conditions. Isokinetic sampling is used since PNA's may be adsorbed on the particulates contained in the flue gas. The sample probe is not heated except by the flue gas itself. The sampled flue gas passes directly from the probe into a series of four glass impingers (See Figure 1). The impingers are immersed in an ice bath and serve to condense as well as trap the PNA's. By the time the flue gas leaves the last impinger its temperature is about 35°F. A small pore size (~0.2μm) filter follows the impinger train to trap any particulates that may be carried through the impinger train. The filter is maintained at about 50°F by the chilled flue gas sample. The sample recovery consists of collecting the condensate from the impinger train, the filter itself, and the acetone wash of the probe, impingers and filter housing. PNA's and other organics are extracted from these three separate parts of the sample using cyclohexane. Analysis of PNA's is done by a combined gas chromatography - UV absorption technique. PNA's are separated into individual fractions on a GC column, and each fraction is analyzed by UV absorption to determine the quantity of the specific PNA contained in the fraction. To account for sample handling and analysis losses C^{14} tagged benzo(a)pyrene and benz(a)anthracene are added to the three parts of the sample before extraction. PNA losses during the analytical procedure are determined from the measured loss of the two radioactive trace components. A detailed description of the analytical procedure is given elsewhere (8).

To determine burner operating conditions, additional measurements were made for CO_2, oxygen, flue draft, flue gas temperature, and fuel flow. Flue gas volumes were calculated from measurement of fuel flow and excess air assuming complete combustion of fuel. Actually measured flue gas flows differed from such calculated flows by no more than 3%. The unit on which the measurements were made was a commercially available hot air furnace with a maximum heat input of 119,000 BTU/hr. The furnace was fired with a conventional high pressure gun burner at a nominal firing rate of 0.75 GPH.

RESULTS AND DISCUSSION

Gaseous Emissions

Figure 2 shows CO emissions as a function of equivalence ratio (E.R.). The equivalence ratio is the ratio of actual air to that required for stoichiometric combustion of the fuel. An E.R. of 1.6 which is typical for field installations, is equivalent to the use of 60% excess air. Results are shown for three fuels differing in gravity, aromatics, and final boiling point. The typical fuel is the only one classified as a No. 2 fuel oil, with the kerosene having a much higher API gravity and the low gravity fuel being too low in gravity. The emissions furthermore are given for two operating conditions, at steady state and for a 5 minute burn - 5 minute off cycle. The results for cyclic operation are time-averaged from the point at which the burner starts to a point 30 seconds after shutdown. The latter is included since the CO emissions tend to be higher immediately after burner shutdown. The CO emissions under steady state conditions are very low even during the relatively fuel rich and smoky operation that is obtained at equivalence ratios lower than 1.4. In fact in the normal operating range to be found in the field (1.5 to 2.0 E.R.), the carbon monoxide in the flue gas is at a lower concentration than in the laboratory combustion air. Even under cyclic operation the CO is low when 40% or more excess air is used. In terms of fuel effects, the high gravity, low final boiling point kerosene gives somewhat lower CO emissions, particularly as less excess air is used. From our point of view it was not considered important to investigate the causes for the observed behavior since under normal operating conditions the CO emissions were low with all three. Differences between fuels occurred under burning conditions which would not normally be used because of smoke limitations.

Figure 3 shows emissions of total hydrocarbons for the same conditions and fuels as previously given for CO. The concentration of hydrocarbons in the flue gas like that for CO is very low, usually less than that contained in the laboratory combustion air except during a short period after startup and after shutdown. Unlike the behavior of CO, under cyclic conditions the hydrocarbons increased at very high excess air levels. As the air velocity tended to become very high, ignition became erratic and in the extreme case the flame would alternately extinguish and reignite for a few seconds at the beginning of the burning cycle. As is clear from Figure 3, there is no effect of fuel composition on hydrocarbon emissions.

Both at steady state and under cyclic conditions, the nitrogen oxide emissions were relatively insensitive to either equivalence ratio or fuel composition. At steady state, emissions averaged about 80 ppm. For the five minute on-five minute off cycle, time-averaged emissions were about 70 ppm.

Smoke and Particulate Emissions

A number of states and localities in the U. S. have laws on the maximum allowable smoke in the flue gas. Smoke behaves much like CO and hydrocarbons in that there is a peaking of the smoke as the burner starts up. As combustion proceeds and the temperature in the combustion zone rises, the smoke decreases. Immediately upon burner shutdown, the smoke in the flue gas again increases to a peak and then drops off to zero as the furnace is swept by ambient air. Startups and shutdowns are not very repeatable in terms of smoke emissions even with the same fuel. The effect of fuel composition on smoke is therefore more clearly seen at steady state operation. Figure 4 shows the Bacharach smoke number as a function of equivalence ratio for four different fuels. It is clear from the figure that there is a difference in smoke number from the four fuels when operating at higher than trace smoke conditions, i.e. less than 70% excess air. A cross plot of smoke number, at for example 50% excess air, against final boiling point shows an excellent linear correlation (Figure 5). Direct substitution of fuels with differing backend volatility could therefore affect the smokiness of combustion. On the other hand these results also illustrate that smoke-free combustion is possible even with fuels having final boiling points substantially higher than found in present No. 2 heating oils, if the excess air is adjusted for the fuel.

As far as domestic heating units are concerned, the smoke number is the only way by which particulate emissions are being characterized. As has been mentioned there do exist federal regulations on mass particulate emissions for very large capacity steam generators. To determine compliance with the regulations, the EPA prescribed a technique to be used for measuring mass particulate emissions. Results of the particulate measurements are given in Figure 6.

Most particulate measurements in our study were made by the EPA procedure. In a limited number of tests, flue gas was sampled in a diluted stream and some measurements were made with a multistage impactor. These measurements are also included in Figure 6. The results shown are for the same fuels for which smoke numbers were given. In addition the figure contains emissions at steady state and for the usual 5 minute on - 5 minute off cycle. Mass particulate emissions are given as a function of smoke number. Most of the measurements were made with a typical heating oil. There is a correlation of particulate emissions with smoke which is quite pronounced at the higher smoke numbers. For operating conditions typical in the field, trace to about a number 4 smoke, the emissions at trace smoke can be just as high as at number 5. Published results of particulate emissions from a field survey of domestic oil heated units also showed no correlation of smoke number with mass particulate emissions (6). The smoke number therefore is influenced not only by mass particle loading of the flue gas but also by the nature of the particles and the particle size distribution. Variations of particulate emissions with operating conditions, i.e. cyclic vs. steady

state, and with different fuels are at a level which is less than the repeatability of the measuring procedure. Unless the smoke becomes very high, mass particle emissions from the gun burner are in the range of 1 to 2 lbs. per 1000 gallons of fuel even with substantial changes in fuel and operating conditions.

Polynuclear Aromatic Hydrocarbons

In the years since polynuclear aromatic hydrocarbons have been identified in the atmosphere, a great many studies of emissions from various sources have been reported in the literature (9). In recent times such studies have concentrated on the automobile engine. Though considerable experience has been accumulated in the experimental approaches to PNA collection one important problem still remains to be solved. That problem is the loss of PNA species during sampling. Although these compounds are easily condensed, they are relatively volatile and easily oxidized. In those parts of the sampling system which are at significantly higher than room temperature the chance for loss is very great. Attempts to quantify such losses in PNA measurements from automobiles (10) by injection of radioactive species into the gas stream sampled, have indicated that under certain conditions, substantially more than half of the reactive PNA's may be lost during sampling. Yet the techniques used to estimate losses raise nearly as many questions as are answered. Our approach to estimate losses consisted of doping the sampling train, exclusive of the probe itself, with known quantities of non-radioactive benzo(a)pyrene and benz(a)-anthracene and then making a normal sampling run. The level of doping was twenty to fifty times the amount of BaP and BaA normally collected in a run. The recoveries measured were 57% for BaP and 46% for BaA. For these two very reactive components perhaps only half of the quantity of each constituent is recovered by the sampling system. As was mentioned previously, losses during the analytical procedure itself were routinely accounted for. In the discussion to follow PNA results reported are those actually measured. They are not corrected for the possible sampling loss described above. Three different types of fuels were run and analyzed for PNA in the fuel and in the flue gas. Results of emissions and fuel aromatic content are shown in Table 1.

TABLE 1

PNA EMISSIONS FROM HEATING OILS
(Lbs./1000 Gals.) x 10^5

	Kerosene		Typical		Low Gravity	
	Fuel	Flue Gas	Fuel	Flue Gas	Fuel	Flue Gas
Pyrene	550	0.8	19,900	6.2	5,700	6.5
Benzo(a)pyrene	12	0.2	190	0.6	124	1.2
Benz(a)anthracene	29	0.04	1,380	0.2	6,340	1.7
Chrysene	110	0.1	3,700	0.2	24,200	0.4
Triphenylene	66	0.2	2,300	0.6	10,100	1.0
Fuel Aromatics - %	13.2		37.1		46.1	

The analytical technique used was able to identify eleven species of PNA's. Results however are reported only for those five species which were consistently found in measurable quantities. In PNA studies from automobiles it had been reported that exhaust emissions were dependent on the aromatic content of the fuel (11-13). As Table 1 shows the three fuels had a big range in aromatic components as well as in fuel PNA content. Looking at benzo(a)pyrene, the differences in emissions between the three fuels are not statistically significant (standard deviation = 0.66), so that the effect of the very large change in aromatic content of the fuel influences the emissions at least of this component to a relatively small extent. As far as BaA is concerned the change in aromatics and PNA content in going from the kerosene to the typical heating oil did not produce a statistically different emission result. Increasing the BaA content of the fuel still further, i.e. moving from the typical to the low gravity fuel, with a relatively small additional increase in aromatics did show a significant increase in BaA emissions though the level is

still quite low. This points to fuel PNA content as influencing emissions more strongly than fuel aromatics. To look at the influence of fuel PNA content, the typical heating oil was doped with pure BaP and BaA without significantly changing other properties.

TABLE 2

EMISSIONS FROM TYPICAL HEATING OIL
(Lbs./1000 Gals.) x 10^5

	As Is		Doped 1		Doped 2	
	Fuel	Flue Gas	Fuel	Flue Gas	Fuel	Flue Gas
Benzo(a)pyrene	190	0.6	1,210	3.6	3,230	4.2
Benz(a)anthracene	1,380	0.2	2,420	0.6	4,800	0.4

The results of the BaP make it clear that increasing the fuel BaP content does increase the level of BaP found in the exhaust. Exhaust BaA on the other hand appears to be less sensitive to BaA level in the fuel. In order to see if significant generation of PNA's occurs in the combustion system the typical heating oil was doped with high boiling aromatics from still bottoms. These heavy fractions contained both PNA's as well as aromatic species in the range of C_{10} to C_{16}.

TABLE 3

EMISSIONS FROM TYPICAL FUEL DOPED WITH HEAVY AROMATICS
(Lbs./1000 Gals.) x 10^5

	Fuel	Flue Gas
Pyrene	47,400	9.4
Benzo(a)pyrene	3,440	<4.5
Benz(a)anthracene	3,700	0.3
Chrysene	5,380	0.3
Triphenylene	4,130	0.9

The results for BaP and BaA are comparable to those of the typical heating oil doped with pure BaA and BaP. The presence of so-called precursors for PNA formation did not show increases in PNA emissions that would not be expected simply from the PNA content of the doped fuel. Regressing the emissions results of the "typical" fuel against the PNA content of the fuel in the normal as well as various doped conditions, allows one, if only approximately, to extrapolate to a zero PNA content. The emissions at this zero intercept should be those which are synthesized in burning that fuel (37% aromatic content). Although these data are scattered, they indicate that even with high aromatics content in the fuel, PNA formation is not significant (about equivalent to that shown from kerosene or less than 0.5×10^{-5} lbs./1000 gals.) and PNA's found in the flue gas are those which survive from the fuel.

Survival of fuel PNA's is very low as shown below.

TABLE 4

RATIO OF FLUE GAS PNA TO FUEL PNA

Pyrene	0.02 - 0.05%
Benzo(a)pyrene	0.1 - 0.3%
Benz(a)anthracene	0.03%
Chrysene	0.002%
Triphenylene	0.01 - 0.02%

These numbers first show that PNA's contained in the fuel are most effectively

destroyed. This is not unexpected in view of the low emissions of hydrocarbons and CO. Secondly, these numbers would permit reasonable estimates of the magnitude of PNA emissions from heating oil combustion if the fuel PNA content is available.

CONCLUSIONS

From the results obtained in this study, a number of conclusions regarding emissions from the domestic high pressure gun burners are evident. First, in the range of practical operating conditions there is no significant effect of fuel composition on the emissions of carbon monoxide, total hydrocarbons, nitrogen oxides, and mass particulates. Second, at a given excess air level an increase in the final boiling point of fuel leads to higher smoke. However, with sufficient excess air, even fuels with very high final boiling points can be burnt essentially smoke free. Third, emissions of polynuclear aromatic hydrocarbons appear to be primarily dependent on the PNA content of the fuel. It is unlikely, however, that differences in exhaust PNA's are measurable over the range of PNA's found in No. 2 fuels in the field.

REFERENCES

(1) Hooper, M. H., "Effects of Combustion Improving Devices on Air Pollution Emissions from Residential Oil-Fired Furnaces", Proceedings of New and Improved Oil Burner Equipment Workshop, National Oil Fuel Institute, September 17-18, 1968.

(2) Wasser, J. H., "Effects of Combustion Gas Residence Time on Air Pollutant Emissions from an Oil-Fired Test Furnace", Ibid.

(3) Howekamp, D. P. and Hooper, M. H., "Effects of Combustion Improving Devices on Air Pollutant Emissions from Residential Oil-Fired Furnaces", Proceedings of New and Improved Oil Burner Equipment Workshop, National Oil Fuel Institute, September 24-25, 1969.

(4) Brema, A., and Lee, W. B., "Use of Staged Air Admission to Reduce Emissions in Combustion of Hydrocarbon Fuels", Proceedings of New and Improved Oil Burner Equipment Workshop, National Oil Fuel Institute, September 23-24, 1970.

(5) Blair, Martin, G., "Use of Fuel Additives and Combustion Improving Devices to Reduce Air Pollution Emissions from Domestic Oil Furnaces", Ibid.

(6) Levy, A., et al., "A Field Investigation of Emissions from Fuel Oil Combustion for Space Heating", API Publication 4099, November 1, 1971.

(7) Barret, R. E., et al., "Field Investigation of Emissions from Combustion Equipment for Space Heating", EPA Report (PB-223148), June 1973.

(8) Gross, G. P., "Gasoline Composition and Vehicle Exhaust Gas Polynuclear Aromatic Content", First Annual Report, CRC-APRAC Project No. CAPE-6-68, December 9, 1970.

(9) "Particulate Polycyclic Organic Matter", National Academy of Sciences, Committee on Biologic Effects of Atmospheric Pollutants, Division of Medical Sciences, National Research Council, Washington, D. C., 1972.

(10) Griffing, M. E., et al., "Applying a New Method for Measuring Benzo(a)Pyrene in Vehicle Exhaust to the Study of Fuel Factors", Papers of Div. of Petroleum Chem., ACS National Meeting, Los Angeles, March 1971.

(11) Begeman, C. R., "Carcinogenic Aromatic Hydrocarbons in Automobile Effluents" Paper 440C presented at SAE Automotive Engineering Compress, Detroit, January, 1962.

(12) Hoffman, C. S., et al., "Polynuclear Aromatic Hydrocarbon Emissions from Vehicles" Div. of Petroleum Chemistry of the ACS, Volume 16, No. 2.

(13) Newhall, H. K., et al, "The Effect of Unleaded Fuel Composition on Polynuclear Aromatic Hydrocarbon Emissions", SAE Paper No. 730834, September, 1973.

FIGURE 1
PNA SAMPLING SYSTEM

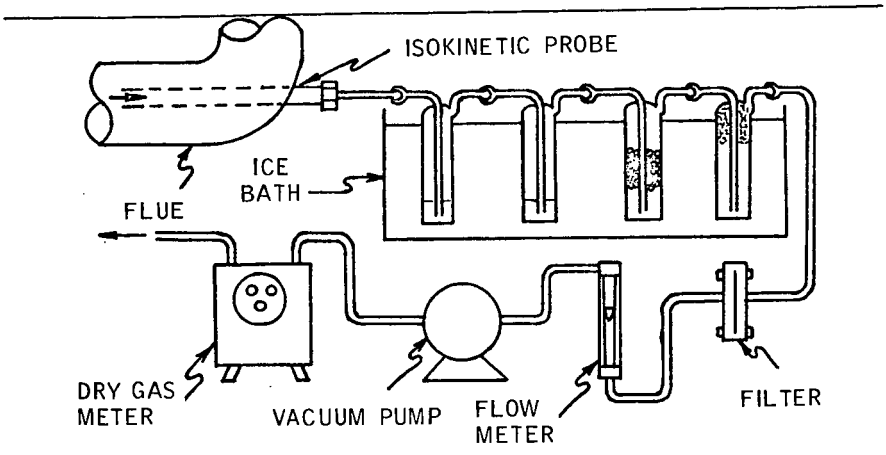

FIGURE 2
CARBON MONOXIDE EMISSIONS

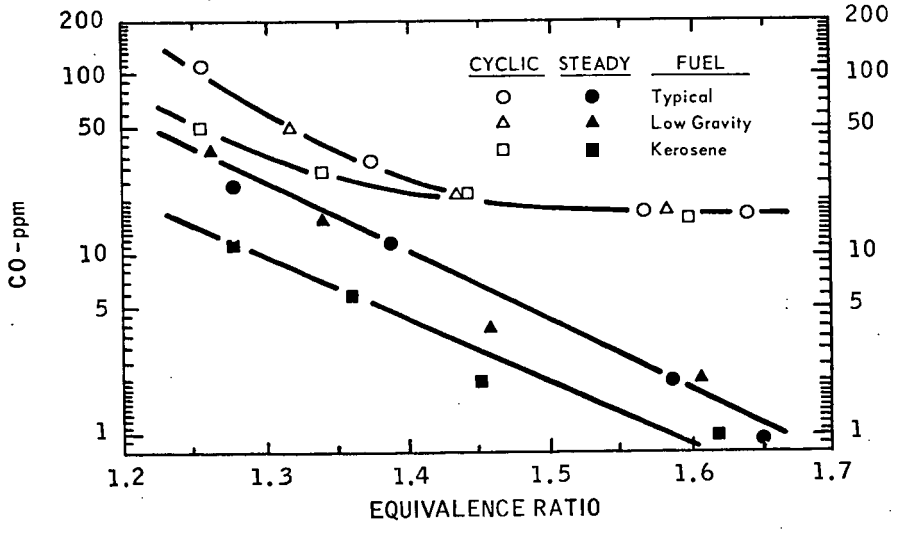

FIGURE 3
HYDROCARBON EMISSIONS

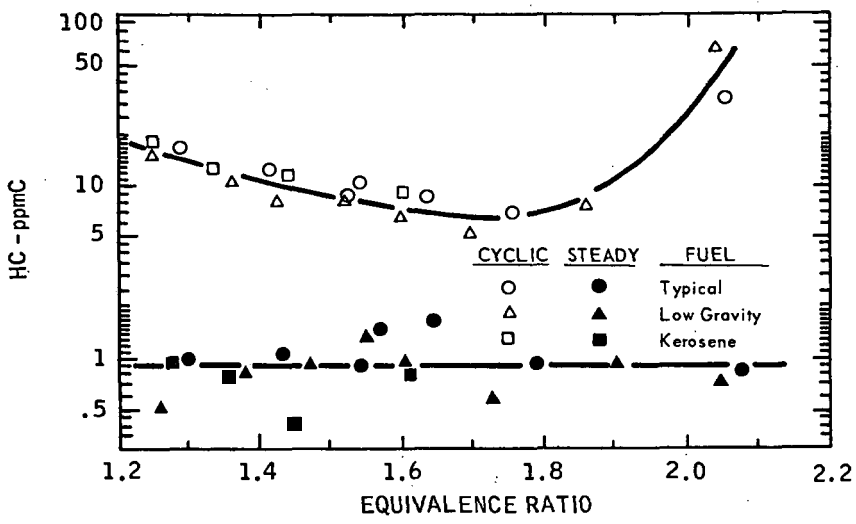

FIGURE 4
FUEL EFFECT ON SMOKE NUMBER

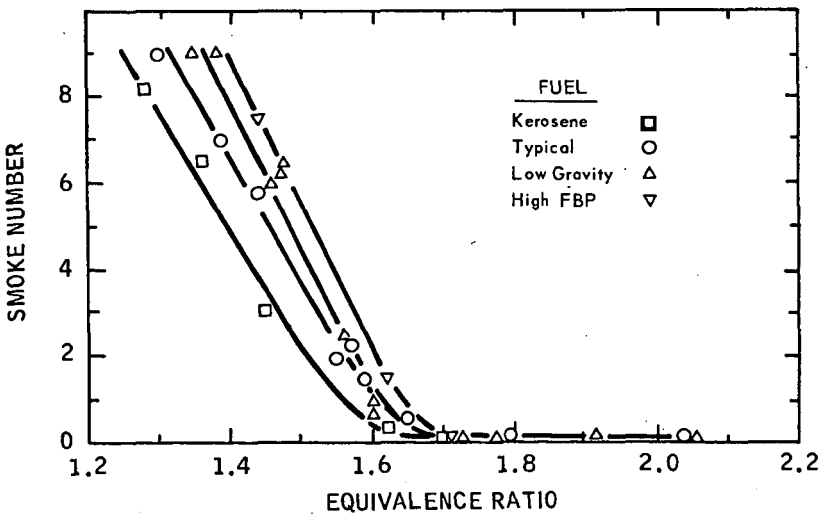

FIGURE 5

INFLUENCE OF FINAL BOILING POINT OF FUEL ON SMOKE

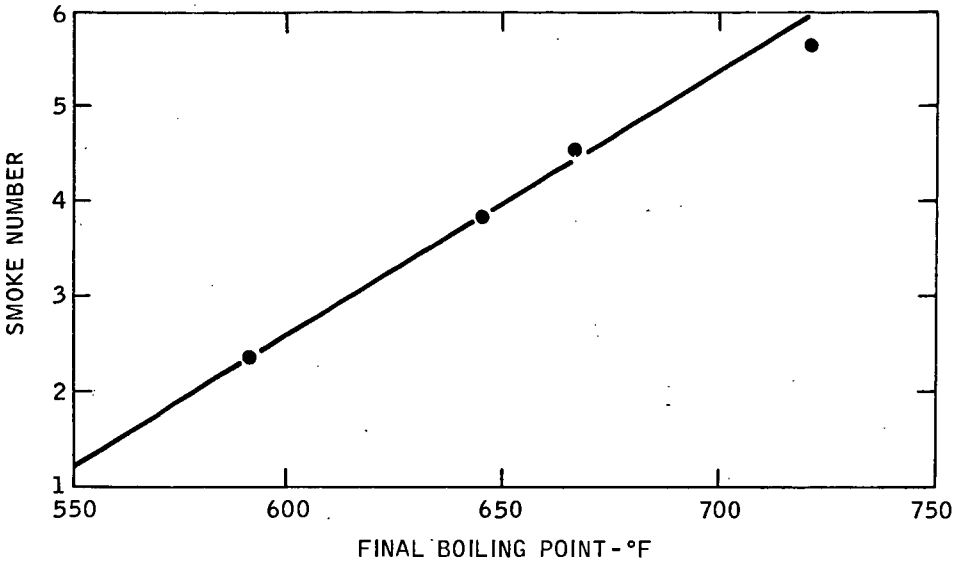

FIGURE 6

PARTICULATE EMISSIONS

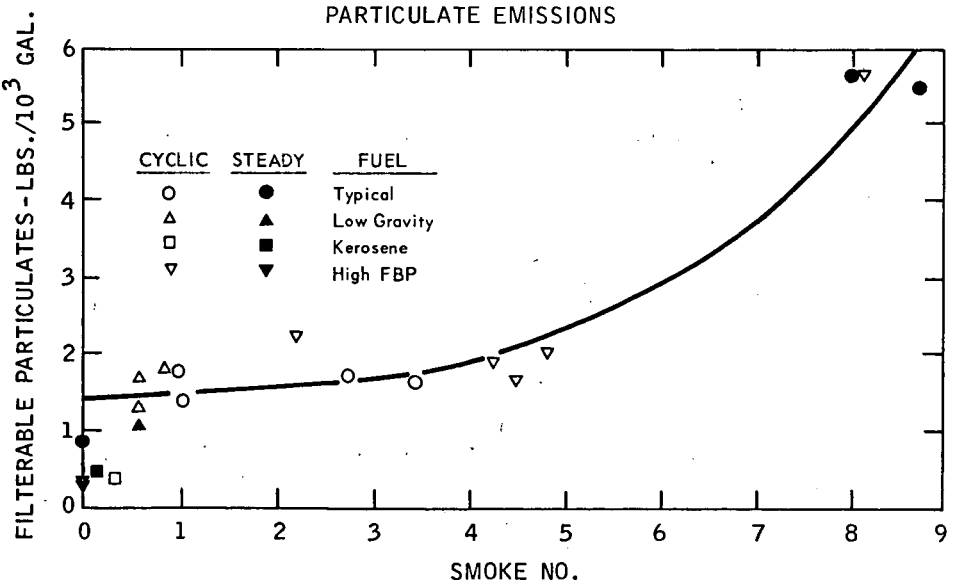

DEVELOPMENT OF A COMPACT, HIGH-CAPACITY FeS_2 ELECTRODE

Hiroshi Shimotake and William J. Walsh

Argonne National Laboratory
9700 South Cass Avenue
Argonne, Illinois
60439

Introduction

High-specific-energy Li-Al/FeS_2 cells are being developed at Argonne National Laboratory (ANL) for off-peak energy storage batteries in electric-utility networks.[1] Similar cells, but with higher specific power, are also being developed at ANL for electric automobile batteries. The cells have a molten-salt electrolyte such as the LiCl-KCl eutectic (mp, 352°C) and operate at temperatures between 375 and 450°C. These cells have been found[2] to be superior to earlier lithium/sulfur cells, in which elemental lithium and sulfur were the active materials. The Li-Al/FeS_2 cells have exhibited stable performance without significant decreases in capacity upon cell cycling and without severe corrosion problems. Engineering-scale Li-Al/FeS_2 cells (150 A-hr capacity) for the energy-storage application have been described.[3] These cells have achieved specific energies of 140 W-hr/kg at the 10-hr rate and cell lifetimes have exceeded 1800 hr.

This paper describes the design and development of the compact, high-performance FeS_2 electrode used in the more recent of the engineering-scale cells. Also discussed is the operation of laboratory-scale cells and the methods used to achieve dimensional control of the FeS_2 electrode. The information gained in the laboratory studies was used for the design of the larger-scale cells. With the improvements in the FeS_2 electrode, significant advances have been made in achieving stable cell capacity with cycling, improving the utilization of the cell reactants, and achieving dimensional stability of the sulfide electrode.

Laboratory-Scale Experiments

Four laboratory-scale cells were operated; the cells were of the design shown in Fig. 1. The positive (FeS_2) electrodes were about 5.7 cm in diameter and had capacities of 12-13 A-hr. The electrode consisted of a bed of finely divided FeS_2 powder encased in a thin layer of zirconia cloth to contain particulates; this structure was, in turn, encased in a basket of molybdenum mesh to provide structural support. The negative electrode was a solid Li-Al alloy that had been electrochemically formed on a substrate of porous aluminum using a method developed at this laboratory.[4]

Iron disulfide power (reagent grade) was purified before use to remove a silicate impurity; this was accomplished by a flotation technique using tetrabromomethane (density, 3.42). The resulting FeS_2 powder was dried and sieved to select a particle size distribution between 80 and 150 μm. This particle

size was chosen to avoid (1) the dimensional instability that would result from the use of a very fine powder (<50 μm) and (2) the decrease in surface area and, hence, a decrease in FeS_2 utilization that would result from the use of a particle size larger than 150 μm.

Several materials were tested for use as current collectors, including Armco iron, nickel, and molybdenum. In test cells, both Armco iron and nickel reacted with the sulfide and eventually were severely corroded. Molybdenum showed no reaction with the cell environment and provided long cell lifetimes. The design of the engineering-scale electrode, therefore, included current collectors of molybdenum. It is believed that a current collector of a more common material can be plated with a thin layer of molybdenum to provide the necessary protection from corrosion. Such a procedure would significantly reduce the cost of the current collectors.

Figure 2 shows typical cell voltage patterns during discharge (lower curves) and charge cycles (upper curves); the two stable voltage plateaus are characteristic of this system. These data were taken for a cell having a molybdenum current collector in the FeS_2 electrode after about 50 hr (Cycle 5) and 200 hr (Cycle 25) of operation. No decrease in capacity with cell cycling was observed; utilization of the cell reactants was about 90%. Because the coulombic efficiency was high (>95%) and the cell resistance was low, energy efficiencies between 60 and 80% were achieved.

Another example of the stability of cell capacity cycling can be seen in Fig. 3. In this cell, a capacity greater than 75% of the theoretical was maintained over a period of 200 hr, at which time the cell operation was voluntarily terminated. In a cell that was operated for 500 hr, a capacity density of 0.43 A-hr/cm^2 (90% of theoretical) was achieved, and no decline in capacity occurred over the entire operating period. The energy efficiency was maintained above 70%.

Design of Engineering-Scale FeS_2 Electrode

The design of the positive electrode developed for the engineering-scale cells is shown in Fig. 4; this electrode has a diameter of 12 cm and a capacity of 150 A-hr. The design was selected to minimize the weight required for current collectors and to maximize the utilization of the FeS_2 reactant. The current collector consisted of five layers of lightweight molybdenum expanded mesh (5-mil thickness) which were cut into circular shape, and joined to a center terminal post with a silver-solder brazing.

The current collector was encased in a thin layer of zirconia cloth to retain the finely divided FeS_2 powder (150 μm); the zirconia cloth was, in turn, encased in a lightweight (∿90 g) molybdenum expanded mesh basket for a structural backing. This basket consisted of two halves which were sewn together with a molybdenum wire (5 mil). The FeS_2 (∿170 g) was poured into the electrode structure through a small opening.

During loading of the FeS_2, the electrode was vibrated to provide a uniform distribution of FeS_2 within the structure and the desired degree of compactness. Thus, the resulting electrode structure contained a porous bed of FeS_2 with sufficient space allowed for the expansion of the cell reactant and the addition of the necessary amount of electrolyte. (This technique was developed during the course of the laboratory experiments.) Finally, the entire basket structure was enclosed in a boron nitride fabric (not shown in Fig. 4), which served as a separator. With this design, the total weight of the sulfide electrode was only 280 g (total cell weight, ∿1200 g).

It is believed that the weight of the electrode can be reduced even further by eliminating the zirconia cloth and molybdenum basket; however, a more suitable form of boron nitride fabric is needed for the electrode separator before this can be accomplished. The boron nitride fabric must be of the proper porosity to retain the finely divided FeS_2 and yet allow sufficient passage of electrolyte; the fabric must also have sufficient strength to give good mechanical backing to the electrode.

Conclusions

The experimental results obtained with the compact FeS_2 electrode have been highly promising. With compact design, engineering-scale FeS_2 electrodes have been constructed with theoretical capacities per unit volume of >1 A-hr/cm^3. We believe that a Li-Al/FeS_2 with this type of positive electrode is capable of achieving a specific energy of ∿180 W-hr/kg. This value exceeds the specific-energy goal for a single cell that has been set in our program to develop a battery for bulk storage of electric energy.

Acknowledgements

The authors gratefully acknowledge the major contribution by Dr. J. E. Battles and Dr. K. M. Myles in examination of materials. Thanks are also extended to J. A. Allen and L. G. Bartholme for preparing the FeS_2 material and cell components, and G. M. Kesser for the editorial assistance on this paper.

This work was conducted under the auspices of the United States Atomic Energy Commission.

References

1. P. A. Nelson *et al.*, "High Performance Batteries for Off-Peak Energy Storage, Progress Report for the Period January 1973-June 1973," USAEC Report ANL-8038, Argonne National Laboratory (March 1974).

2. D. R. Vissers *et al.*, "A Preliminary Investigation of High-Temperature Lithium/Iron Sulfide Secondary Cells," J. Electrochem. Soc. *121*, 665 (May 1974).

3. W. J. Walsh *et al.*, "Development of Prototype Lithium/Sulfur Cells for Application to Load-Leveling Devices in Electric Utilities," IECEC Meeting, San Francisco, California (August 1974).

4. N. P. Yao *et al.*, "Solid Lithium-Aluminum Alloy Electrode in High Temperature Secondary Cells," Abstracts, 144th Meeting of the Electrochemical Society, Boston, Mass. (October 1973).

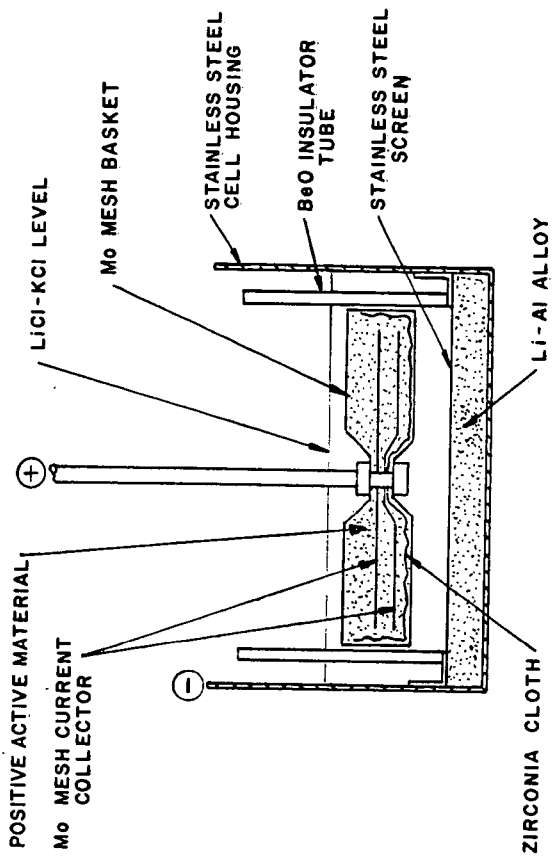

Fig. 1. Laboratory-Scale Li-Al/FeS_2 Cell

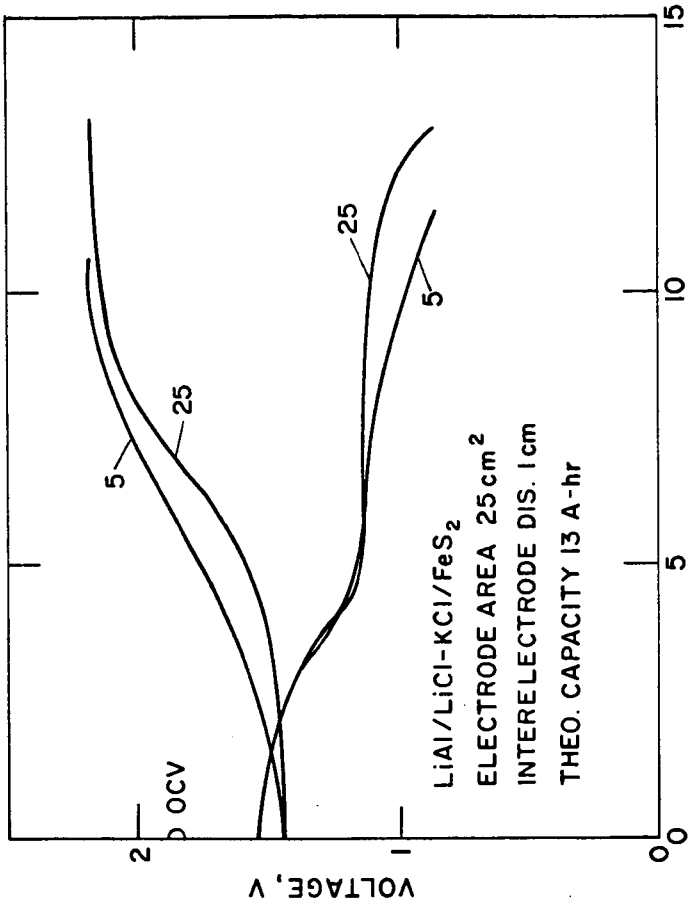

Fig. 2. Typical Measurements of Voltage *vs.* Capacity in Laboratory-Scale LiAl/FeS_2 Cells

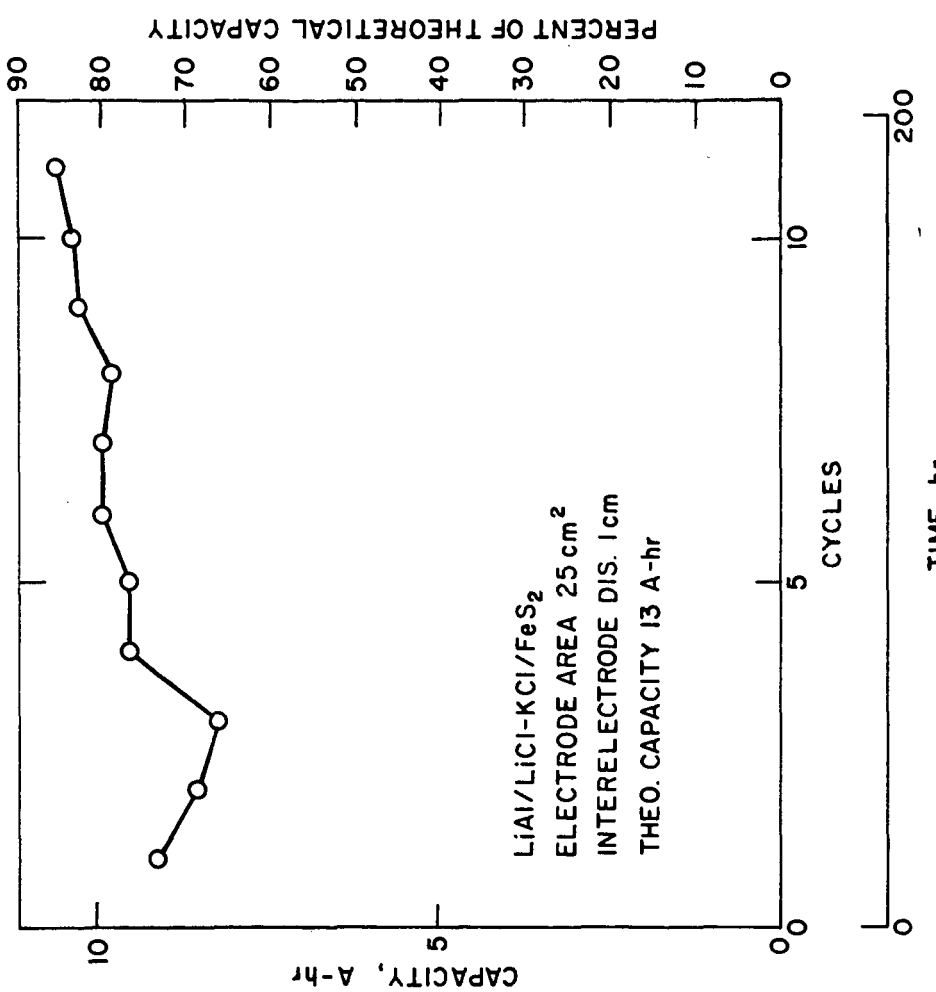

Fig. 3. Capacity of Li-Al/FeS_2 Laboratory-Scale Cell as a Function of Operating Time

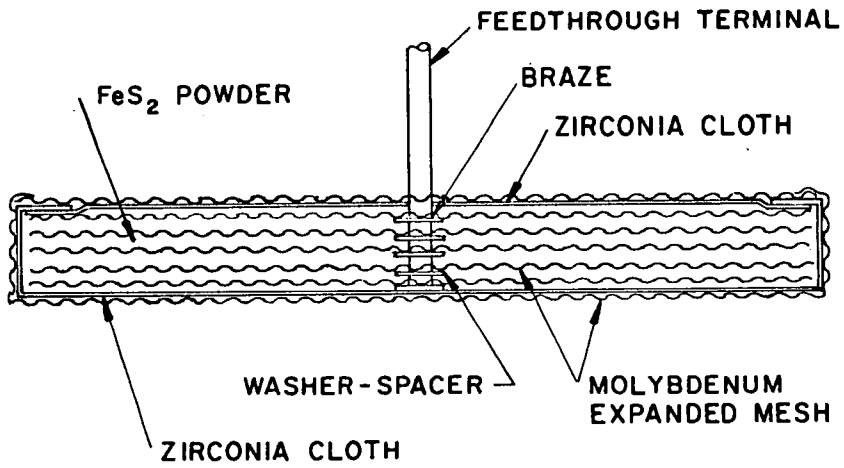

Fig. 4. Design of Engineering-Scale FeS_2 Electrodes

PURIFICATION OF WASTE WATER FROM COKING AND COAL GASIFICATION PLANTS USING ACTIVATED CARBON

Harald JÜNTGEN and Jürgen KLEIN

Bergbau-Forschung GmbH, Essen (W.-Germany)

I. Introduction

Under environmental aspects the purification of waste water containing organic substances becomes more and more important. It is known that the conventional processes, especially biological techniques, are not able to remove all organic compounds out of the wastes. These resistant compounds inhibit, especially if they are toxic, the biological process of cleaning. So they accumulate in the effluent water causing a pollution increase of our streams, lakes, and seas.

In recent times different methods are discussed to solve this problem, e.g. reverse osmosis, precipitation by special agents, the burning of high concentrated wastes, and the adsorption on suitable adsorbents.

Under the industrial wastes the phenolics from coking and other coal-using plants are most undesirable. They contain some compounds in such a high concentration that they are particularly noxious. The concentration range of some compounds contained in waste water from coking plants is listed in table I. Depending on the special kind of treatment systems of coke oven gas there are two or three types of waste water: the condensate, the ammoniacal liquor, and the decanter waste water. We consider now only the condensate and the waste water after the ammonia decanter. Fig. 1 shows a simplified scheme of a treatment system of coke oven gas. The water coming from the tar separator is called condensate, and after decanting the uncombined ammonia decanter waste water.

The main methods to clean this waste water are:

- extraction by benzene or isopropylether
- biological treatment
- adsorption on activated carbon

One of these techniques, the adsorption, is indicated in fig. 1 as a possible step of waste treatment to get clean water.

The extraction needs further steps of purification because the removal of organic carbon by this process reaches only about 55 %.

The biological treatment is loaded with many difficulties.

Some of them will be discussed herein short. As table II shows there are some compounds, e.g. benzene, naphthalene, anthracene, HCN, that cause a high value of TOC or COD, but the BOD-value is zero, that means these compounds are not decomposable by microbes. Thereby differences can be caused in the valuation of the grade of purification. Up to now in the BRD the quality of effluents are often measured by BOD- and COD_{Mn}-values. But as to be seen in table II a low BOD-value of a

treated waste is no guaranty for sufficiently cleaned water. On the other side many of the inorganic salts or ions cause a high COD_{Mn}-value, that cannot be reduced by biological decomposition.

Moreover, the operation of a biotreatment plant is very complicated. Particular conditions are to be adhered to, to enable a high efficiency of the purification process. The limiting values of some contraries to the three main decomposing compounds of coking plant effluents are set out in table III. It shows that these compounds exercise a strong influence of the decomposition of each other.

The adsorption on activated carbon nowadays often used in advanced treatment systems for reclamation of drinking water can help to solve the problems of purification of high concentrated industrial effluents like phenolic wastes. In the following it shall be pointed out, which parameters lead to the design of an adsorption plant and how it works.

II. Determination of design parameters

The use of activated carbon for industrial wastes postulates special characteristics of the carbon and the process of adsorption and reactivation. The carbon must have a high internal surface area per unit volume and special adsorption affinity to the waste water compounds, furthermore, from the economic point of view an extreme hardness and low reactivity of the carbon is important to make its reactivation and reuse possible. The design of the adsorption unit and the operation of the adsorption process must allow the best use of the adsorption capacity of the carbon to minimize the cycling amount of activated carbon. The reactivation of the charged carbon has to be performed at such carefully controlled conditions that the adsorption capacity of the carbon is fully regained and the carbon loss is at a minimum. Bergbau-Forschung has developed a process of waste water treatment by activated carbon that combines these requirements. To determine the design parameters of such an integrated adsorption/reactivation plant we use a serie of tests that will be discussed now in brief.

II.1 Adsorption isotherms

Knowing the waste water analysis and the desired quality of the effluent, adsorption isotherms would be run on various representative samples to determine the feasibility of using activated carbon to remove the organics from this waste and to find the most suitable carbon as well as its grain size for the sorbable components. This test consists of contacting a fixed quantity of waste with varying amounts of carbon for a given time. The amount of organic removal at the varying dosages is determined by TOC-measurement and gives an indication of the amount of carbon required to treat this particular waste.

II.2 Column test

With the knowledge of kind and grain size of activated carbon the next test is to be run. The waste water at a constant but in several runs varying flow-rate passes through a carbon column of a suitable length and diameter which depends on the used grain size. By measuring the concentration of sorbable compounds in several heights of layer as a function of time or throughput the so-called curve of breakthrough can be achieved by equation 1.

$$\frac{c}{c_o} = f\ (\text{time}) \qquad 1)$$

Using the mass-transfer-zone concept it is possible to determine from these curves the essential parameters for design as it is shown in the scheme of fig. 2. At first the velocity of the mass-transfer-zone between the layer heights H_1 and H_2 has to be determined by equation 2.

$$v_F = \frac{H_2 - H_1}{t_{H_2} - t_{H_1}} \qquad 2)$$

In the continuous process v_F is equivalent to the velocity of activated carbon $\dot{V}_C$ circulating the adsorption/reactivation plant, calculated by equation 3.

$$\dot{V}_C = v_F \cdot A \qquad A = \text{sectional adsorber area} \qquad 3)$$

The width of the mass-transfer-zone H_{MTZ}, given by equation 4,

$$H_{MTZ} = v_F \cdot (t_2 - t_1) \qquad 4)$$

depends on the slope of the breakthrough curve and gives the minimum height of the adsorption layer. In the ideal case v_F and H_{MTZ} are independent from the position of layer, and constant during the process of adsorption. A very important factor is the achieved adsorbate loading of the carbon layer, calculated by equation 5.

$$Q(t) = \frac{\dot{V}_w(t)}{M_C} \int_o^t (c_o - c)\, dt \qquad 5)$$

$\dot{V}_w(t)$ = mass flow of waste water

M_C = carbon amount in adsorber

The higher the loading, the less carbon is required per unit volume of waste and consequently the less is the consumption of energy and carbon loss during reactivation.

To have an idea of the adsorption tests some isotherms are shown in fig. 3. The upper diagram on the left hand side shows isotherms of three types of activated carbon treated with the same waste. The slope of the curves and the values of charge indicate which of the three carbons are the most suitable ones for cleaning the special waste. To get the specific adsorption capacity per unit volume the values of adsorbate loading are to be multiplied by the bulk density of the carbon. The lower diagram shows isotherms of three different types of coking plant effluents treated with the same activated carbon. As to be seen the isotherms differ remarkably due to the different kind and content of compounds. On the right hand side in the upper diagram two adsorption isotherms are shown. They are determined by treatment of one carbon with condensate (curve 1) and decanter waste (curve 2) of the coking plant Kamp-Lintfort. Here the higher TOC-content causes a higher value of charging. In the lower diagram two curves are shown which are calculated from the breakthrough curves of pilot column tests. Although the TOC-contents of the wastes are equal to those from the curves in the upper diagram, the achieved values of charge on the same carbon are different. The effect can be explained by the different conditions of lab-scale test and pilot column test. In the lab test the isotherms are got at decreasing concentration, in the column test the carbon is treated at quasi-constant concentrations. As we have found out for different types of wastes with a complex mixture of compounds, differing in adsorption affinity to the carbon, in the first phase of adsorption

a higher loading is achieved at decreasing concentration. Lateron it might happen that the higher concentration in the column test causes a higher adsorbate loading, but often the active centers of the carbon are blocked so that no increase in charge is possible.

Fig. 4 shows representative breakthrough curves measured in pilot column tests with decanter waste of a TOC-content of 1000 mg/l at a flow-rate of 10 m/h. The steep slope of the curves is brought about by the fast kinetics of adsorption standing out for the main compounds of the waste. Furthermore, the curves are parallel to each other showing a constant velocity of the mass-transfer-zone. Steep and parallel curves indicate a small zone of mass-transfer, that means the required height of carbon layer is low.

II.3 Regeneration test

Is the adsorption in general well understood, the thermal regeneration of the loaded carbon, although of great importance, has been not sufficiently investigated till now. Our investigations show that there are two steps: first the desorption of reversibly bonded compounds and second the reactivation with steam or similar gases to destroy those compounds that are irreversibly bonded or decomposed on the internal surface of the carbon during the heating phase. With a special arrangement of thermal-balance, gaschromatograph and mass-spectrometer, we have investigated the desorption process. Thereby it is not only possible to identify the adsorbed substances, we get also information about the quantity of desorbed products and the possibility of recovering valuable by-products from the waste. Furthermore, it can be checked in which position of the adsorber unit the single components of the waste are adsorbed. Fig. 5 shows desorption curves of compounds out of different wastes. The curves in the lower diagram are gained from carbons loaded in decanter waste water with a TOC-content of 1000 mg/l, taken from a position of the column near the water inlet. The main substances are phenol, cresol, naphthalene and SO_2 from decomposition of sulphorous compounds. Is the carbon charged in the condensate after the tar separator the main substances are as shown in the upper diagram: phenol, cresol, naphthalene, but additional dimethylphenol and hydrocarbons C_3 and C_8.

Fig. 6 shows desorption curves from carbon samples in different positions of a column treated with decanter waste. The carbon of the adsorber outlet is mainly charged with phenol and sulphorous compounds. In the middle of the column also cresol is adsorbed, and in the first layer of carbon at the column inlet naphthalene is predominantly adsorbed. From this experiments one can get a concentration profile of adsorbed substances over the length of the carbon column, as shown in fig. 7.

The simultaneous processes of desorption and reactivation are studied in lab-scale fluidized bed which was operated batchwise. With this set-up the conditions for the regeneration of loaded carbons are experimentally determined. After the column test the charged carbon is regenerated in this fluidized bed by varying temperature, residence time, and partial pressure of steam or other reactive gases. By measuring the adsorption activity and the carbon loss of the reactivated carbon the conditions for regeneration are optimized. These data and the amount of circulating carbon lead to the design of the reactivation unit.

III. Pilot plant

With the data obtained in the above described tests it is possible, on principle, to design an integrated adsorption/reactivation plant. But for commercial purposes it is necessary to run tests for some time with a pilot column at the waste producing plant, because the operational wastes can strongly change in amount and concentration due to the rhythm of production.

Bergbau-Forschung, as a research institute of the mining companies of Western Germany, has investigated with priority the waste water from coking plants. A pilot adsorption plant with a maximum throughput of 300 l/h was in operation for two years, and some of the results shall now be pointed out. The flow scheme of the pilot adsorption plant is shown in fig. 8. A side stream of decanter waste water is pumped to a water receiver through a prefilter, to remove the mechanical impurities. From this the waste water flows from bottom to top through the adsorption columns. The discharge of the adsorbent can take place through a special outlet mechanism during operation. The filling-up of the carbon is carried out hydraulically by water from the receiver. The flow-rate through the adsorber was changed between 1 and 20 m/h. To have the possibility of measuring the breakthrough of the mass-transfer-zone in different heights the carbon column has a length of 5 m and the TOC-content as a function of layer height was continuously recorded. The typical curves of breakthrough, measured in this pilot columns, are already shown in fig. 4. To get a sufficiently cleaned water the TOC-measurement in the layer height of 2.50 m was taken as setting-means for carbon discharge. A reaching of breakthrough of 95 % input-concentration at this position led to the discharge of this completely loaded carbon layer during operation, and the filling-up of the 2.50 m column with fresh resp. reactivated carbon.

Fig. 9 presents the data of TOC-removal over an operation time of 10 months. As to be seen the input TOC ranges between 800 and 1900 mg/l, the output between 80 and 250 mg/l. It was possible to show that the output TOC was caused by cyanides and thiocyanates. The loaded carbon was reactivated in a reactivation pilot plant on the Bergbau-Forschung area. From fig. 9 it can be seen that in the ten months of operation the whole adsorber filling was reactivated 29 times.

A more detailed information gives fig. 10. Here the TOC and BOD-content is plotted against the operation time. As to be seen the removal of COD is different from that of TOC. The percentage removal ranges for TOC between 90 and 95 % and for BOD between 82 and 99 %. For these tests we used different activated carbon with the same grain size of 2 mm and different flow rates to determine their influence on the important parameters like width, H_{MTZ}, and velocity, v_F, of the mass-transfer-zone, and the loading of the used carbon. In fig. 11 H_{MTZ} is plotted as a function of flow rate and bulk density. Within the range from 340 to 500 g/l bulk density has no remarkable influence, but a change in the flow rate from 5 to 20 m/h doubles the value of H_{MTZ}.

In a similar way the velocity of the mass-transfer-zone v_F is influenced by bulk density and flow rate as shown in fig. 12. The achievable charge of the carbon does not appreciably depend on bulk density, flow rate, and concentration as shown in fig. 13.

The success of reactivation is shown in fig. 14. It was possible to operate at such conditions that the adsorption activity, set forth for loading and H_{MTZ}, could always be regained for any number of adsorption/reactivation cycles. For the operation costs the knowledge of the carbon loss is very important. Fig. 15 shows that after a first period of different conditions in the reactivation unit the carbon loss got into its stride of 2 to 2.5 %. During the two years of pilot plant operation we got the average values of removal of the main impurities of the waste listed in table IV.

Impurities	Content (mg/l)	Removal (%)
phenols	650 - 1400	> 99
cyanide	5 - 35	45 - 70
thiocyanate	120 - 450	30 - 80
iron	40 - 150	30
solids	300 - 3000	> 99
TOC	800 - 2000	85 - 95
COD_{Mn}	2000 - 4000	80 - 99

Table IV: Content of main impurities in decanter waste and its removal by adsorption

IV. Demonstration plant

The good results of pilot plant operation gave rise to plan a demonstration plant with a throughput of 25 m^3/h, that is the effluent of a medium sized coking plant. Table V gives the essential design data obtained from pilot plant results. Fig. 16 shows a scheme of the projected plant. From a tank 1 the waste water is pumped through a two-stage prefilter, then uniformly distributed by a suitable system over the cross section of the adsorber flowing from the bottom to the top where it leaves the adsorber sufficiently cleaned. The distribution system allows also a plane parallel discharge of the charged activated carbon. With an air-lift pump 5 the carbon is transported up to a dewatering screen 6 and then dosed with a feeding-screw 9 into the reactivation unit 10. The reactivated carbon is completely wetted in the quench tank 11 and then fed back into the adsorber. The detail engineering of this plant has begun, and we hope that it will be under construction by the end of the year.

waste amount	25	m^3/h
average TOC-content	1000	mg/l
flow rate	10	m/h
activated carbon: bulk density	450	g/l
grain size	2,0	mm
TOC-removal	95	%
adsorbate loading	70	kg C/m^3
circulating carbon	0.3	m^3/h
carbon loss	0.14	kg/m^3 waste

Table V: Design data for the demonstration plant

V. Waste water from gasification plants

Due to the rising demand of energy, coal gasification has become urgent. Also in the BRD investigations are made to develop new technologies of gasification. As carbonization is the first step of the gasification process it is obvious that the compounds contained in the produced waste water are similar to those contained in coking plant effluents. Lab tests with waste water from a semitechnical gasification plant which operates at 40 atm and temperatures of about 900 °C to gasify 5 kg coal per hour with steam in a fluidized bed, have shown that the removal of the organic impurities by adsorption on activated carbon is possible. At a TOC-content of 700 mg/l the achieved adsorbate loading on the carbon AW2-450 is even higher than that of the same carbon treated with decanter waste. As we found the calculated values of width and velocity of the mass-transfer-zone are in the same magnitude as those determined with decanter waste. To get design parameters for commercial plants we plan pilot column tests at a gasification pilot plant which is under construction and will have an throughput of 200 kg coal per hour, resp. a waste production of about 0.5 m^3/h.

VI. Conclusion

In the investigations described in this paper it was the aim to optimize the adsorption and regeneration step in order to achieve a high adsorption efficiency and a low carbon loss. By integrated operation of the adsorption in a moving bed and the regeneration in a fluidized bed it is possible to purify coking plants effluents sufficiently, and regenerate the loaded carbon at a carbon loss less than 3 %, restoring the adsorption capacity simultaneously. These promising results have led to the design of a demonstration plant for purification of 25 m^3/h decanter waste.

Compared with the conventional waste water treatment systems the following advantages of an integrated adsorption/reactivation system have to be pointed out

1. removal of organic contamination to minimal concentrations
2. no additional disposal or pollutional problems are created
3. adaptability to changes in quality and amount of the effluent in a wide range by change in amount of carbon circulating the adsorp-

tion/regeneration plant

4. regeneration of the carbon allows its reuse for many cycles
5. a very small floor space required.

These advantages result in the fact that adsorption on activated carbon is a suitable process for the purification of concentrated industrial wastes.

Table I: Composition of waste water from coking plants

compounds	condensate (mg/l)	ammoniacal liquor (mg/l)	decanter waste water (mg/l)
NH_3 (total)	6000 - 8000	8500 - 15000	20 - 4500
NH_3 (uncombined)	2000 - 6000	8000 - 12000	20 - 1000
CO_2	2400 - 3900	3000 - 14000	-
H_2S	300 - 900	1000 - 5000	2 - 50
HCN	55	200 - 2000	0 - 20
HCNS	50	700 - 1200	0 - 800
phenols	700 - 3200	2000 - 3000	50 - 2500
pyridinebases	200 - 500	100 - 200	-
fix. acids		3400 - 5600	20 - 600
pH-value	8,0 - 9,0	9,0 - 9,5	5,0 - 11,5

Table II: Characterising values of compounds from coking plant effluents

compound in solution (100 mg/l)	TOC (mg/l)	COD_{Mn} (mg/l)	BOD_5 (mg/l)
NaCl	0	3,3	-
NH_4Cl	0	9,1	-
Na_2CO_3	11,3	1,8	-
NH_4SCN	15,8	64	-
H_2S	0	190	187
HCN	70,5	0,2	0
phenol	76,6	238	178
o-cresol	77,7	173	164
m-cresol	77,7	172	170
pyridine	75,7	0,6	115
benzene	92,5	0,8	0
naphthalene	93,6	23,4	0
anthracene	94,5	16,2	0
Cl-ion	0	5,5	-
SCN-ion	20,7	77,6	-
SO_3-ion	0	19,7	-

Table III: Limiting values for biological treatment of coking plant effluents

temperature: 25 - 35 °C
pH-value: 6,5 - 8,0
phenol-content: < 500 mg/l

compounds to decompose	contraries	limiting values (mg/l)
phenols	ammonium	1700
	thiocyanate	250
	sulphide	25
	metal-ions	5
thiocyanate	ammoniumchloride	1000
	thiosulphate	100
	phenols	25
	metal-ions	5
ammonia	phenols	50
	thiocyanate	10
	cyanide	10

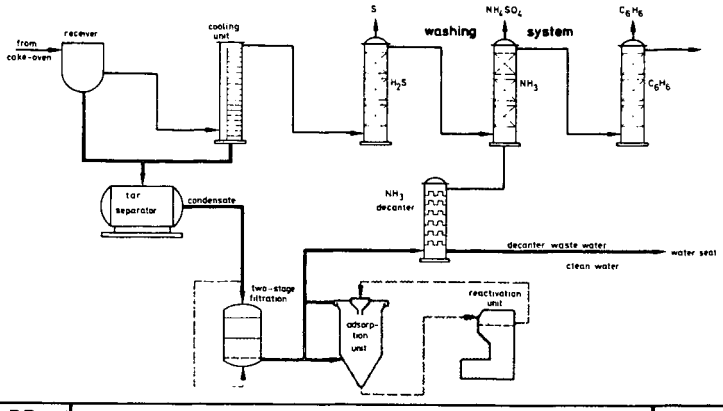

BF 1974	Fig. 1: Treatment system of coke oven gas - simplified scheme -	5179

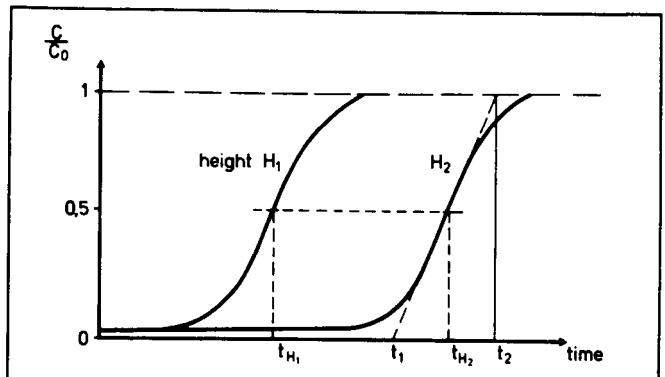

(1) $\frac{C}{C_0} = F(t)$ (3) $\dot{V}_E = v_F \cdot A \left[\frac{m^3}{h}\right]$ (5) $Q(t) = \frac{\dot{V}_W(t)}{M_C} \int_0^t (C_0 - C_t)dt$

(2) $v_F = \frac{H_2 - H_1}{t_{H_2} - t_{H_1}} \left[\frac{m}{h}\right]$ (4) $H_{MTZ} = v_F \cdot (t_2 - t_1)\ [m]$ (5a) $Q(t) = \frac{v_A}{v_F} \cdot (C_0 - C) \left[\frac{g}{l}\right]$

BF 1974	Fig. 2: Mass-transfer-zone concept for determining process parameters	5201

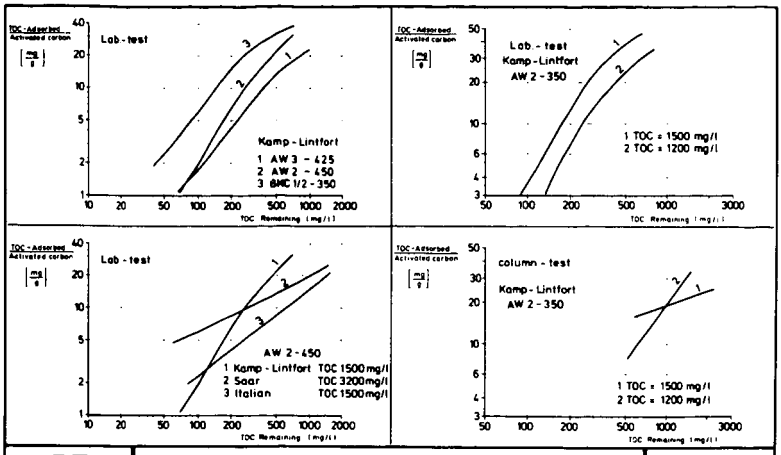

BF 1974	Fig. 3: Adsorption isotherms for different wastes and activated carbons	5189

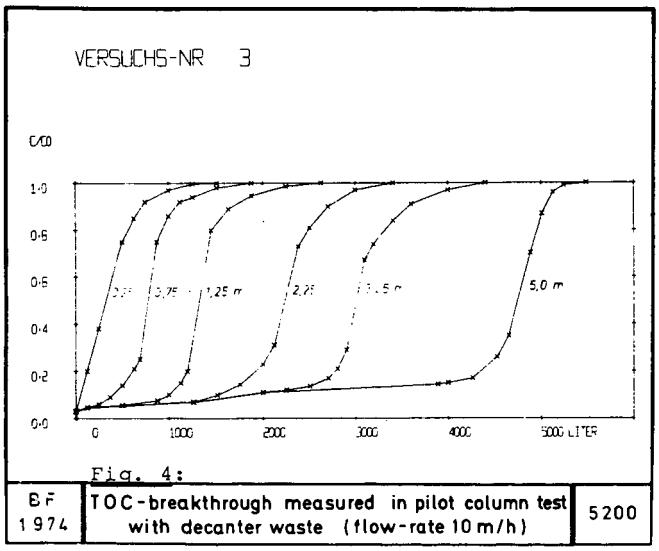

Fig. 4:

BF 1974	TOC-breakthrough measured in pilot column test with decanter waste (flow-rate 10 m/h)	5200

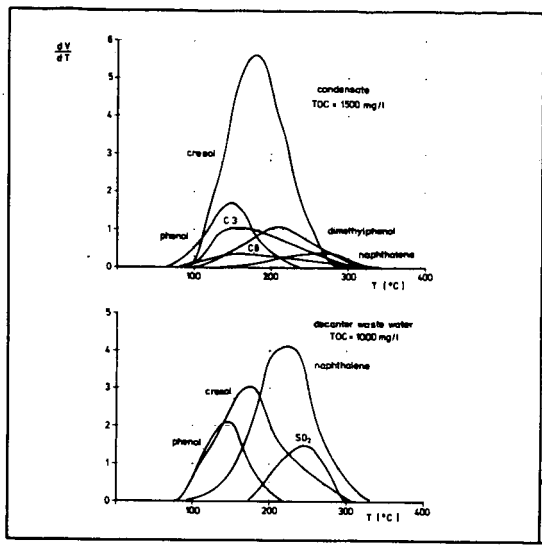

BF
1974

Fig. 5:
Non-isothermal desorption of compounds from activated carbon

5203

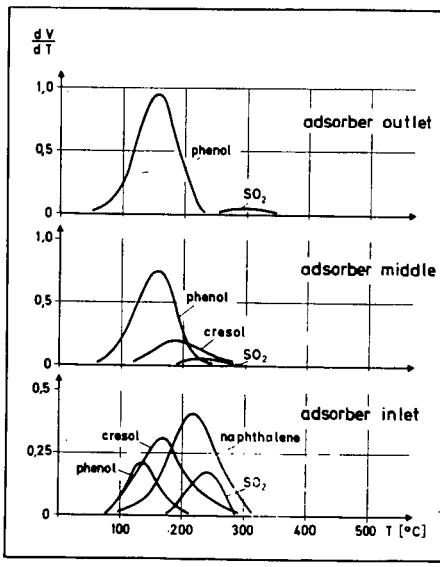

BF
1974

Fig. 6:
Desorption of waste compounds from activated carbon (columntest)

5 1 9 2

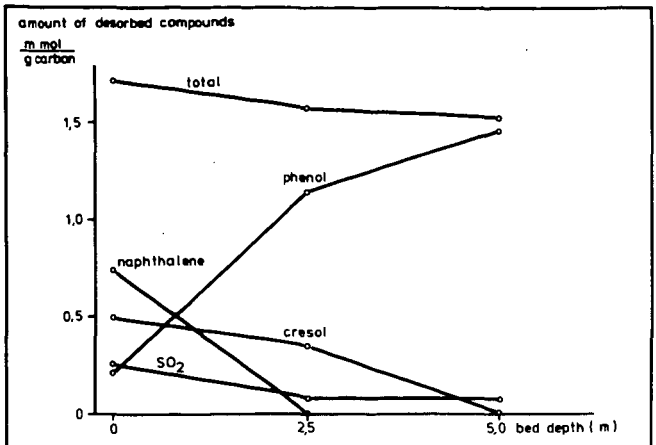

Fig. 7:

BF 1974	Desorption of compounds from activated carbon (columntest)	5191

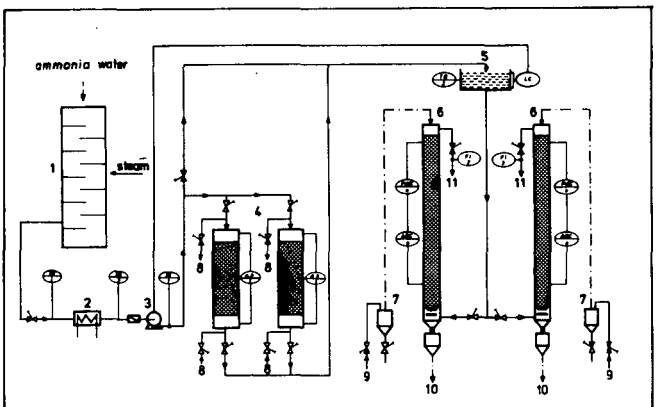

BF 1974	Fig. 8: Purification of coking plant effluents - pilot plants flow sheet -	5190

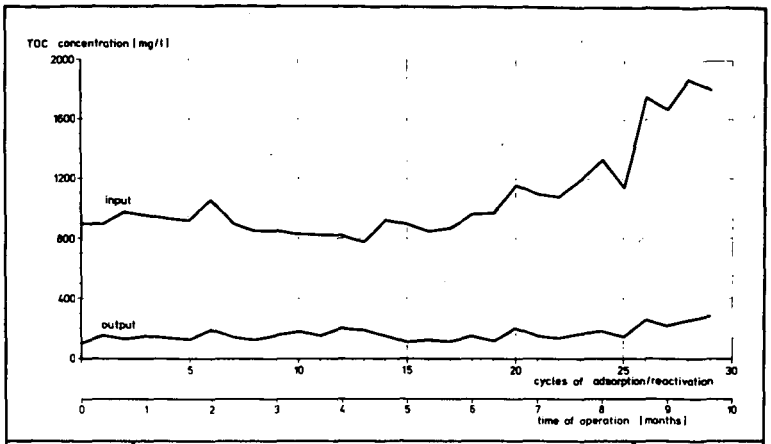

BF 1974	Purification of coking plant effluents - results of pilot plant operation -	5181

Fig. 9:

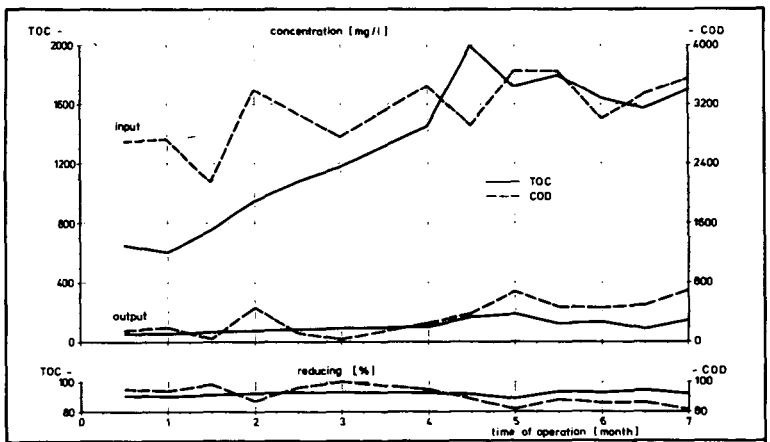

BF 1974	Purification of coking plant effluents - results of pilot plant operation -	5180

Fig. 10:

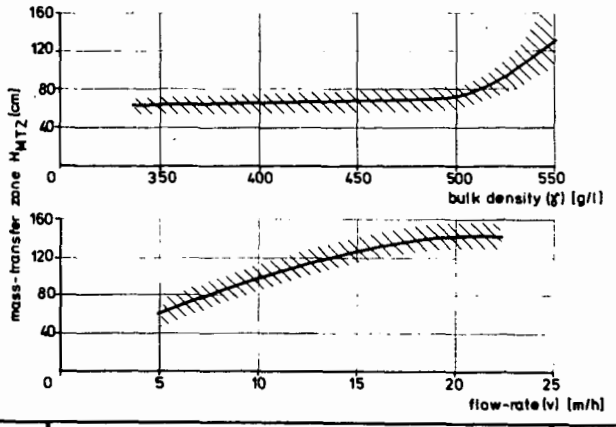

BF 1972	Fig. 11: Purification of coking plant effluents – results of pilot plant operation –	5212

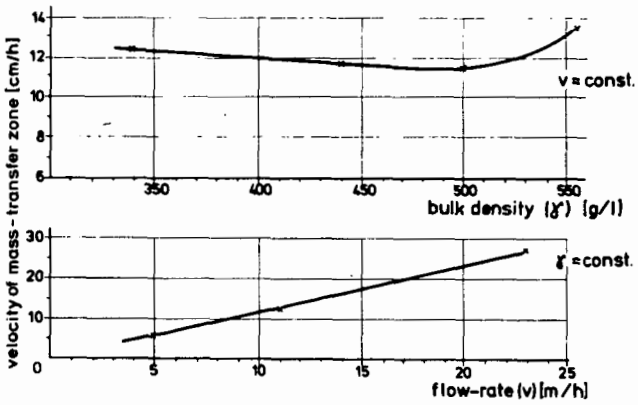

BF 1972	Fig. 12: Purification of coking plant effluents – results of pilot plant operation –	5210

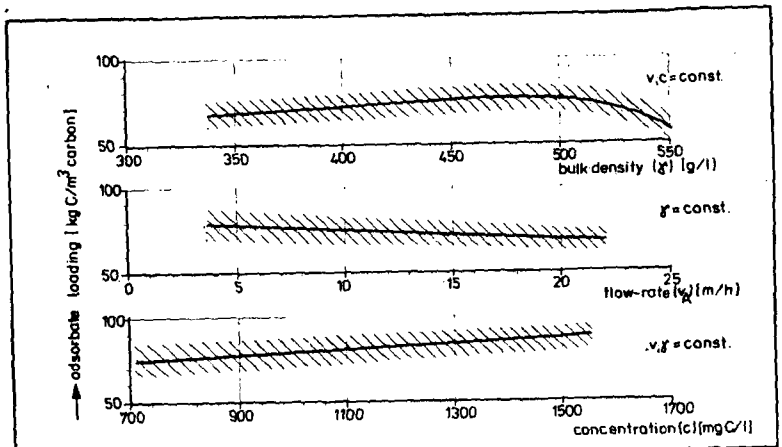

BF 1972 | Fig. 13: Purification of coking plant effluents – results of pilot plant operation – | 5214

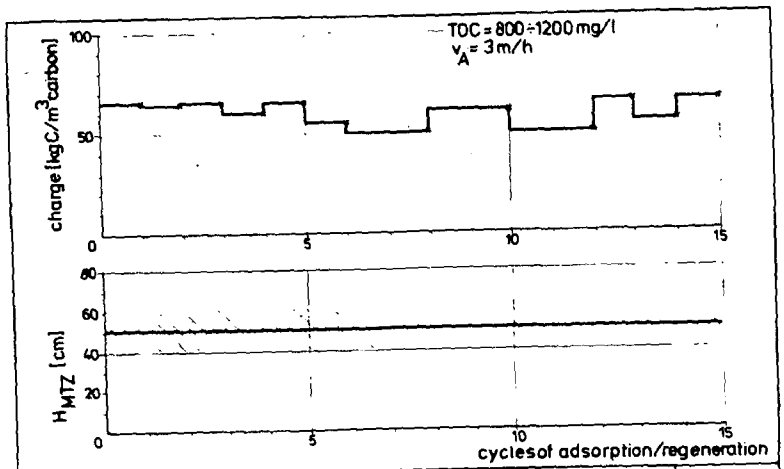

BF 1972 | Fig. 14: Purification of coking plant effluents – results of pilot plant operation – | 5211

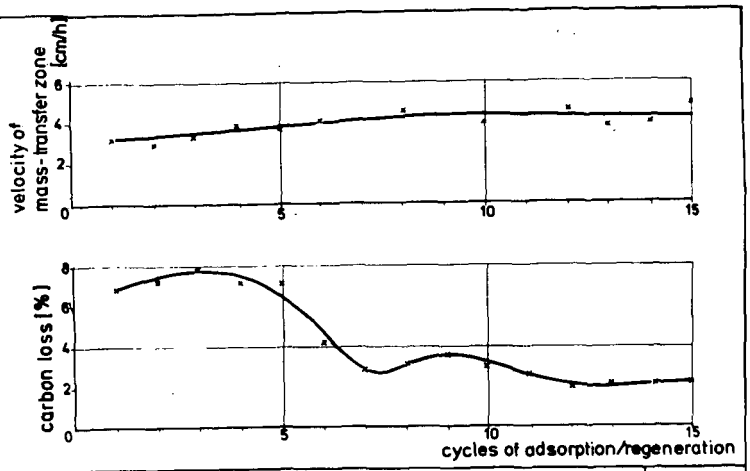

BF 1972	Fig. 15: Purification of coking plant effluents results of pilot plant operation	5213

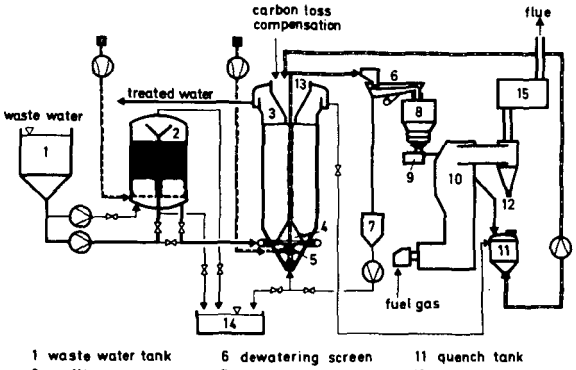

1 waste water tank
2 prefilter
3 adsorber
4 water distribution
5 air lift pump
6 dewatering screen
7 receiver
8 intermediate vessel
9 feeding screw
10 reactivation unit
11 quench tank
12 cyclone separator
13 receiver
14 tank
15 afterburner

BF 1974	Fig. 16: Scheme of demonstration plant 25 m³/h	5193

COAL GASIFICATION AND THE PHENOSOLVAN PROCESS

Milton R. Beychok

Consulting Engineer, Irvine, California

On the basis of current trends in the supply and demand of energy, the world faces a serious shortage of petroleum crude oil. In the U.S., the shortage of crude oil is compounded by an equally serious dwindling of natural gas supplies. Unless alternative energy supplies are developed, we face a tremendous economic drain on our capital resources from the high cost of imported crude oil.

Because of this situation, there has been a dramatic acceleration in the development of plans to produce clean-burning gas from coal (1). By 1976-1977, two such projects should be coming onstream in the Four Corners area of New Mexico (1,2), each producing 250 million standard cubic feet per day of substitute natural gas (SNG). Other coal gasification projects are under consideration and design for Wyoming, Montana and the Dakotas.

The New Mexico projects will each gasify about 25,000 tons per day of coal, and will each produce about 105-110 tons per day of byproduct crude phenol (2) -- as well as other byproducts. The gasification process uses steam, as a source of hydrogen, to produce methane SNG from the coal carbon. Byproduct crude phenol is recovered from the phenolic steam condensate (gas liquor) which results from condensing and removing the excess gasification process steam.

The projects in New Mexico will use the Lurgi* coal gasification process -- and the bulk extraction of crude phenol from the phenolic gas liquor will utilize Lurgi's Phenosolvan liquid-liquid extraction process.

COAL GASIFICATION

Figure 1 presents a simplified flow diagram of the process steps involved in the Western Gasification Company's project in New Mexico (2,3). As shown in Table 1, that project will process 52,700 tons/day of coal, steam, water and oxygen -- to produce 5,440 tons/day (250 MM SCFD) of SNG, plus 47,260 tons/day of byproducts which include the 105 tons/day of crude phenol (2,3). The pertinent process steps can be briefly summarized as (2,3):

Gasifiers -- reaction vessels wherein coal, steam and oxygen are reacted under controlled conditions to yield a crude gas containing methane, hydrogen, carbon oxides, excess steam, and various byproducts and impurities. Only some 40% of the plant's endproduct methane SNG is

---

* Lurgi Mineralöltechnik GmbH, Frankfurt (Main), Germany. The projects in Wyoming, Montana and the Dakotas also plan to use Lurgi technology.

produced in the gasifiers. Subsequent reaction steps produce the remainder of the methane.

Gas Cleaning -- the cooled gas is cooled and scrubbed with water to remove tars, heavy oils and phenols. The tars and oils are recovered as byproducts. The phenolic water (gas liquor) is processed in a subsequent step (Phenosolvan extraction) for recovery of byproduct phenol.

Shift Conversion -- excess carbon monoxide in the crude gas is catalytically "shifted" (converted) to carbon dioxide to provide the 3-to-1 ratio of hydrogen-to-carbon monoxide required for additional methane synthesis in the subsequent methanation step.

Gas Cooling -- the shifted gas is again cooled to remove additional oil byproducts and any residual phenolic gas liquor.

Acid Gas Removal -- the Rectisol absorbtion process, using low temperature methanol, selectively removes hydrogen sulfide and carbon dioxide from the cooled gas. Pre-cooling at the Rectisol unit entry recovers byproduct naphtha.

Methanation -- carbon monoxide and hydrogen are catalytically combined to form methane and byproduct water. About 60% of the endproduct SNG is produced in this step.

Compression -- the final dry and purified gas is compressed and then delivered to the pipeline with a heating value of about 980 Btu/SCF.

Phenosolvan -- the gas liquors, from the gas scrubbing and gas cooling steps, are processed in a Phenosolvan unit. Crude phenol is extracted and recovered as a byproduct. The residual water effluent is further processed in a biotreating unit and then reused within the plant.

Auxiliary Services -- the auxiliary units include cryogenic air fractionation to supply oxygen to the gasifiers, a Claus sulfur plant to convert gaseous hydrogen sulfide (removed by the Rectisol unit) to byproduct sulfur, a steam boiler plant, a cooling water system, and wastewater treating and reuse systems.

PHENOSOLVAN PROCESS

The Phenosolvan process is a liquid-liquid extraction process developed by Lurgi and first commercialized in about 1940. The process was originally developed to extract phenols from the aqueous gas liquor obtained in coke oven plants. Since 1940, about 32 commercial Phenosolvan plants have been installed worldwide, ranging in capacity from 2 to 1000 gallons per minute of gas liquor throughput.

Figure 2 presents a simplified flow diagram of the Phenosolvan process as proposed for use in the New Mexico coal gasification projects (2). The incoming gas liquor is filtered through a gravel bed and then contacted with solvent (isopropyl ether) in multi-stage mixer-settlers. The phenol-rich solvent (extract) is distilled to recover lean solvent for reuse, and then stripped to remove and recover residual solvent. The dephenolized liquor (raffinate) is gas-stripped to remove and recover solvent. The liquor is then steam-stripped to remove acid gases (hydrogen sulfide and carbon dioxide), followed by steam-stripping to remove ammonia.

Some knowledge of the phenols and other organics, that may be present in the gas liquor, is needed to predict the extraction performance of the Phenosolvan unit. In general, the Phenosolvan process will extract more than 99% of the mono-hydric phenols, but the gas liquor will contain organics other than mono-hydric phenols.

As a generic term, "phenols" include 6,7 and 8-carbon aromatics with one hydroxyl group -- the mono-hydric phenol, cresols, xylenols and ethylphenols. "Phenols" also include poly-hydrics having two or more hydroxyl groups such as catechol and resorcinol, which are benzene $[C_6H_4(OH)_2]$ isomers (4).

The expected composition of the gas liquor produced in a coal gasification plant is proprietary information. It will vary with different coal supplies and it will vary with different gasification processes and conditions. However, based on published literature (5,6, 7,8) furnished by Lurgi, the mono-hydric phenols may constitute as much as 75-85% of the organics in the gas liquor. The poly-hydrics in the gas liquor may be as much as 34% of the total phenols(7). The gas liquor may also contain organic bases (pyridines), neutral oils, and perhaps other organic acids (for example, naphthenic acids). Lowenstein-Lom's studies (9) of gas liquors from Czechoslovakian coal carbonization plants confirms that the phenolic extracts may contain as much as 75-80% mono-hydrics, and as much as 30-35% poly-hydrics including pyrocatechol, resorcinol and their homologues.

For the purposes of this paper and based on the above published literature, it has been assumed that the crude phenol extracted from the coal gasification gas liquor will contain (on a water- free basis):

85% mono-hydric phenols
15% poly-hydric phenols
5% other organics

We may also assume that the mono-hydric phenol distribution coefficient (K_D) for the system isopropyl ether-phenol-water is 20, and that the weight flow ratio of liquor to solvent (W/S) is 10 for a typical design(5). With these assumptions, we may use the following equation for multi-stage extraction with a perfectly lean solvent (4) to predict the extraction recovery of mono-hydric phenols:

$$x_w/x_n = \frac{E^{n+1} - 1}{E - 1} \qquad 1)$$

where: $E = K_D(S/W) = 20(1/10) = 2$
n = equilibrium extraction stages
x_w = phenols in entering liquor
x_n = phenols in exiting liquor
$x_w/x_n = 1000$ for 99.9 % extraction

Equation 1 confirms that 9 equilibrium extraction stages will extract 99.9% of the mono-hydric phenols, and that number of equilibrium stages would probably be a reasonable design.

Based on Weisner's paper furnished by Lurgi (8), the Phenosolvan process may extract as much as 70% of the organics other than mono-hydric phenols. Lowenstein-Lom (10) determined phenol and catechol

distribution coefficients for over 40 possible solvents, including 6 aliphatic ethers. For the ethers, his data indicate that the catechol K_D averaged 35% of the phenol K_D (the range was 20-52%). If we therefore assume a catechol K_D of 7 (which is 35% of the phenol K_D of 20 used above), and we use 9 equilibrium stages, we can obtain from Equation 1:

$$x_w/x_n = \frac{0.7^{10} - 1}{0.7 - 1} = 3.24$$

$$\text{If } x_w = 100, \text{ then } x_n = 30.8$$

Thus, the catechol extraction would be about 70% which generally confirms Weisner's (8) statement regarding extraction of organics other than mono-hydric phenols.

For the purposes of this paper, based on the above, it has been assumed that extraction recoveries in the coal gasification plant Phenosolvan unit will be about:

99.5% for mono-hydric phenols
60.0% for poly-hydric phenols
15.0% for other organics

Finally, based on a gas liquor rate of 2,700 gallons per minute for the Western Gasification Company's project (2,3), Table 2 presents a calculated material balance for the Phenosolvan unit using the assumptions derived above. As shown in Table 2, the 105 tons/day of extracted byproduct crude phenol represents an overall removal of 75% of the organics that may be contained in the gasification plant gas liquor.

Using BOD_5 factors that can be obtained from stoichiometric oxygen demands, and the assumption that BOD_5 is 68% of the stoichiometric, Table 2 estimates that the incoming gas liquor will have a BOD_5 of about 13,000 ppm. This will be reduced about 84% to yield an effluent liquor with a BOD_5 of about 2,150 ppm. [For those who are unfamiliar with BOD_5 and stoichiometric oxygen demands, Beychok has published a fairly complete discussion of these and other terms related to wastewater quality (11)]

SUMMARY

A number of large coal gasification projects are under serious consideration in the Western United States. Two of these should start full-scale operations in New Mexico during 1976-1977 -- each gasifying about 25,000 tons/day of coal and each producing about 250 MMSCFD of methane SNG. These New Mexico projects will each produce about 105 ton/day of byproduct crude phenol.

The crude phenol byproducts will be extracted in Phenosolvan units, which have been extensively used in similar applications worldwide since about 1940. The Phenosolvan process uses isopropyl ether solvent for the liquid-liquid extraction of phenolics from the liquors produced from coal gasification. For the Western Gasification Company coal gasification project, planned for New Mexico, this paper has estimated that the Phenosolvan process will recover 105 tons/day of

crude phenol from 2,700 gallons per minute of gas liquor containing about 142 tons/day of various phenols and other organics. The estimated phenol recovery will reduce the gas liquor BOD_5 about 84% and the effluent liquor from the Phenosolvan unit will be further processed in a biotreater before being completely reused within the plant.

The author wishes to acknowledge the help of Herr Paul Rudolph of Lurgi GmbH who kindly furnished many of the references which made this paper possible.

REFERENCES

(1) "Clean energy via coal gasification", M.R. Beychok and A.J. Paquette. 18th Annual New Mexico Water Conference, New Mexico State University, Las Cruces, April 1973.
(2) Federal Power Commission, Dockets CP73-131 and CP73-211. Application filings for proposed coal gasification plants in New Mexico.
(3) "Coal Gasification : A Technical Description", brochure by the Western Gasification Company, Farmington, New Mexico, 1973.
(4) Manual on Disposal of Refinery Wastes, Volume on Liquid Wastes, Chapter 10. American Petroleum Institute (written under contract by M.R. Beychok).
(5) "Recent developments in the Phenosolvan process", R. Jauernik, Erdol und Kohle, April 1963.
(6) "Recovery of phenols from coker gas liquor by the Phenosolvan process", Hans-Joachim Wurm, Gluckauf 104, S.517/523, 1968.
(7) "Recent developments in water usage and effluent disposal in the gas industry", I.G.E. Journal (British), Dec. 1967.
(8) "Dephenolization of effluents (from coke-oven plants) by the Phenosolvan process", P. Weisner. Symposium at ISCOR-Steelworks, Pretoria, South Africa, Feb. 1974.
(9) "A new dephenolization process for low-temperature carbonization plants", W. Lowenstein-Lom, Petroleum, Feb. 1951.
(10) "The Phenosolvan process", W. Lowenstein-Lom et al, Petroleum, Apr. 1947.
(11) "AQUEOUS WASTES from petroleum and petrochemical plants", M.R. Beychok. John Wiley and Sons, Ltd., London-New York-Sidney, 1967.

TABLE 1

LURGI GASIFICATION MATERIAL BALANCE

(Basis: 250 MMSCFD of SNG product gas)

		Short Tons per day	Weight %
INPUTS:			
	Sized coal	21,860	41.48
	Steam and water	25,160	47.74
	Oxygen	5,680	10.78
	TOTAL	52,700	100.00
OUTPUTS:			
	Product gas	5,440	10.32
	Crude phenol	105	0.20
	Ash	5,876	11.15
	Reuse water	17,851	33.87
	Byproduct water[a]	3,730	7.08
	Tars, oils and naphtha	1,475	2.80
	Offgas to sulfur plant[b]	792	1.50
	CO_2 vent gas	16,631	31.56
	Ammonia and water[c]	800	1.52
	TOTAL	52,700	100.00

Notes:

a -- Water produced in methanation reaction, and also reused.
b -- Contains 183.7 tons/day of sulfur in form of hydrogen sulfide
c -- Contains approx. 180 tons/day of free ammonia

TABLE 2

CALCULATED PHENOSOLVAN MATERIAL BALANCE

(for coal gasification gas liquor)

	FEED LIQUOR		EFFLUENT		CRUDE PHENOL	
	lbs/hr	ppm	lbs/hr	ppm	lbs/hr	wt %
Water, 10^6 lbs/hr	1.35	-	1.35	-	-	-
Mono-hydric phenols	7,475	5,537	37	27	7,438	85
Poly-hydric phenols	1,458	1,080	583	432	875	15
Other organics	2,913	2,158	2,476	1,834	437	5
TOTALS, water-free	11,846	8,775	3,096	2,293	8,750	100
TOTALS, water-free, tons/day	142	-	37	-	105	-
BOD_5 (estimated), ppm	-	12,976	-	2,151	-	-

Basis:

(a) 2700 gallons per minute (1.35 x 10^6 lbs/hr) of water flow

(b) 105 tons/day of extracted crude phenol

(c) Assumed composition of crude phenol:
85% mono-hydric phenol
15% poly-hydric phenol
5% other organics

(d) Assumed extraction recoveries:
99.5% for mono-hydric phenols
60.0% for poly-hydric phenols
15.0% for other organics

(e) BOD_5 factors:
mono-hydric phenols = 1.7
poly-hydric phenols = 1.9
other organics = 0.7

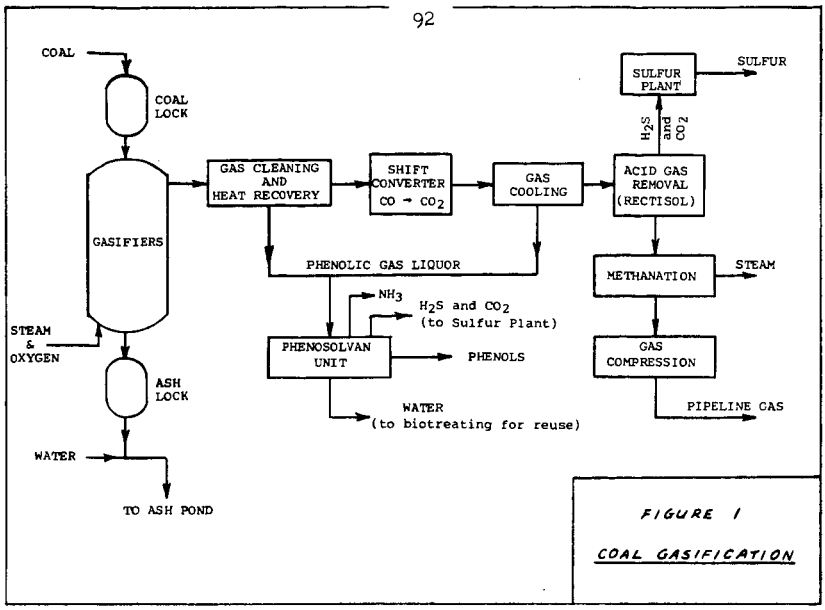

FIGURE 1

COAL GASIFICATION

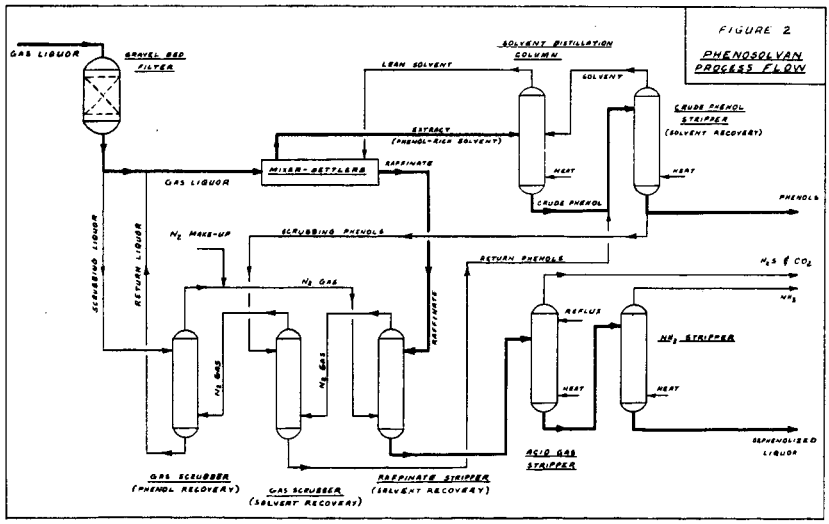

FIGURE 2

PHENOSOLVAN PROCESS FLOW

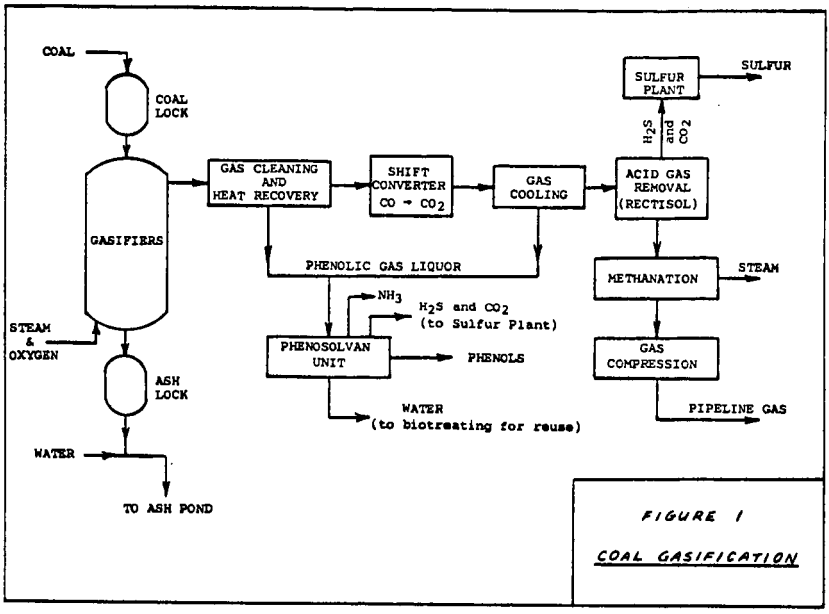

FIGURE 1

COAL GASIFICATION

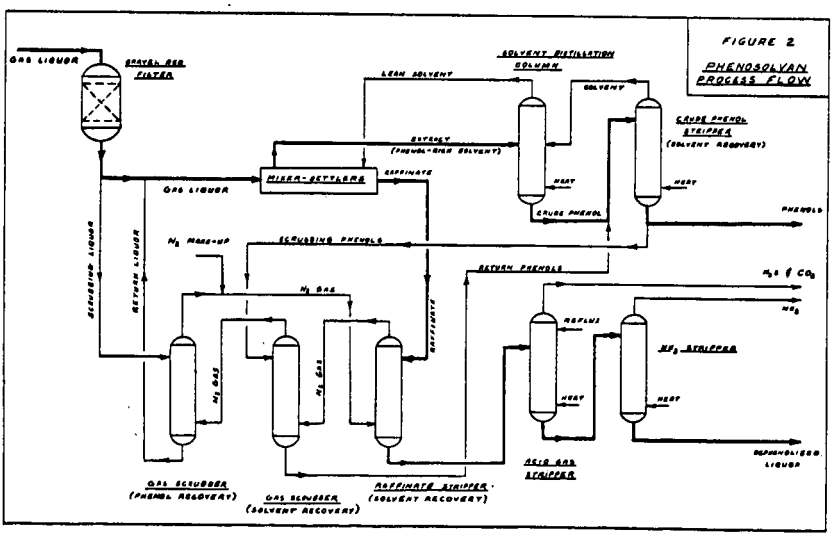

FIGURE 2

PHENOSOLVAN PROCESS FLOW

EFFLUENT TREATMENT AND ITS COST FOR THE SYNTHANE COAL-TO-S.N.G. PROCESS

Joseph P. Strakey, Jr., Albert J. Forney, William P. Haynes
U. S. Bureau of Mines, 4800 Forbes Avenue, Pittsburgh, Pa.

Kenneth D. Plants
U. S. Bureau of Mines, P. O. Box 880, Morgantown, W. Va.

Introduction

A full scale coal gasification plant will convert coal containing large amounts of ash and sulfur into 250 x 10^6 scfd of S.N.G. which can be utilized in an environmentally-acceptable manner. The gasification plant itself will require extensive controls to prevent the release of large quantities of pollutants to the environment. The SYNTHANE process (1) is one of four new coal-to-S.N.G. processes that is proceeding to the large pilot plant scale (it will gasify 75 tons of coal/day). One of the principal objectives of the pilot plant is to determine the environmental aspects of the process and to develop the necessary treatment techniques. A complete and accurate accounting of the environmental aspects will await the operation of the pilot plant. In the study presented here, we have used the data collected in the small (20-40 lb./hr) gasifier to project the environmental impact of a full scale SNYTHANE plant and estimate the cost of controls. The gasifier is the same as the large gasifier except in scale and the effluents should be a reasonable representation of those to be expected from a full scale plant. The chars, tars, gases, and water from this gasifier have been extensively analyzed and reported (2).

Gaseous Effluents

Coal storage and preparation would be the same as that for a 1800 MWe coal-fired power plant and no special problems are anticipated. In the 75 ton/day SYNTHANE pilot plant, the coal pulverizer is swept with a clean hot flue gas from an oil-fired furnace to dry and transport the coal. In a full scale plant, the mill could be swept with heated air. A baghouse will remove particulates from the discharge, and no increase in emissions would result.

The lock hoppers used to introduce the coal into the system at 1000 psig are pressurized with CO_2 recovered from the acid gases. A Stretford plant removes H_2S from the acid gases in the 75 ton/day pilot plant so the CO_2 is relatively pure. If a Claus plant is used in place of the Stretford, the CO_2 will contain sulfur compounds and the lock hopper gas should be vented through the boiler in order to convert all the sulfur compounds to SO_2. If the lock hoppers are vented through the boiler or directly to the atmosphere, filters would be used to remove coal dust.

Pretreatment of the coal when required, is done at pressure and the offgas is mixed with the product gas from the gasifier and no effluents are created. Char is withdrawn from the bottom of the gasifier and is passed through a char cooler where the temperature is lowered from 1800° F to 600° F by a water spray. The steam generated here is used in the shift reactor, and no gaseous effluent results. The char is brought to atmospheric pressure in lock hoppers pressurized with steam. The char is low in volatile matter so no problems are anticipated in handling the lock hopper steam.

No gaseous effluents are created in the gas cleanup section of the plant or in the shift reactor.

The acid gases removed in the hot carbonate system are treated in the Stretford or Claus plant and the treatment of the effluents is discussed below. Final sulfur cleanup and methanation introduce no gaseous effluents.

The major gaseous sulfur effluent results from the combustion of the char produced in the gasifier. In the SYNTHANE process, the amount of char produced is just sufficient to supply the energy needed for steam generation so a "balanced" condition results. This balance point occurs when the carbon conversion upon gasification is approximately 65%. The sulfur content, and analyses, of four different coals and the chars produced from them, is shown in Table 1. Sulfur content of the chars varies from 0.2 to 1.8% S. These data were selected from runs where the carbon conversion was near 65%. For the high sulfur eastern coals, combustion of the char will result in SO_2 emissions in excess of present emission standards.

In the control strategy presented here, the char-fired boiler is also used as an incinerator to dispose of sulfur bearing streams produced in other parts of the plant. One such stream is produced in the water treatment plant where the ammonia stripping step produces an offgas containing CO_2, H_2S, and HCN. This offgas is incinerated in the boiler where the H_2S is converted to SO_2 and the very small amount of HCN is converted to H_2O, CO_2, N_2 and perhaps some NO_x. The sulfur in this offgas is small in proportion to the sulfur in the char, ranging from 4 to 11% of the char sulfur for the different coals.

The tailgas from the Stretford or Claus plant is also incinerated in the char-fired boiler. The Stretford tailgas contains only very small quantities of sulfur compounds and incineration of this stream serves mainly to prevent objectionable ground level concentrations of CO_2.

The SO_2 emissions for the Stretford case are shown in the first row of table 2 in pounds of SO_2 per million Btu's of char fired. Also shown is the percent removal of SO_2 needed to meet the New Source Performance Standard of 1.2 lb. of SO_2 per million BTU. The high sulfur eastern coals will require SO_2 scrubbing of 36 and 67% No scrubbing is required for the western coals.

Another option which was considered is the combustion of the tars (see table 1) produced in gasification along with the char. These tars can furnish from 16 to 24% of the necessary heat; their sulfur content varies from 1.1 to 2.7%. In this case, the char would be gasified to a higher carbon conversion to maintain balanced operation. Emissions were calculated for this case by assuming equal percentage gasification of the C,H,N,O,S to give the desired reduction in char mass and heating value. The emissions are shown in the second row of table 2. For the Illinos coal, the percent removal of SO_2 needed is increased from 36 to 52% but is almost unchanged for the western Kentucky coal. The western coals still require no SO_2 scrubbing.

Another option is to desulfurize this tar before combustion. This has been done for one SYNTHANE tar in the Bureau's SYNTHOIL pilot plant (3,4). The sulfur content was reduced from 1.8% to 0.56% when hydrodesulfurized under relatively mild conditions of 425° C and 2000 psi. Based on experience with coal tars, it is believed that the sulfur levels could be reduced to 0.1% by operating at 450° C and 4000 psi. Assuming this fractional sulfur removal, the emissions have been calculated for the case of combustion of char plus desulfurized tar including the sulfur from the ammonia stripping step. The results are shown in the third row of table 2. Only a relatively small decrease in emissions over the case of char combustion alone results and the added cost of the desulfurizing step would not be justified.

A Claus plant could be operated in place of the Stretford process. The feed gas to the Claus plant would contain about 4% H_2S for the high sulfur coals. While operation with such a lean gas is not normal practice, plants have operated with as low as

1.9% H_2S (5) with recoveries of 70%. It is unlikely that a Claus plant could be used with the low sulfur western coals. To compare the emissions for this case, a sulfur recovery efficiency of 80% was assumed with the tailgas being incinerated in the boiler. A significant increase in emissions results as shown in the fourth row of table 2. Approximately 80% removal efficiency is required for the SO_2 scrubbing system which is well within the realm of present technology. Emissions are also shown for the case where the tars are combusted along with the char.

The recovery of H_2S from the acid gases could be omitted entirely and the sulfur could be removed as SO_2 from the boiler after incineration. This would require removal efficiencies in excess of 90% for the eastern coals, as shown in table 2, which would not be practical, but for the western coals this is a definite possibility. For the western coals, the removal efficiencies needed would be 70 and 86%. Also shown in table 2 are the emissions for combustion of the tar along with the char. The NO_x emission limits can be met by proper design of the boiler using techniques such as tangential firing and overfire air.

An estimate of the cost of air pollution controls can be made. It has been assumed here that the Stretford or Claus plant is part of the basic coal gasification process even though it is actually included to reduce emissions and its cost has not been included. The cost of the SO_2 scrubbing system is taken to be equivalent to $35/KW based on the boiler size. The char fired boiler would have an equivalent generating capacity of about 514 MWe.

For the worst case (W. Kentucky coal), conventional lime or limestone scrubbing of nearly all of the flue gas would be needed to achieve the removal efficiency of 67% with the Stretford plant and 80.8% with the Claus plant. The capital cost would then be $17,987,000. The operating cost, at 2 mills/kwh (a moderate to high number) would be $8,140,000 per year, or $ .0987 per thousand ft^3 of S.N.G. If Illinois No. 6 coal is used, scrubbing would only be necessary on about half of the boiler output if the Stretford process is used. The cost would be correspondingly reduced.

Solid Effluents

The major solid effluents will be sulfur, ash, and lime sludge. A 250 x 10^6 scfd plant gasifying one of the eastern coals will produce about 24 ton/hr of elemental sulfur from the Stretford plant. Although it is salable in the near future, this situation is unlikely to continue and disposal methods such as returning the sulfur to the worked-out mine may ultimately be necessary.

All of the coal ash will end up as particulates in the char fired boiler. Particulate emissions here are quite high. The char is both high in ash and low in heating value. The particulate emissions are shown below along with the percent removal needed to meet the New Source Performance Standard of 0.1 lb of particulate per million BTU.

Particulate Emissions from Char fired Boiler

	Lb ash/10^6 BTU	% Removal
Illinois No. 6	24.52	99.59
Wyoming	64.20	99.84
W. Kentucky	28.26	99.65
Lignite	25.97	99.61

Removal efficiencies of 99.6 to 99.8% will be needed. This will require the best available technology in precipitators or venturi scrubbers. The recovered ash could also be returned to the coal mine.

A lime sludge will be produced in the SO_2 scrubbers and in the lime leg of the ammonia stills. The total volume will be about 17 tons/hr when Illinois No. 6 coal is used. It may be possible to reduce the volume by using the sludge from the ammonia stills in the SO_2 scrubbers. The only proven disposal method at present is ponding. Since the gasification plants will be mine-mouth plants, adequate land area for a pond should be available.

Some spent catalysts and sorbents will be generated. Spent shift catalyst and sponge iron, used in final sulfur cleanup, can be disposed of by burial. The activated carbon also used in final sulfur cleanup will also require periodic replacement and the used carbon could be returned to the gasifier. The Raney nickel and the second stage conventional methanation catalyst contain a high proportion of nickel, and we are currently investigating techniques to recover the nickel from spent catalyst.

Liquid Effluents

The water and steam flows for a 250 x 10^6 ft.^{3}/day SYNTHANE plant are shown in figure 1. These flows are based on the design for the 75 ton/day pilot plant. A total of 1.25 lb of steam/lb coal is used in the pretreatment and gasification of the coal. A steam decomposition of 40% in the gasifier has been assumed. Most of the water is condensed in the scrubber along with several contaminants. A portion of the water recovered in the knock-out trap after the shift converter is sprayed into the char cooler to reduce the char temperature from 1800 to 600° F. The steam generated is then blended with the shift reactor feed gas.

No contaminated effluents are created in the purification and methanation steps of the process. The hot potassium carbonate (Benfield) acid gas scrubbing process can be operated at a net steam deficit. An analysis of the water produced in the methanation reaction (133,000 lb/hr) is shown below. It is relatively uncontaminated and should be suitable as a boiler feed water. The high iron concentration is a result of reaction with the carbon steel piping in the pilot plant.

Methanation Byproduct Water Analysis 1/

pH	5.4
Suspended solids	47
Phenol	0.003
COD	39
Ca	8
Mg	0.1
Fe	25
HCO_3	23

The water collected downstream of the gasifier in the scrubber-decanter requires extensive treatment. The condensates collected from the small SYNTHANE gasifier (20-40 lb/hr) have been analyzed (2) and the results are shown in the following table:

1/ mg/l except pH

Byproduct water analysis from SYNTHANE gasification of various coals, mg/l (except pH)

	Coke plant	Illinois No. 6 coal	Wyoming subbituminous coal	Illinois char	North Dakota lignite	Western Kentucky coal	Pittsburgh seam coal
pH	9	8.6	8.7	7.9	9.2	8.9	9.3
suspended solids	50	600	140	24	64	55	23
Phenol	2,000	2,600	6,000	200	6,600	3,700	1,700
COD	7,000	15,000	43,000	1,700	38,000	19,000	19,000
Thiocyanate	1,000	152	23	21	22	200	188
Cyanide	100	0.6	0.23	0.1	0.1	0.5	0.6
NH_3	5,000	[1] 8,100	9,520	2,500	7,200	10,000	11,000
Chloride	-	[2] 500	-	31	-	-	-
Carbonate	-	[2] 6,000	-	-	-	-	-
Bicarbonate	-	[2] 11,000	-	-	-	-	-
Total sulfur	-	[3] 1,400	-	-	-	-	-

[1] 85 percent free NH_3.

[2] Not from same analysis.

[3] $S^{=}$ = 400
$SO^{=}$ = 300
$SO_4^{=}$ = 1,400
S_2O_3 = 1,000

Approximately 60% of the coal nitrogen is converted to ammonia. The concentration of cyanide is notably small (0.6 mg/l or lower). Thiocyanates are also low compared to coke plant weak ammonia liquor. There is a wide variation in phenols for the different coals, from 1,700 to 6,600 mg/l. The water condensed after the shift reactor would be similar in character but more dilute; it would contain only about 9 mg/l of phenol.

A treatment process was developed to serve as the basis for an economic estimate. It is shown in figure 2. The flows and amounts are based on an Illinois No. 6 coal with a nominal 2000 mg/l of phenol and 12,000 mg/l of ammonia. The use of other coals will undoubtedly change these quantities but should not greatly affect the cost estimate.

The ammonia water from the scrubber decanter is first fed to ammonia stills where free ammonia is released in the free ammonia leg and the fixed ammonia is liberated in the fixed leg after reaction with milk of lime. Heat is supplied to the stills by adding live steam at 15 psig. The tops of the stills are equipped with dephlegmators which cool the gas to 185° F and condense a portion of the steam which acts as reflux.

The ammonia leaving the stills proceeds to a washer column where it is cooled to 90° F and washed with a water spray which reacts with the NH_3 to produce NH_4OH. This, in turn, removes CO_2, H_2S, and HCN. The wash solution passes to a dissociator where it is heated to drive off the acid gases. The acid gases are washed with incoming feed water to recover the NH_3. The purified ammonia product is absorbed in water to produce a 30% aqueous ammonia product for sale. An anhydrous ammonia product could also be produced. Lime sludge consisting of unreacted components in the lime and the calcium salts formed in the ammonia stills is removed as a slurry from the lime leg and pumped to the pond for the SO_2 scrubber.

The stripped water is withdrawn from the base of the fixed ammonia leg and cooled to 100° F in an air cooled heat exchanger and stored for 48 hours in a holding tank to permit separation of any remaining tars. Water from the holding tank is combined with water from the knockout drum following the shift converter for feed to the aeration tanks. Antifoam and phosphoric acid (biological nutrient) are added and sulphuric acid is used as needed to control the pH at 8.0 and temperature is adjusted to 90° F.

Biological oxidation is used to oxidize phenols, other organics, cyanides, and thiocyanates. A similar system has been used by Bethlehem Steel Co. at its Bethlehem, Pa. plant (6) where phenols are reduced to as low as 0.1 mg/l and thiocyanates are re-

duced by an average of 70%. This plant has been operating for over 10 years. In the aeration tanks, surface aerators supply the necessary oxygen. The water from the aerators flows to clarifiers where the sludge is separated and returned to the aerators. A portion of the sludge is wasted by filtering the clarifier underflow and adding the waste sludge to the coal fed to the gasifiers.

The overflow from the clarifier containing 0.2 mg/l of phenol and less than 50 mg/l of NH_3 flows to polishing towers, where gasifier char removes the remaining phenols. The spent char is filtered and returned to the gasifier. The treated water can then be used as cooling tower make-up. Blowdown will, of course, ultimately result in discharge to a stream.

The design of this water treatment process is based on related commercial experience such as the Bethlehem Steel water treatment plant. We are currently investigating several aspects of the process with the condensate from the small SYNTHANE gasifier and the results will be reported at a later date. More research is needed in the area of water treatment to adequately define the effluents from these treatment processes.

The economic evaluation of this process based on early 1972 costs yielded a total construction and total plant cost of $11,098,900. The total incremental investment including interest during construction and working capital is $13,185,500. The annual operating cost with a 90% operating factor is $3,019,700. Allowing a credit of $35 per ton of NH_3 produced, the net annual operating cost is $1,173,500. This is equivalent to $0.0142 per thousand ft^3 of S.N.G. produced.

Conclusion

In summary, this preliminary study indicates that the gaseous, solid, and liquid wastes from a full-scale SYNTHANE plant can be controlled in an acceptable manner at an acceptable cost. The cost of controlling the gaseous pollutants is estimated at $0.0987 per 1000 ft^3 of S.N.G., and that of the water pollutants is $0.0142 per 1000 ft^3 of S.N.G.

TABLE 1. - Coal, Char, and Tar Analyses
Weight percent

	Illinois No. 6	Western Kentucky	Wyoming Sub-Bituminous	North Dakota Lignite
COALS:				
Moisture	7.8	4.3	10.4	21.1
Volatile Matter	37.7	34.6	35.3	32.3
Fixed Carbon	43.2	44.5	36.4	38.3
Ash	11.3	16.6	17.9	8.3
Hydrogen	5.3	4.7	5.0	5.7
Oxygen	15.6	10.9	25.1	32.9
Carbon	63.2	62.7	50.7	51.3
Nitrogen	1.1	1.2	0.7	0.7
Sulfur	3.5	3.9	0.6	1.1
CHARS:				
Moisture	1.0	0.9	0.6	1.4
Volatile Matter	3.6	4.6	3.1	8.8
Fixed Carbon	69.1	65.4	47.8	63.2
Ash	26.3	29.1	48.5	26.6
Hydrogen	1.0	1.0	0.8	1.1
Oxygen	1.3	0.9	1.1	2.6
Carbon	69.9	66.5	49.1	68.3
Nitrogen	0.5	0.7	0.3	0.3
Sulfur	0.9	1.8	0.2	0.5
Carbon Conversion,%	65.5	68.4	68.3	64.0
LB Char/LB Coal	0.310	0.437	0.363	0.250
TARS:				
Hydrogen	6.6	6.0	7.2	7.7
Oxygen	6.6	6.9	8.5	6.4
Carbon	83.0	84.0	81.9	83.8
Nitrogen	1.1	1.4	1.2	1.0
Sulfur	2.7	1.7	1.2	1.1
LB Tar/LB Coal	0.051	0.045	.038	0.025

TABLE 2. - SO_2 Emissions for Various Control Options

LB SO_2 / 10^6 BTU

[ ] = percent removal required

STRETFORD PLANT	Ill. #6	Wyoming	W. Kentucky	Lignite
Char	1.87 [35.9%]	0.57 [0%]	3.63 [67.0%]	1.04 [0%]
Char + Tar	2.30 [52.0%]	0.77 [0%]	3.43 [66.8%]	1.10 [0%]
Char + Des. Tar	1.51 [27.0%]	0.47 [0%]	3.11 [63.4%]	0.89 [0%]
CLAUS PLANT				
Char	5.45 [78.0%]	1.24 [3.6%]	6.24 [80.8%]	2.49 [51.7%]
Char + Tar	5.88 [81.2%]	1.45 [23.4%]	6.03 [81.1%]	2.55 [55.5%]
No H_2S Removal				
Char	19.78 [93.9%]	3.96 [69.7%]	16.64 [92.8%]	8.28 [85.5%]
Char + Tar	20.21 [94.5%]	4.16 [73.3%]	16.44 [93.1%]	8.34 [86.4%]

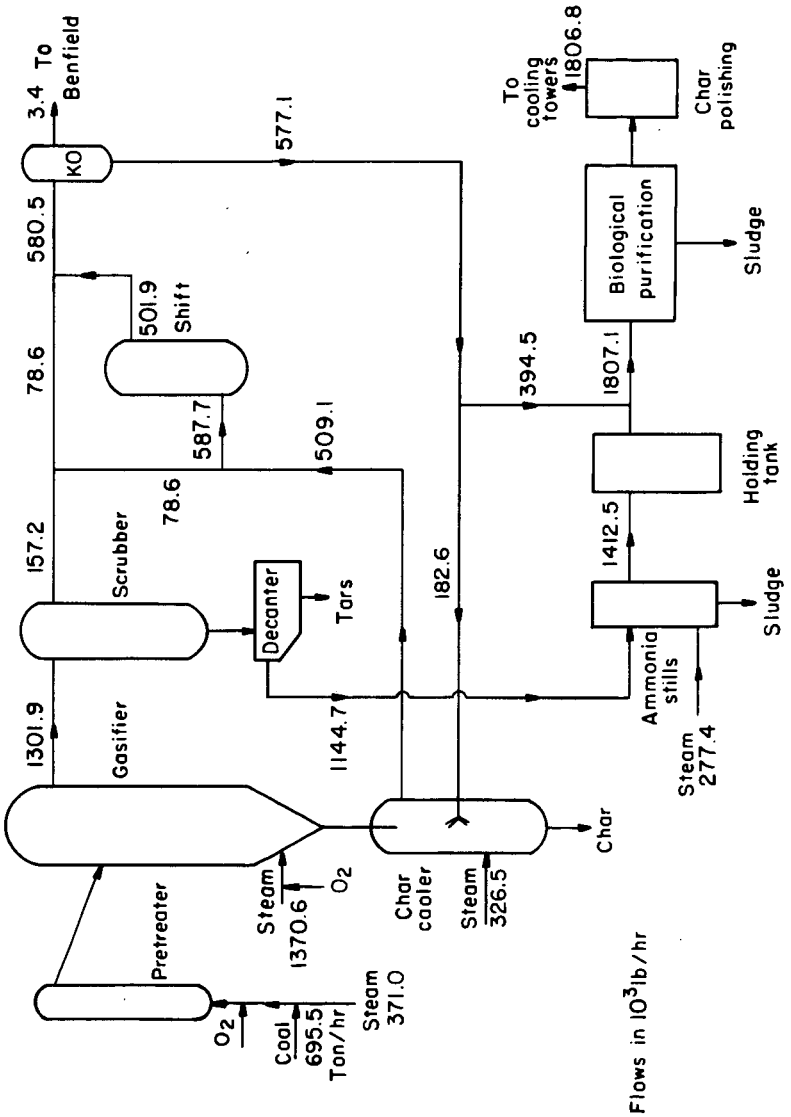

FIGURE 1 - Water and steam flows - 250×10^6 SCFD SYNTHANE plant.

L-13756

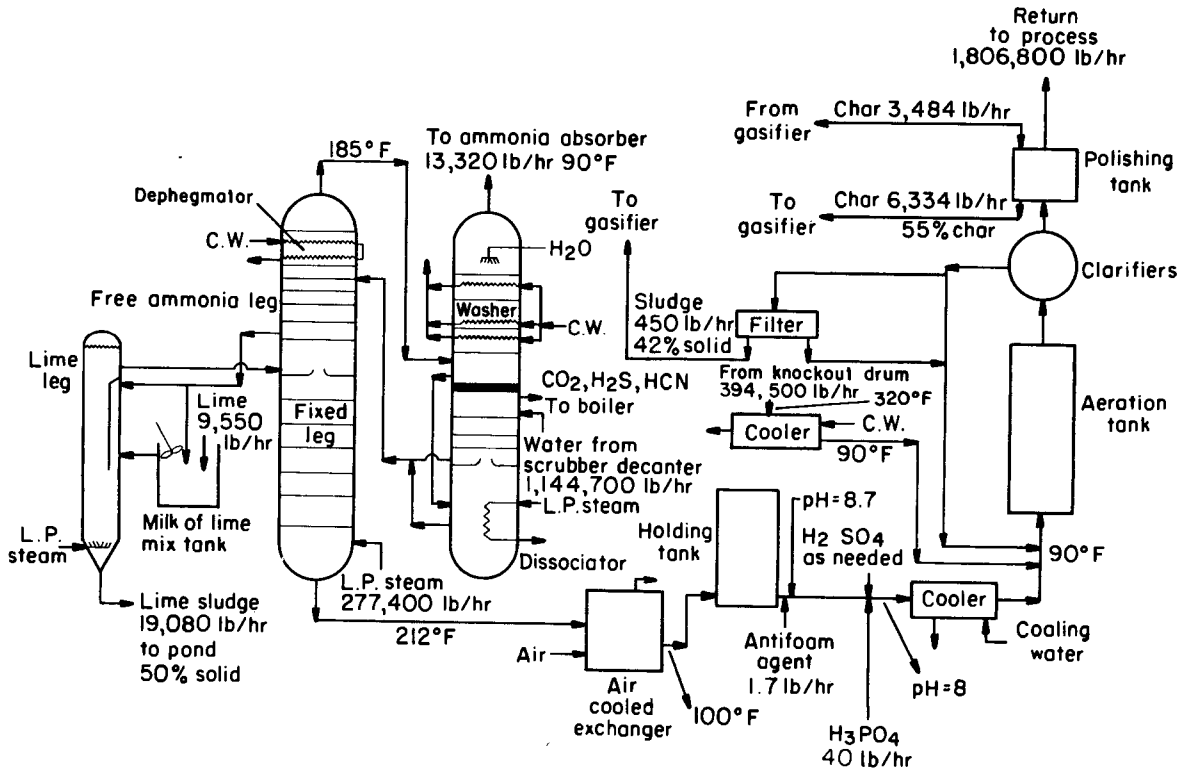

FIGURE 2 – Flow sheet, water treatment.

L-13757

BIODEGRADATION OF ^{14}C-PHENOL BY ACTIVATED SLUDGE

H. C. Alexander, F. A. Blanchard, I. T. Takahashi

The Dow Chemical Company - Midland, Michigan

Phenol, C_6H_5OH, is in widespread use as a raw material for manufacturing synthetic resins, medical, and industrial compounds. Various phenols (substituted hydroxy derivatives of benzene) are waste products of oil refineries, coke plants, some chemical plants, and human and animal refuse. The presence of such compounds in natural waters can affect fish. The threshold limit of toxicity for some fish is a few mg/l and at even lower concentrations fish can acquire an obnoxious taste. Phenolic materials can impart a bad taste to drinking water. "The removal of phenolic tastes from a water supply offers a serious challenge at the treatment plant" (1). McKee and Wolf (2) note that "despite the fact that it (phenol) is used as a bactericide in strong concentrations, weak phenol solutions are decomposed by bacterial and biological action in streams". Responsible manufacturing practice and good product stewardship cause management to increasingly call upon us to establish the ultimate fate of such compounds which may find their way into the environment. Contact with activated sludge from a waste treatment plant provides a rapid test of aerobic biodegradability.

The Dow Midland Division in its Phenolic Wastewater Treatment Plant commonly removes phenol from a waste stream at 80 ppm as judged by the 4-aminoantipyrene test (1). A trickling filter system takes the concentration down to about 30 ppm. Then, activated sludge reduces it to less than 1 ppm. Chemical oxygen demand (COD) and bio-chemical oxygen demand (BOD) and total oxygen demand (TOD (3)) data indicate that the phenol is consumed.

A C-14 radiotracer study has now been carried out to confirm these observations, to follow this decomposition more directly, and to establish a method useful for examining compounds of widely varying biodegradability. By radioassay, the fate of the ^{14}C-labeled phenol including the distribution of C-14 between evolved CO_2 and cell material has been determined after various contact times. Reaction rates under these conditions have been measured for unacclimated sludge and for specially acclimated sludge.

Methods

A laboratory system designed to contain the activated sludge culture plus the degradable substrate is shown in Figure 1. The oxidation cylinder is aerated through a fritted glass bottom with CO_2-free air at 60-100 ml per minute. Air from the cylinder is dried; the respired CO_2 passes through the infrared (IR) detector and into the scrubbers to be absorbed.

Return sludge (the settled solids at about 2% concentration) from the Dow Phenol Waste Treatment Plant for a preliminary trial or from the Dow General Waste Activated Sludge Plant (for other trials) was the starting culture. This was placed in a 2-liter cylinder fitted with an air sparger. The solids were settled, the free liquid decanted off, then an equal volume of fresh water was added. Experimental trials 1 and 2 were run on this sludge with only its inherent acclimation. Additional acclimation was given for a preliminary experiment and for Experiment 3 as follows: Phenol was added to a concentration of 100 ppm and the culture was aerated overnight. This procedure was repeated daily to provide a fresh supply of phenol to the sludge.

On the ninth day a test run was carried out in the oxidation cylinder. An IR CO_2 curve was obtained on the preliminary experiment. Measurements of phenol by the 4-AAP Method (1) on filtered, single distilled samples were made COD and TOD (1,3) were run on the filtered supernate. All these tests showed no phenol after the CO_2 peak.

For each run, sufficient settled return sludge to give a mixed liquor volatile solids (MLVS) concentration of approximately 3,000 mg/l was placed in the oxidation cylinder. Labeled phenol was added. Then water was added to bring the volume to 1.7 liters. The uniformly-labeled ^{14}C-phenol was obtained from New England Nuclear Corp. with a specific activity of 1.57 mCi/millimole. Its chemical purity by gas chromatography was 93.4% and by thin-layer chromatography 98.2%. For use, a working solution of 30.07 mg/ml in water was prepared. From this stock, 1.5 ml, 5 ml or 10 ml were added to the oxidation cylinder to obtain 27 ppm, 88 ppm and 177 ppm for Experiments 1, 2, and 3 respectively. A 200-ml sample was removed at the start to measure volatile solids and to do radioassays.

After the initial sampling, the oxidation cylinder contents was sampled at various time intervals over a 1 day period for ^{14}C-analysis. A hypodermic syringe (#17 needle) was used to withdraw 20 ml of sludge from a rubber tubing connection near the base of the cylinder. Formalin (1.0 ml) was added as a preservative. Respired CO_2 was collected in a mixture of 40% monoethanolamine in Dowanol® EM[a] ethylene glycol methyl ether. The total trap contents was removed as a sample and the absorbent replaced at each sampling time.

Radioassays were done by liquid scintillation counting using a Packard TriCarb[b] 3380 liquid scintillation spectrometer. Samples of trap contents were prepared by diluting a 3 ml aliquot in 15 ml of Econofluor[c] scintillation solution/methanol (60:90 v/v). Total sludge samples (0.2 ml) were combusted using a Harvey Biological Oxidizer, then counted. Supernate samples were obtained by centrifuging the sludge suspension for 2 minutes and removing a 0.2 ml aliquot. This was mixed with 10 ml Aquasol[c] water solubilizing liquid scintillation fluid and then counted. All ^{14}C quantities are calculated and reported as the equivalent amount of ^{14}C-phenol.

A test of the nature of the activity remaining in total sludge samples after a period of biodegradation was made. Samples of Experiment 2 at 2 and 8 hours were acidified and extracted twice with ethyl ether. Data from radioassay of this ether was converted to the equivalent ppm phenol that was extractable from the sludge. A water control was also run.

Results

The radioassay results from all the experiments are summarized in Table I. CO_2 given off by the respiration of the sludge system rose to a maximum in 1-2 hours after dosing with phenol as shown by the IR data and the corresponding respired $^{14}CO_2$ data in Figure 2. Some of the IR response is due to endogenous respiration of original non-radioactive cell material, whereas the $^{14}CO_2$ must all come from the ^{14}C-phenol.

---

a Trademark of the Dow Chemical Company.
b Trademark of the Packard Instrument Co.
c Trademark of the New England Nuclear Corp.

In the unacclimated cases as shown in Figures 2 and 3 there is a lag time of about 0.5 to 1 hour before very much $^{14}CO_2$ is respired. There was only a 0.25 hour lag with the acclimated sludge system. Even during these initial lag times, however, the compound was being removed from solution and taken up by the solids. Compare Figures 3 and 4. After 6 hours less than 25% remained in solution. A major part of the $^{14}CO_2$ release occurred within 8 hours (39-45% of original compound released as $^{14}CO_2$). Figure 3.

The peak rates for the unacclimated runs were 0.95 and 2.04 mg phenol/g MLVS/hr for Experiments 1 and 2 respectively at 2.5 and 3.5 hours. The highest rate observed was 16.9 mg phenol/g MLVS/hr from the acclimated sludge in Experiment 3.

After 1 day of exposure the distribution of the initially supplied radioactivity was:

	Radioactivity Found %			
Experiment	In Solution	Sludge Solids*	CO_2	Recovery
preliminary	0.8%	29.5%	62.1%	92.4%
1	3.0	43.0	62.1	108.1
2	2.6	37.8	54.2	94.6
3 (8 hours)	17.6	30.6	38.6	86.8

The activity in the solids does not behave like phenol in solution. It is scarcely accessible to ether extraction. The extraction recoveries from 2 and 8 hour total sludge samples of Experiment 2 were only 44% and 0.2% (72% and 4.9% if from supernate alone). The water control gave a 98% extraction recovery of the phenol.

Discussion and Conclusions

The mode of disappearance of phenol during biodegradation by activated sludge seems to be that it is first absorbed into the cell mass, then metabolized with a major portion going to CO_2 and the rest to cell material.

The biodegradation built up to a rapid rate then decreased. It approached the original endogenous respiration rate of the activated sludge after 8-10 hours. The phenol itself was being removed from solution even before much $^{14}CO_2$ respiration had occurred. Most of the ^{14}C-material left in the solids and in solution after 8 hours was probably not phenol.

The distribution of the phenol's carbon atoms between CO_2 and solids as observed in this ^{14}C-phenol biodegradation is in general agreement with data from standard BOD tests. H. C. Alexander has previously measured a BOD_5 of phenol as 1.82 parts 0_2 per part phenol. The theoretical oxygen demand of phenol is calculated from the following balanced reaction:

$$C_6H_5OH + 7\ O_2 \longrightarrow 6\ CO_2 + 3\ H_2O$$

$$\frac{224\ \text{M.W. } O_2 \text{ consumed}}{94.1\ \text{M.W. phenol}} = 2.38 \text{ parts } 0_2/\text{part phenol}$$

The BOD_5, if considered as being due to phenol oxidation to CO_2, represents 76% of the phenol present, the remaining 24% going into new cell growth. As noted previously the ^{14}C-phenol after 1 day of biodegradation showed 54-62% respired CO_2 and 30-43% retained in solids.

* By difference: total sludge minus supernate.

Because of the relatively rapid biodegradation of the phenol, it was possible to observe the CO_2 release by both IR and by radioassay. The radiotracer technique, however, has much greater sensitivity so that it can be used to get data on compounds degrading over a month long period rather than several hours. This extends even further the experimental capability of this relatively rapid activated sludge biodegradation technique.

Summary

The ultimate biodegradation of phenol by activated sludge was confirmed by collecting and measuring $^{14}CO_2$ released from a ^{14}C-labeled phenol. Infrared detection confirmed that the evolved material was CO_2. In 1 day, 54-62% of the supplied compound was converted to $^{14}CO_2$, 30-43% was found in the sludge solids. Three percent or less remained in the solution. For unacclimated sludge a peak degradation (at about 3 hr.) proceeded at a rate of (1-2) mg ^{14}C-phenol per gram mixed liquor volatile solids per hour. An acclimated sludge reached a rate of 17 mg ^{14}C-phenol per gram mixed liquor volatile solids per hour. Lag times of 0.5 to 1 hour were evident for the unacclimated sludges but only 0.25 hour for an acclimated one. The ^{14}C-activity left in the sludge after 8 hours did not freely extract with ether as did known phenol in solution.

This procedure is a useful tool in evaluating the biodegradability of an organic compound. Where needed, sensitivity is available for observing biodegradation of compounds whose degradation rate is several thousand times slower than that of this phenol.

Acknowledgements

The authors wish to thank Dave Gransden, on loan from Chemical Biology Research, for his assistance in the radioactive analyses.

Authors

H. C. Alexander, F. A. Blanchard, and I. T. Takahashi are, respectively, Laboratory Supervisor, Waste Control Laboratory and Analytical Specialists, Special Analysis Laboratory Midland Division Analytical Laboratories of the Dow Chemical Company.

References

1. "Standard Methods for the Examination of Water and Wastewater", 13th Edition, American Public Health Association, New York, N.Y., 281, 508-510 (1971).
2. McKee, J. E. and Wolf, H. W. Editors, "Water Quality Criteria", The State Water Resources Control Board, California, 2nd Edition, 237 (1963).
3. Clifford, Dennis A. "Automatic Measurement of Total Oxygen Demand: A New Instrumental Method", 23rd Annual Purdue Industrial Waste Conference, Purdue University, Layfayette, Ind. (1968).

TABLE I - RESULTS OF TRAP, SLUDGE AND SUPERNATE RADIOASSAYS

Experiment Number	Sampling Time, Hr	$^{14}CO_2$ Collected (as µg phenol)		^{14}C-Activity Concentration (as ppm phenol)	
		Trap 1	Trap 2	Total sludge Suspension	Supernate
Preliminary	1.5	21,400			
(100 ppm)	3.0	31,900			
	8.0	22,100			
	24.0	14,400		30.3	0.8
1	0			32.2	25.6
(26.5 ppm)	0.5	18	.0	24.3	20.6
	1.0	151	-.1	22.9	13.5
	1.5	1612	-.1	19.5	5.2
	2.0	2228	.4	17.2	4.0
	3.0	4217	.6	14.8	3.4
	4.0	2047	.6	14.9	2.4
	6.0	3767	1.6	18.5	2.5
	8.0	2668	0.5	13.7	1.8
	22.0	7056	16.6	12.2	0.8
2	0			73.0	82.1
(88.4 ppm)	0.5	169	0.2	64.3	74.6
	1.0	1672	0.4	64.1	64.6
	1.5	3444	0.5	66.2	55.4
	2.0	3991	0.4	65.2	50.0
	2.5	2998	0.5	70.5	47.1
	3.0	4017	0.7	61.4	38.2
	3.5	4558	1.9	64.4	29.9
	4.0	4207	0.8	55.6	24.0
	6.0	17332	6.8	48.9	2.8
	8.0	8759	8.5	43.7	2.8
	22.0	14148	21.8	35.7	2.3
3	0			87.8	147.4
(176.9 ppm)	0.25	116	-0.5	79.2	122.0
	0.50	7174	-0.6	135.0	67.8
	0.75	17536	-0.5	87.2	84.1
	1.0	15275	-0.4	122.3	80.2
	1.25	7260	-0.5	124.6	75.2
	1.5	5159	-0.4	116.7	76.8
	1.75	3763	-0.3	108.8	64.4
	2.0	3343	2.1	120.1	69.3
	2.5	5212	36.4	109.5	58.9
	3.0	4838	-0.3	107.7	46.3
	4.0	4661	-0.1	93.5	44.2
	5.0	5126	-0.5	91.8	44.3
	6.0	5543	0.2	92.4	36.1
	8.0	8782	1.1	85.4	31.2

Figure 1

LABORATORY ACTIVATED SLUDGE BIODEGRADATION SYSTEM

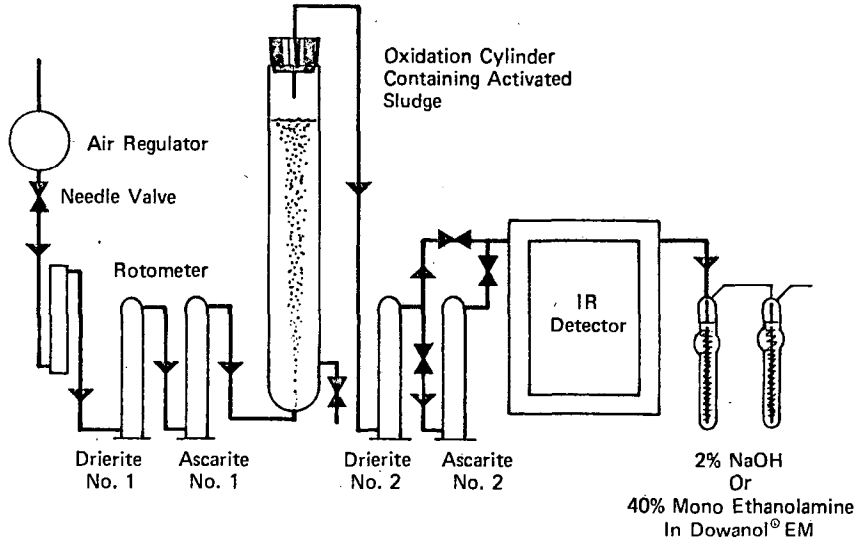

Figure 2

CO_2 AND $^{14}CO_2$ RESPIRED

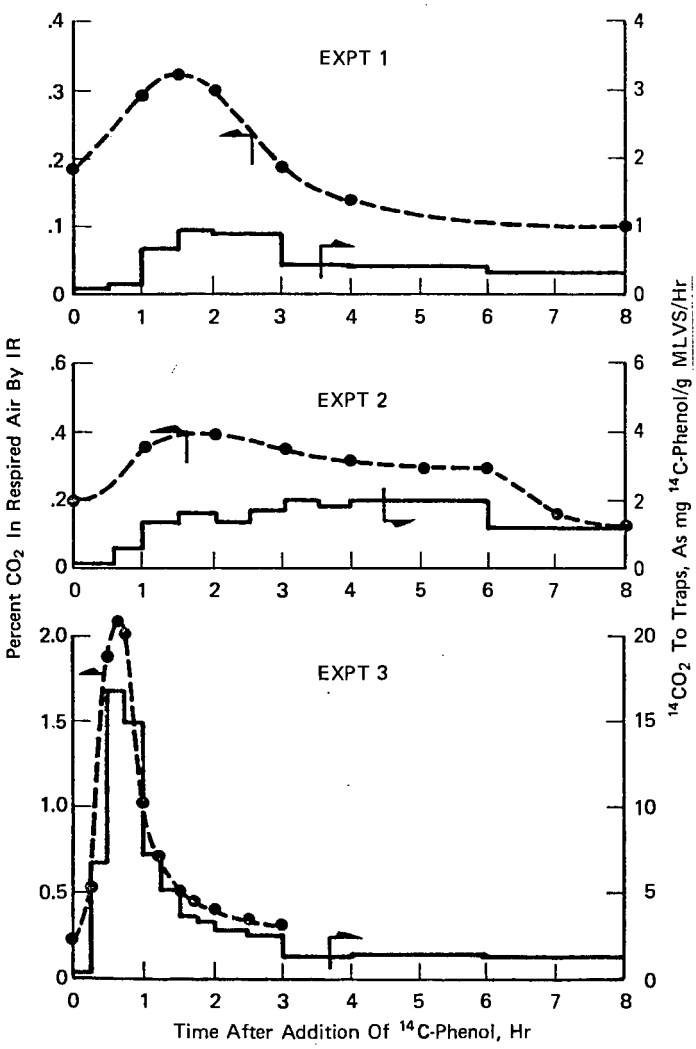

Figure 3

CUMULATIVE $^{14}CO_2$ COLLECTED IN TRAPS

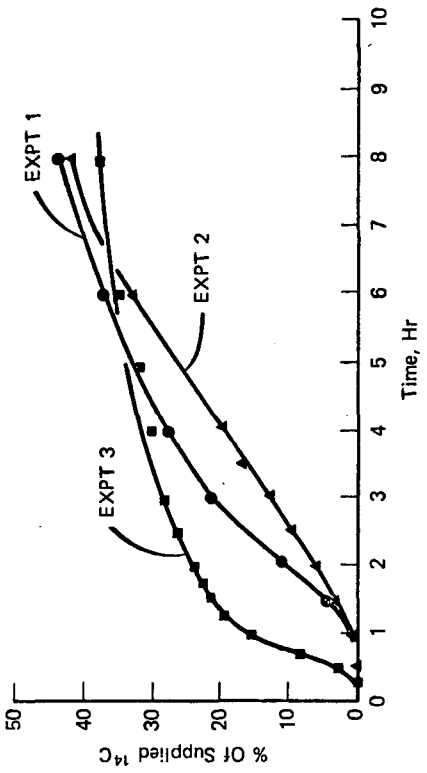

Figure 4

^{14}C-ACTIVITY REMAINING IN SUPERNATE

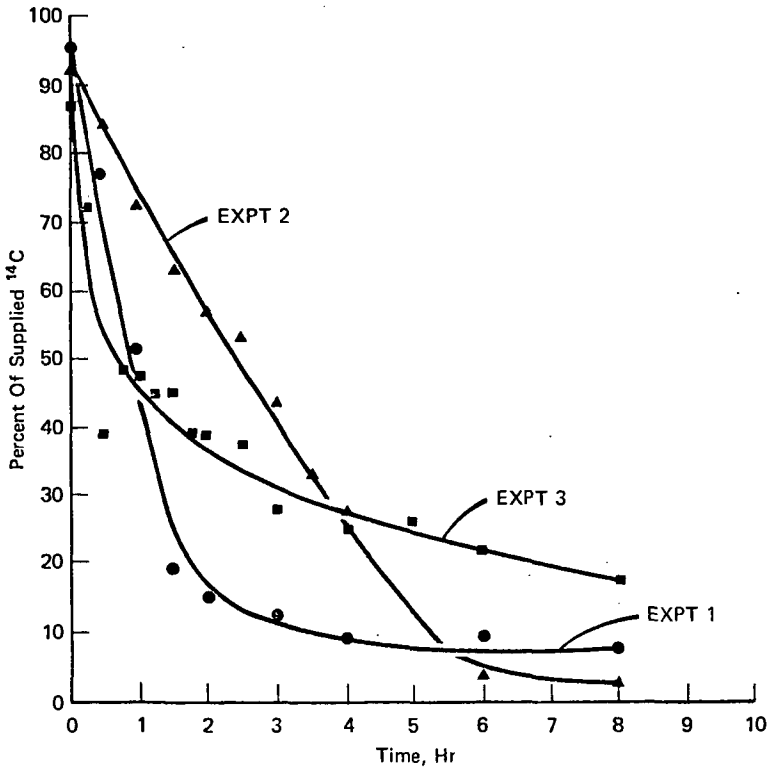

PETROLEUM REFINING PHENOLIC WASTEWATERS

by

Thomas E. Short, Ph.D.*, Billy L. DePrater**, and Leon H. Myers***

INTRODUCTION

The phenolics content of petroleum refining wastewater has been a concern of both regulatory agencies and refiners for some time. This is primarily due to toxicity to aquatic organisms and the characteristically high oxygen demand that phenolics can and do impose on receiving streams. In addition, there is the taste and odor problem caused when very low concentrations of phenolics are present in potable water supplies. This is particularly true when waters containing phenolics are disinfected with chlorine. The resulting chloropholics produce a very noticeable taste and odor problem.

---

*Chemical Engineer, Petroleum-Organic Chemicals Wastes Section, Treatment and Control Technology Branch, Robert S. Kerr Environmental Research Laboratory, Ada, Oklahoma.

**Supervisory Research Chemist, Petroleum-Organic Chemicals Wastes Section, Treatment and Control Technology Branch, Robert S. Kerr Environmental Research Laboratory, Ada, Oklahoma.

***Supervisory Chemist, Petroleum-Organic Chemicals Wastes Section, Treatment and Control Technology Branch, Robert S. Kerr Environmental Research Laboratory, Ada, Oklahoma.

This paper presents major sources of phenolics in petroleum refining wastewater; also, consideration is given to the amounts of phenolics produced by refiners which must either be controlled or treated before discharge. Additionally, it reviews the problems in analyzing for phenolics content; and finally, presents an examination of the treatment methodology for these wastewaters.

Methods of Analysis for Phenolics

Phenols are defined as hydroxy derivatives of benzene and its condensed nuclei.

The EPA manual (Methods of Chemical Analysis for Water and Wastes 1971) recommends that Standard Methods for the Examination of Water and Wastewater or "ASTM Method D-1873-70" be used for analysis of samples for phenolics. In these procedures, samples obtained in the field for analysis of phenols are fixed by the addition of copper sulfate and phosphoric acid. Even with the preservatives the sample must still be kept iced and the analysis must be done with 24 hours.

There are numerous test methods available to assess phenolic concentration in a waste stream. "Standard Methods" lists a Gas Chromatographic procedure and the 4-Aminoantipyrine procedure. In addition, the derivative electron capture detector method and an ultra violet bathochrome shift method are scheduled for round robin testing. Some water pollution laboratories make use of the Technicon Auto Analyzer system and report good results. By far, the most common method is the 4-Aminoantipyrine test.

In this test procedure, phenols react with 4-Aminoantipyrine at a pH of 10.0 ± 0.2 in the presence of potassium-ferricyanide to form a colored antipyrine dye. The light absorbance of this dye is measured by use of a spectrophotometer at 460 mμ wavelength. The absorbance relates directly to the amount of phenol which is present in the sample.

Phenol decomposing bacteria, oxidizing and reducing substances, and alkaline pH cause interference in the testing for phenol. By using the fixing reagents mentioned earlier and by distillation of the sample, most interferences can be eliminated. Further extraction of the distillate by chloroform can concentrate the phenol so that very low values can be detected colorimetrically. Presumably, the 4-Aminoantipyrine method does not measure parasubstituted phenols in which the substitution is an alkyl, aryl, nitro, benzoyl, nitroso or aldehyde group. It has also been reported that triaryl phosphates are positive intereferences in the 4-Aminoantipyrine test. Unfortunately, color response of the 4-Aminaontipyrine test is not the same for all phenolic compounds. Because phenolic wastes usually contain a variety of phenols, it is not feasible to determine the exact quantity of phenols in a sample. For this reason pure phenol is selected as the standard for the test and all results are expressed or reported as phenol.

Because of the obvious deficiencies of the 4-Aminoantipyrine test, EPA has assigned certain laboratories to continue evaluation of other testing procedures for phenolics.

Sources of Phenolics From Refining

The majority of phenols present in refinery wastewater originate from the catalytic cracking process. The reaction products from the cat cracker contain steam and the subsequent main fractionator uses stripping steam. Thus the main fractionator overhead reflux drum produces sour, foul condensate containing ammonia, light hydrocarbons, hydrogen sulfide, cyanide, and of course phenols. Caustic treatment of cracked gasoline removes sulfur compounds (mercaptans and thiophenols) and phenolic compounds. Hence, spent caustics are another source of phenol.

Thermal cracking also produces a similar foul condensate. Thermal cracking processes include visbreakers, delayed coking, and steam crackers which produce ethylene, propylene, and petrochemicals. Similarily hydrocrackers may also produce phenolic wastewaters.

Another possible source of phenolics is loss of phenol used as a solvent in extraction processes such as the Duo-Sol process.

EPA/API Survey of Refinery Raw Waste Loads

In 1972 the American Petroleum Institute and the Environmental Protection Agency cooperated in a study whose primary purpose was to evaluate the amounts and constitutents of raw aqueous wastes that were generated by the refining industry. Raw wastes were defined to be those wastes which have received no treatment other than gravity separation. Another objective of the study was the evaluation of treatment

efficiencies of activated sludge units handling refinery wastewaters. The goal of the study was to produce a "real life" data base for this industry.

API contacted every known refinery in the United States and solicited their cooperation for the study. Each refinery was requested to sample and analyze each of the raw waste streams in the refinery. Results of the analyses were then reported on a uniform questionnaire; 135 questionnaires were received and accepted for use in the study. These 135 refineries represented approximately 85 percent of the nation's crude refinery capacity.

The survey results pertaining to phenolics in raw wastewaters are presented in Table 1. The amounts of phenolics produced by each class of refinery surveyed is listed according to the API refinery classification system utilized in the study. Each class is defined by the following:

Refinery Class	Processes
A	Crude Distillation
B	Cracking
C	Cracking and petrochemicals
D	Cracking and lubes
E	Cracking, lubes, and petrochemicals

Generally, as the refinery class goes from A through E, the complexity of the refinery increases.

The effect of refinery classification on phenolics production is quite apparent from Table 1. Class A refineries (no cracking) produce only

TABLE 1

REFINERY PHENOLICS RAW WASTE LOAD SURVEY

Class	No. of Refineries	Total Crude Capacity	Median pounds Phenolics per 1000 BBL Crude	pounds Phenolics/day
A	13	204,900	0.03	1,809
B	71	3,448,900	1.54	16,620
C	27	3,416,830	4.02	27,668
D	11	1,068,450	2.18	4,317
E	13	3,354,470	2.67	18,430
Total	135	11,493,550	-	68,844

0.03 lbs of phenolics per 1000 BBL refined. Whereas classes B through E (with cracking) produce much higher levels of phenolics (1.54--4.02 lbs/1000BBL). As Table 1 indicates, the refineries surveyed (with 85% of the nation's crude capacity) produce about 69,000 lbs of phenolics per day which are contained in their raw wastewaters.

In order to validate the study's results, 10% of the surveyed refineries were selected at random. EPA representatives visited the refineries to observe the sampling and to obtain "split samples" which were preserved and returned to the Robert S. Kerr Environmental Research Laboratory for analysis. The refinery laboratory or the consulting laboratory for the refinery also analyzed the split samples.

The results of this split sampling are shown in Table 2. As can be seen, there are considerable differences between some of the measurements made by EPA and API on the same split sample. However, a statistical analysis of the results (student's T test) indicates the average difference between the results obtained by two laboratories is not significant. Since "average" data were to be used in the EPA/API study, the results were considered acceptable. These results brought about concern for those cases where a limited number of samples might be analyzed and compared, such as could occur in an environmental enforcement action. The most apparent reason for this analytical difference was analyst deviation from the EPA methodology.

Following the EPA/API study, an inquiry was received from the Oklahoma Petroleum Refiners Waste Control Council (OPRWCC) expressing

TABLE 2

EPA/API SPLIT SAMPLING RESULTS FOR PHENOLICS

EPA	API	DIFFERENCE	% DIFFERENCE
0.01	0	.01	100.0
1.6	1.5	.1	6.3
0.01	0.02	- .01	-100.0
2.3	0.02	2.28	99.1
0.01	0.1	- .09	-900.0
0.9	0.1	.80	88.9
140.0	115.0	25.0	11.9
0.01	0.0	.01	100.0
4.6	4.7	- .1	- 2.2
7.6	7.7	- .1	- 1.3
0.01	0.004	.006	160.0
0.01	0.013	- .003	- 30.0
0.02	0.023	- .003	- 15.0
0.01	0.05	- .04	-400.0
2.90	3.5	- .6	- 20.7
0.01	0.0017	.0083	83.0
4.55	0.3330	4.217	92.7
0.01	0.	.01	100.0
0.01	0.0037	.0063	63.0
0.39	0.32	.07	18.0
2.2	2.2	.00	.0
0.01	0.	.01	100.0
2.46	1.9	.56	22.8
12.2	5.9	6.3	51.6
3.1	2.5	.6	19.4
0.01	0.0	.01	100.0
410.0	115.0	295.0	72.0
0.1	0.038	.062	62.0
0.06	0.016	.044	73.3
64	26.7	37.3	58.3
0.52	0.412	.108	20.8
0.6	0.441	.158	26.3
0.01	0.0	.01	100.0
0.48	0.6	- .12	- 25.0
0.48	0.063	0.417	86.9
0.01	0.027	- .017	-170.0
8.2	6.1	2.1	25.6
0.001	0.015	- .014	-1400.0
0.01	0.01	0.0	0.0
0.02	0.02	0.0	0.0
500.0	600.0	-100.0	- 20
1.4	0.97	.43	30.7
13.8	1.51	12.3	89.1
3.6	0.025	3.585	99.6
2.2	2.3	- .1	- 4.5
525.0	280.0	245.0	46.7
14500.0	2400.0	12100.0	83.4
4.5	0.01	4.49	99.8
0.4	0.01	.39	97.3
0.4	0.255	.145	36.3
13.1	0.295	12.805	97.7
0.6	0.49	.11	18.3
2.5	0.94	1.56	62.4
0.01	0.0	.01	100.0
0.01	0.0	.01	100.0
0.01	0.0	.01	100.0
0.43	0.4	.03	7.0
5.4	5.3	.1	1.9
0.65	1.0	- .35	- 53.8
0.52	0.5	.02	3.8
0.52	0.5	.02	3.8
62.0	67.0	-5.0	- 8.1
0.38	0.4	- .02	- 5.3
0.38	0.4	- .02	- 5.3
0.03	0.0	.03	100.0
0.01	0.14	- .13	1300.0
0.01	0.0	.01	100.0
31.0	32.0	-1.0	- 3.2
3.2	0.1	3.1	96.9

Average Difference 183.36

σ Difference 1,456.47

N 69

T 1.0457

their concern over analytical variances experienced in analyzing industrial wastewater samples. This organization, composed of 11 refinery members has employed a self-reporting system for wastewater discharge analyses since 1955. Each month, the individual refineries report analytical data to the Oklahoma State Corporation Commission.

To attain the major and ancillary objectives of a study to define intra and interlaboratory repeatability and reproducibility, a steering committee including one EPA, one State, and three refinery representatives was formed. Formation of the study plan was the responsibility of the committee while the liaison and project direction were responsibilities of RSKERL personnel.

Participant selection from the Council was voluntary, with the agreement that any refiner who volunteered would, of necessity, have to participate in the total program. Eight of the eleven member refiners agreed to participate in the project. Those refiners who did not choose to participate represent refineries which either contract the analysis of their wastewater samples or could not participate due to internal restrictions. Refinery size of the participants varied from 12,000 to 112,000 barrels of crude per calendar day. The size distribution of the participating refineries is shown below:

CAPACITY OF PARTICIPANTS

Refinery	Thousand Barrels/Calendar Day
A	12.0
B	25.0
C	28.5
D	29.5
E	48.5
F	51.0
G	87.0
H	112.0

Size variance of the participants is an important factor since the population (industrial participants) involved in the study should represent a spectrum from small to large. Refinery size also reflects laboratory capabilities for wastewater analyses since the analytical staff size is dependent on refinery size.

Two Oklahoma State agencies, which are currently involved in analyzing industrial wastewaters, requested participation in the program. These State agencies were the Oklahoma State Health Department, whose responsibilities include analyses of petroleum refinery wastewater for the Oklahoma Corporation Commission (Oklahoma's Pollution Control Enforcement Agency for industrial discharges) and the Zoology Department of Oklahoma State University (OSU). The Zoology Department has performed bio-assays on petroleum refinery wastewaters since 1956 and regularly analyzes refinery wastewaters.

EPA laboratories participating in the study were the Robert S. Kerr Environmental Research Laboratory at Ada and the Methods Development

and Quality Assurance Research Laboratory located in Cincinnati, Ohio. MDQARL participation was primarily that of a referee laboratory while RKSERL duties included project liaison, sampling, intralaboratory analyses, data analyses, and report preparation.

The research program developed by the steering committee called for a two-phase study. In the first phase, a uniform sample of refinery wastewater would be obtained. The participating laboratories would handle the analysis in a routine fashion. Following the first phase, each analyst or his representative attended a seminar in which the analytical procedures were discussed. The purpose of the seminar was to achieve uniformity in analytical techniques. After the seminar, another set of samples would be analyzed to measure the effect of instruction.

Wastewater for the first phase was obtained from a final clarifier effluent at a petroleum refinery. The water had been biologically treated and represented all the wastewater sources in the refinery with the exception of sanitary sewage.

Wastewater for the second phase was obtained from the discharge of the API separator. This water was not biologically treated.

The sampling method used for the study involved pumping the water into a 35 gallon drum which had an inert inner liner. Calculated amounts of preservatives were added to the sample and an electric stirrer was used to mix the sample thoroughly. After five minutes

of mixing, replicate samples were withdrawn through a valve located near the bottom of the barrel into previously numbered one-quart plastic or glass containers. The numbered containers were filled at random. The samples were then placed into ice chests to assist in sample preservation.

To insure uniformity of starting time, the participants were instructed to begin analysis at 10:00 a.m. (CDT). Since the samples were obtained about 16 hours previous, the samples could be air delivered to MDQARL, Cincinnati, Ohio.

The phenolic analytical results of the study are presented in Tables 3 and 4. As can be seen, there is a very noticeable improvement in the coefficient of variation (standard deviation divided by the mean) for the results after the seminar. This is demonstrated graphically in Figure 1. Plotted are the standard deviations from this study versus the concentrations of phenolics. Also indicated on this plot are a range of standard deviations that can normally be expected. This range is based on results reported in the literature on analytical procedures. As can be seen, before the seminar, the standard deviation for the interlaboratory results is well above the normal range. After the instruction seminar, the standard deviation is brought down within the normal range. This indicates that instruction in proper analytical technique is essential to obtaining optimal analytical results.

TABLE 3

PHENOL ANALYTICAL METHOD EVALUATION

Phase I

(Results obtained before Instruction)

Intralaboratory Evaluation:

Lab No.	Phenol (µg/l)	Duplicate (µg/l)
01	15.0	11.3
01	14.4	11.3
01	9.7	10.2
01	14.0	11.2
01	13.9	11.7
01	13.9	9.8
01	13.5	10.8

Average Phenol = 12.2 µg/l

Standard Deviation = 1.8 µg/l

Interlaboratory Evaluation:

Lab No.	Phenol (µg/l)	Duplicate (µg/l)
02	14.0	15.0
05	24.0	21.9
08	3.3	4.0
10	20.0	17.0
11	29.0	29.0
13	4.0	4.0
16	15.6	20.7
17	12.5	3.8
20	12.0	13.0

Average Phenol = 15.2 µg/l

Standard Deviation = 8.1 µg/l

Combined Evaluation:

Average Phenol = 13.9 µg/l

Standard Deviation = 6.3 µg/l

Coefficient of Variations = 45.3%

TABLE 4

PHENOLICS ANALYTICAL METHOD EVALUATION

Phase II

(Results obtained after Instruction)

Intralaboratory Evaluation:

Lab No.	Phenolics (µg/l)	Duplicate (µg/l)
01	5480	5367
01	5470	5500
01	5480	5150
01	5320	5367
01	5320	5283
01	5070	4800

Average Phenolics = 5300.6 µg/l

Standard Deviation = 206.5 µg/l

Interlaboratory Evaluation:

Lab No.	Phenolics (µg/l)	Duplicate (µg/l)
02	6338	6088
05	6600	6720
08	6600	5000
10	4250	4400
11	6150	6200
16	5400	5500
17	5100	5200
20	6080	6550

Average Phenolics = 5761.0 µg/l

Standard Deviation = 795.8 µg/l

Combined Evaluation:

Average Phenolics = 5563.7 µg/l

Standard Deviation = 650.4 µg/l

Coefficient of Variation = 11.7%

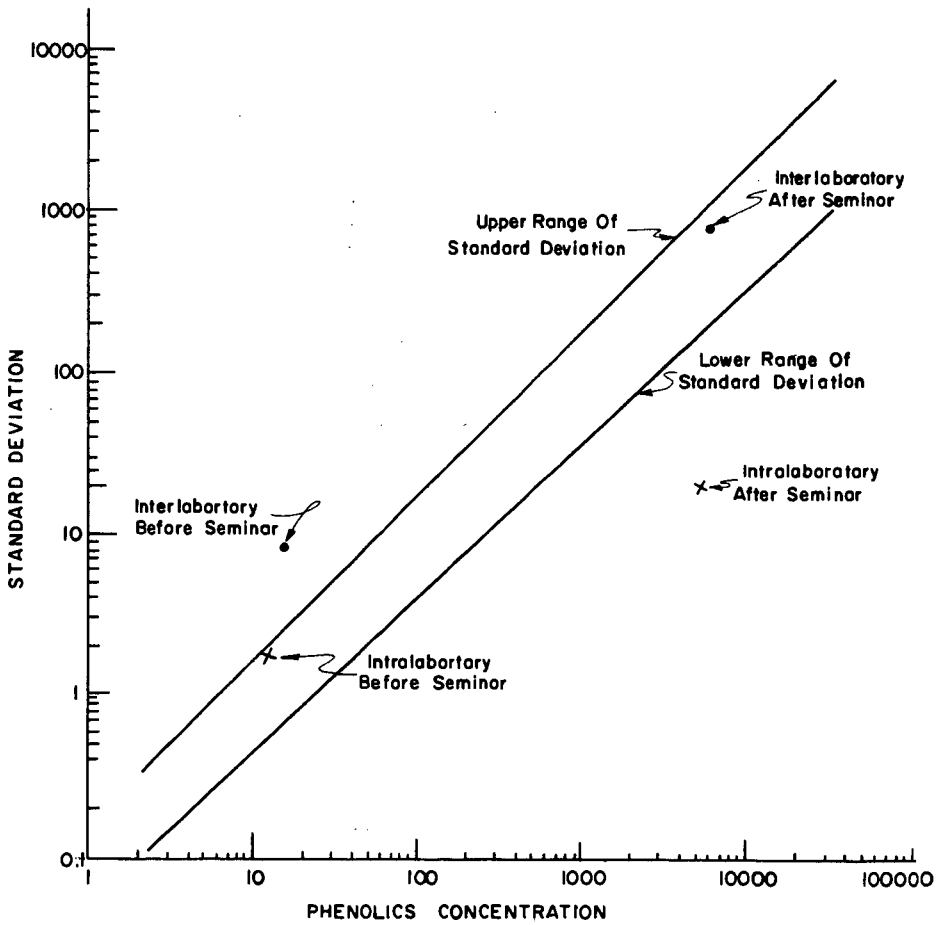

FIGURE 1 — PHENOLICS ANALYTICAL VARIABILITY

Treatment Efficiency Study

Another part of the EPA/API study was to evaluate the pollutant removal capability of activated sludge units which treat refinery wastewaters. Six existing full-scale refinery waste treatment systems were selected for this study. Each activated sludge unit was sampled for a two-week period. Grab samples were taken every two hours and composited for 24-hour periods. Influent to the treatment system (normally from the API separator) and the effluent (normally from the final clarifier) were studied to determine the amount of each pollutant removed.

The refinery treatment systems selected for this study were of sound design and operated in an effective manner. Another criterion in the selection was location. Selection was made so that the distribution would approximately follow the density or distribution of the entire refining industry. The refineries selected had capacities ranging from 35,000 to 117,600 BPD. Two of the refineries were class C, the other three were class B.

Refinery No. 9973 is a 56,000 barrel per day, class B, refinery located in the midwest. A flow diagram of the refinery wastewater treatment is shown in Figure 2. Refinery process wastewater from the API separator is held in an equalization basin with a retention time of about 7 1/2 hours. The wastes then flow into an activated sludge unit with 12 hours detention time in the aeration basin. On the average, this

REFINERY NO. 9973

Class B
Refinery Capacity = 56,000 BPD

Location Midwest

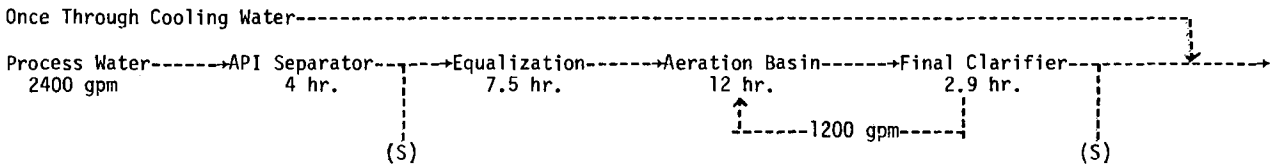

Median Influent Phenolics = 11.0 mg/L
Median Effluent Phenolics = 0.01 mg/L
Median Phenolics Removal = 99.9%

FIGURE 2

Activated Sludge Treatment Efficiency Study

(S) denotes sample point

unit handled wastewater with 11 mg/L of phenolics and reduced it to less than 0.01 mg/L for a typical removal of over 99.9%. A graphical presentation of the daily results is presented in Figure 3. Note that there is some variation in influent concentration. However, for the most part, this variation is small. As a result, the effluent concentration is relatively constant and the removals are quite good on a day-to-day basis. However, one sample (the 12th day) showed a substantial increase in phenolics for no apparent reason.

Refinery No. 2115 is an 88,000 BPD, class B refinery located in the northwest. The oily refinery wastewaters from the API separator are discharged to a primary clarifier, then to a trickling filter, and finally to an activated sludge unit with a detention time of 2.7 hours in the aeration basin. A diagram of the refining wastewater treatment system is shown in Figure 4. For this treatment system, samples were collected following the API separator, the trickling filter, and final clarifier. During the sampling period the median influent to the treatment system was 10.45 mg/L. The trickling filter reduced this to 0.99 mg/L. Finally the activated sludge reduced the phenolics to 0.35 mg/L for a total removal of 99.6%. Figure 5 shows the daily results of the sampling. As can be seen, the final concentration of the activated sludge unit responds very sensitively to the concentration from the trickling filter. Note that between the second and third day into the study, a small increase in phenolics from the trickling filter resulted in a very sharp increase in the discharge from the

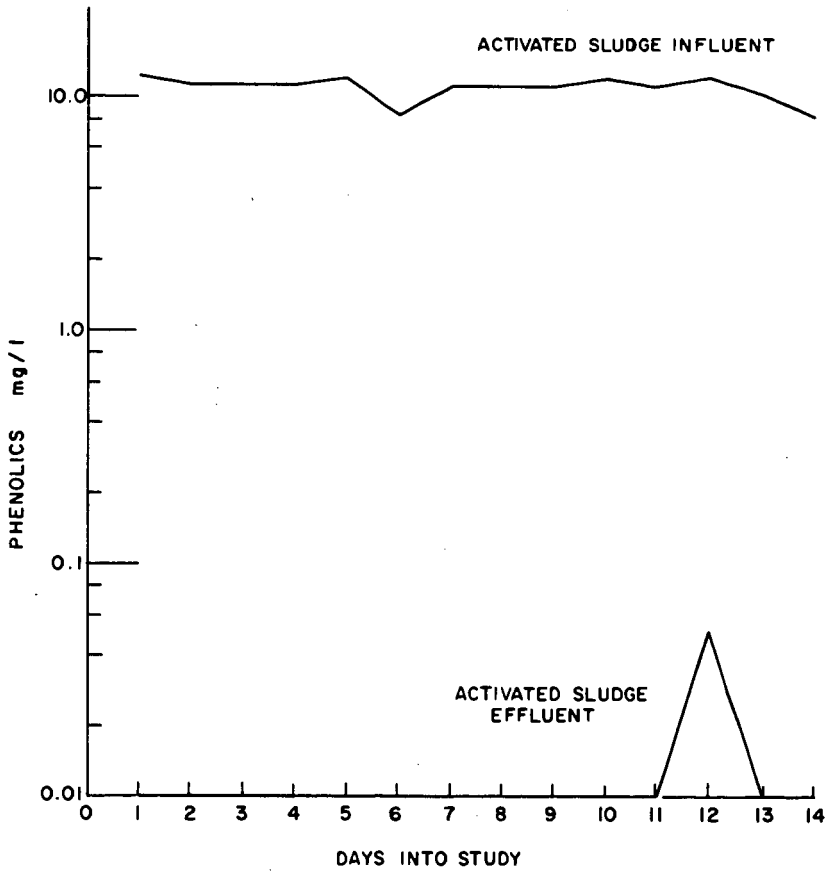

FIGURE 3 – TREATMENT EFFICIENCY STUDY RESULTS
REFINERY NO. 9973

REFINERY NO. 2115

Class B
Refinery Capacity 88,000 BPD

Location Northwest

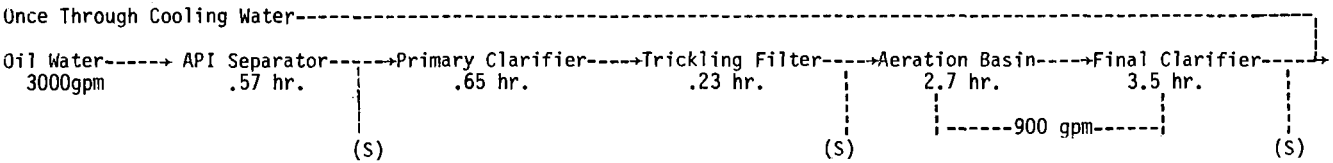

Median Influent Phenolics = 10.45 mg/L
Median Trickling Filter Phenolics Effluent = 0.99 (90.5% removal)
Median Effluent Phenolics = 0.035 mg/L
Median Phenolics Removal = 99.6%

FIGURE 4

Activated Sludge Treatment Efficiency Study

(S) denotes sample point

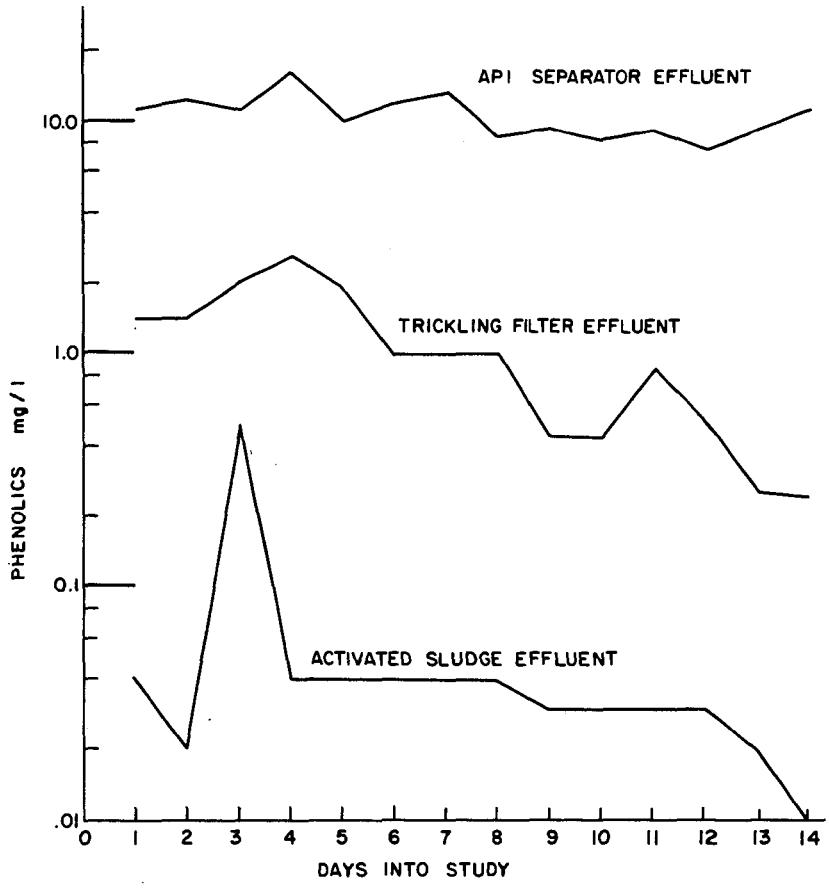

FIGURE 5 - TREATMENT EFFICIENCY STUDY RESULTS
REFINERY NO. 2115

activated sludge system. On the other hand, at about 11 days into the study the trickling filter showed a fair increase in concentration where as the activated sludge indicated no change. The major difference between these two situations is that the first increase ("upset") occurring 2 days into the study resulted in a 2.5 mg/L concentration going into the activated sludge. Whereas the second "upset" resulted in a concentration of only 0.85 mg/L. Thus, it appears reasonable to expect that the effect of an "upset" is related not only to the relative change in concentration, but is also highly dependent upon the maximum concentration of the upset.

Refinery No. 0288 is an 117,600 BPD, class C refinery located in the midwest. The refinery's oily wastewater from the API separator is treated by air flotation and then treated by an activated sludge system whose aeration basin has a 13-hour detention time. A diagram of the refinery wastewater treatment system is shown in Figure 6. In the study of this refinery, samples were obtained from the air flotation unit and the final clarifier effluents. The median phenolics concentration of the wastewater sent to the activated sludge unit was 2.5 mg/L. The median effluent from the activated sludge unit was 0.01 mg/L, for a median removal for phenolics of 99.4%. Figure 7 shows the daily concentration during the study. In the first week of the study the feed concentration increased very significantly twice (3rd and 5th days). As expected, the effluent from the activated sludge also increased in response to the feed concentration. In the second week, there was a slight increase in feed concentration, however, the effluent from the final clarifier did not indicate

REFINERY NO. 0288

Class C

Refinery Capacity, 117,600 BPD

Location Midwest

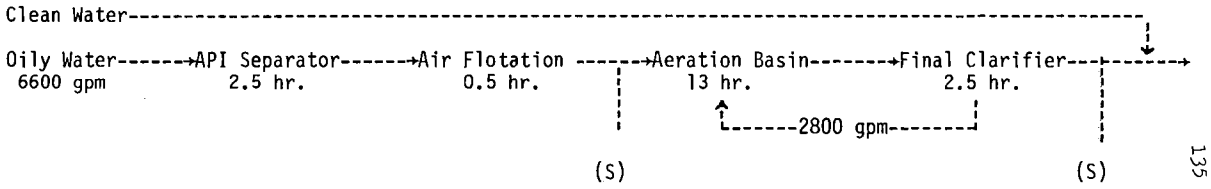

Median Influent Phenolics = 2.5 mg/L
Median Effluent Phenolics = 0.01 mg/L
Median Phenolics Removal = 99.4%

FIGURE 6

Activated Sludge Treatment Efficiency Study

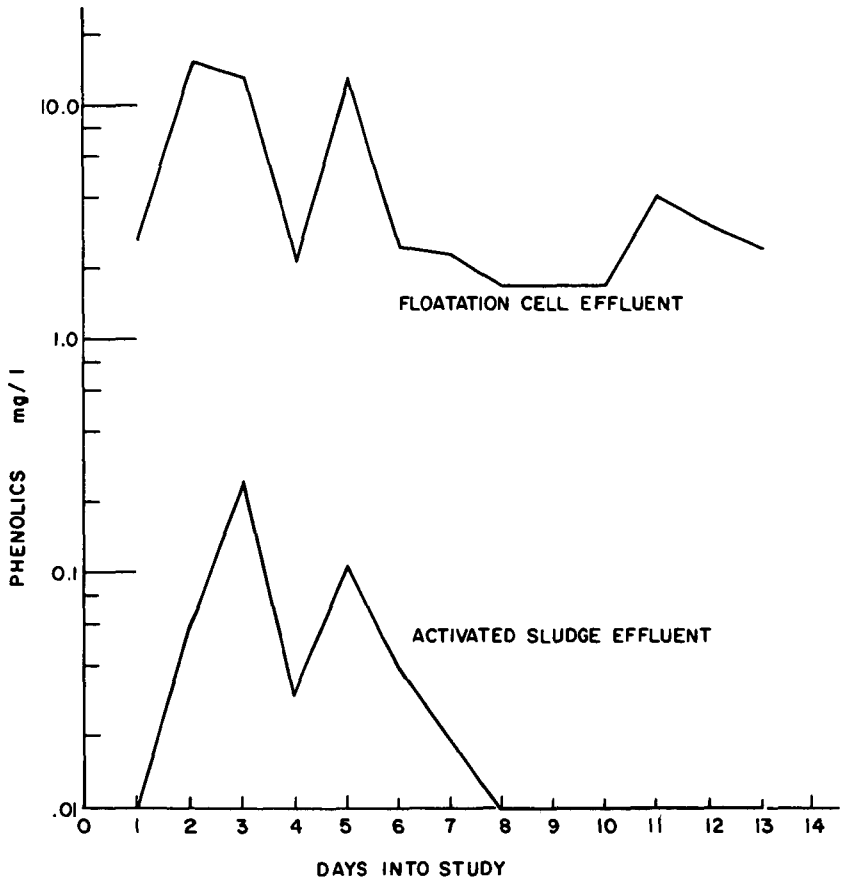

FIGURE 7 - TREATMENT EFFICIENCY STUDY RESULTS
REFINERY NO. 0288

any effect. Apparently, the feed concentrations were not high enough to adversely effect the performance of the treatment system.

Refinery No. 6512 is a 90,000 BPD, class C refinery, located in the southwest. All of the wastewater from the refinery flows through an API separator to an equalization basin. From there, the water is treated by chemical coagulation and then by an activated sludge treatment system which has a total detention time of 12 hours. A diagram of this waste treatment facility is shown in Figure 8. From the equalization basin the median phenolics concentration is 0.61 mg/L. The effluent from the activated sludge is about 0.01 mg/L for 97.6% removal of phenolics. Figure 9 shows the daily concentration from this study. During the first week, there were two periods in which the phenolics in the effluent were running higher than normal (3rd and 5th days). These periods generally correspond to periods when the feed concentration was higher than normal. During the second week, a very high effluent concentration was noted at the 11th day, although the feed concentration remained fairly level. There is no apparent explanation for this "upset." It was also noted that during this period the sulfide content of the activated sludge effluent was abnormally high.

Refinery No. 6693 is a 35,000 BPD, class B refinery located in the southwest. All of the refinery wastewater flows through an API separator to an activated sludge unit whose aeration basin has a 48-hour detention time. Figure 10 contains a diagram of the refinery

REFINERY NO. 6512

Class C

Refinery Capacity 90,000

Location Southwest

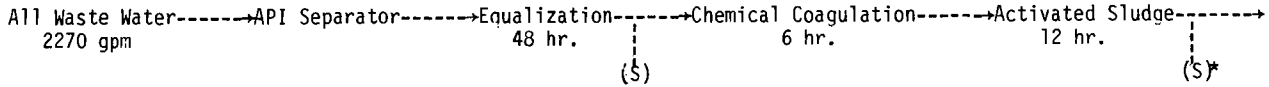

Median Influent Phenolics = 0.61
Median Effluent Phenolics = 0.01
Median Phenolics Removal = 97.6%

*Sample was taken of clarified effluent from combined aeration-clarifier unit.

FIGURE 8

Activated Sludge Treatment Efficiency Study

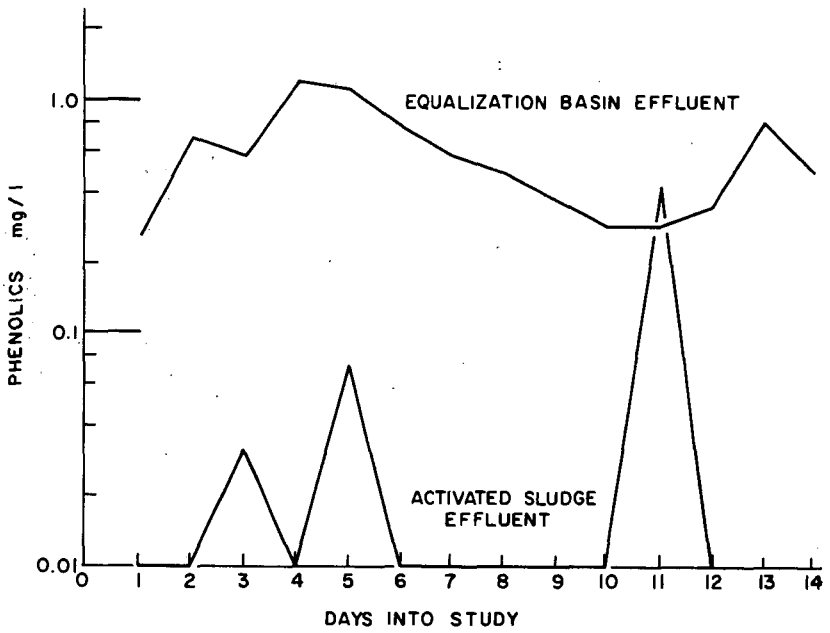

FIGURE 9 - TREATMENT EFFICIENCY STUDY RESULTS
REFINERY NO. 6512

REFINERY NO. 6693

Class B

Refinery Capacity 35,000 BPD

Location Southwest

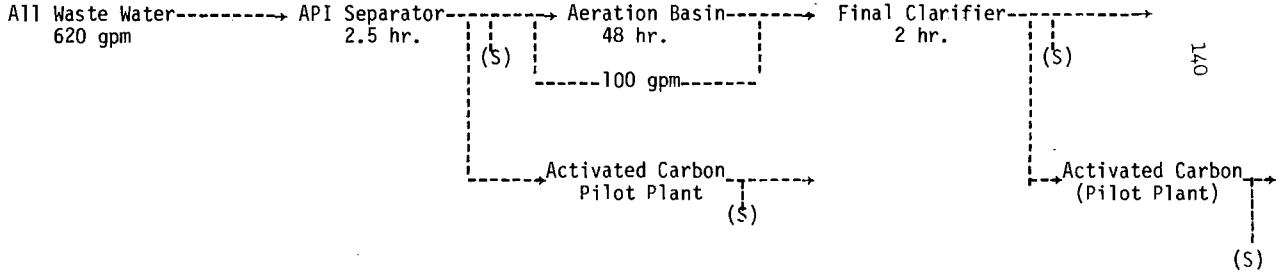

Median Influent Phenolics = 3.38 mg/L
Median Biotreatment Effluent Phenolics = 0.013 mg/L (99.6% removal)
Median Carbon Treatment Effluent Phenolics = 0.003 mg/L (99.91% removal)
Median Bio-Carbon Treatment Effluent Phenolics = 0.001 mg/L (99.97% removal)

FIGURE 10

Activated Sludge and Activated Carbon
Treatment Efficiency Study

(S) denotes sample
point

wastewater treatment system. For this treatment system, samples were collected at the API separator effluent and the final clarifier effluent. As an additional study, this treatment system was chosen for an evaluation of activated carbon treatment of refinery wastewater. Sample streams from the API separator and final clarifier were sent to an activated carbon pilot plant.

In the first pilot plant, activated carbon was the sole treatment process for the API separator effluent (i.e., secondary). In the second pilot plant, a biologically treated effluent from a final clarifier was "polished" using the activated carbon adsorption process (i.e., tertiary). Two complete pilot plants were installed and operated simultaneously.

Figure 11 is a flow diagram of the pilot activated carbon treatment systems. The wastewater to be treated first flows through a dual-media filter constructed of a 4" pipe. This filter consisted of an 18" layer of sand over pea gravel, topped with a 6" layer of anthrafilt. The purpose of the dual-media filtration pretreatment was to reduce the suspended solids and oil content to an acceptable level. Pretreatment for oil and suspended solids removal is a necessity in the handling of refinery wastewater with activated carbon since excess solids or oil will plug off the column prematurely.

After pretreatment, the wastewater entered a "Calgon" activated carbon pilot plant. This pilot plant was set up so that the wastewater flowed down three of the 5" ID columns. The first column contained

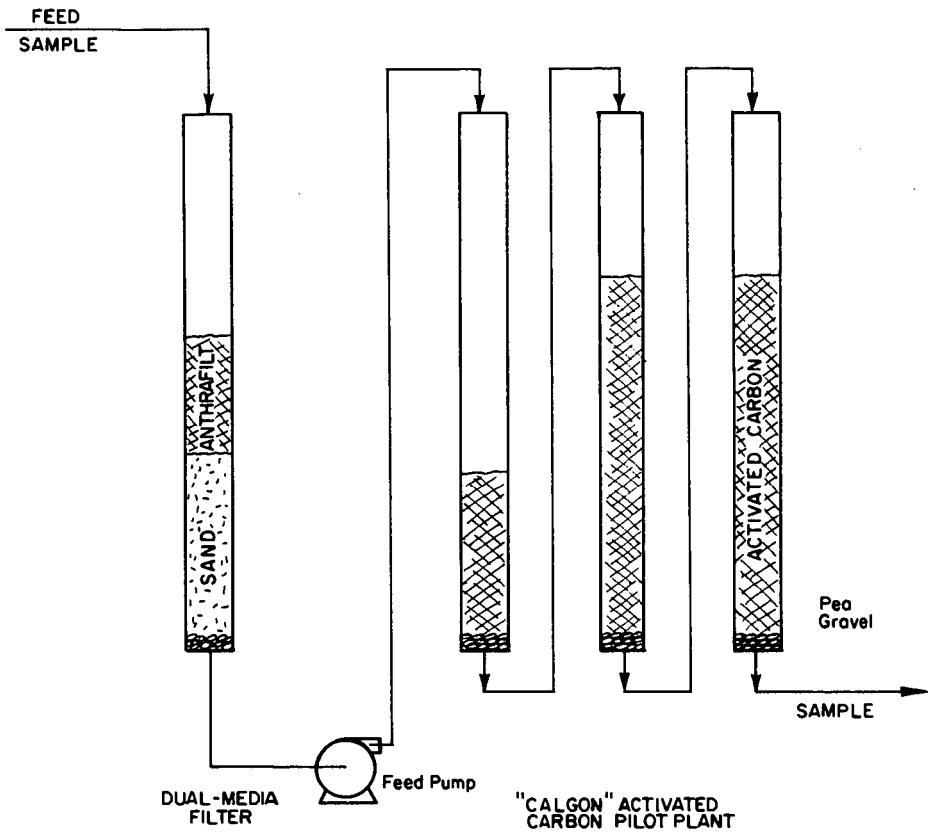

FIGURE 11 - ACTIVATED CARBON PILOT PLANT
FLOW DIAGRAM

an 18" layer of granular activated carbon while the remaining columns had a 36" layer of carbon.

The flow rate through each pilot plant was adjusted to about 1/4 gpm. During the operation of the pilot plant, samples of the API separator effluent, biological treatment effluent, and both pilot plants' effluents were taken every two hours. These samples were composited and preserved according to recommended EPA methods. Twenty-four hour composite samples were analyzed daily for a spectrum of water pollution control parameters using EPA analytical methodology and analytical quality control techniques.

The dual-media filter and carbon columns were backwashed whenever the pressure in the first column exceeded 20 psi.

The median phenolics content of the API separator effluent was 3.38 mg/L. The activated sludge effluent contained a median 0.013 mg/L for a 99.6% removal. The activated carbon treatment system treating API separator effluent had a median 0.003 mg/L effluent concentration for a 99.91% removal. The activated carbon system following biological treatment had an effluent concentration of 0.001 mg/L for a 99.97% removal.

Figure 12 is a graphical presentation of the API separator effluent and the activated sludge effluent. For the most part the influent concentration was fairly free of any sharp increases of phenolics. With the exception of the first 2 or 3 days, the activated sludge effluent was fairly constant. During the last 5 days of the study the feed showed a gradual increase in concentration. However, there was no apparent effect on the effluent.

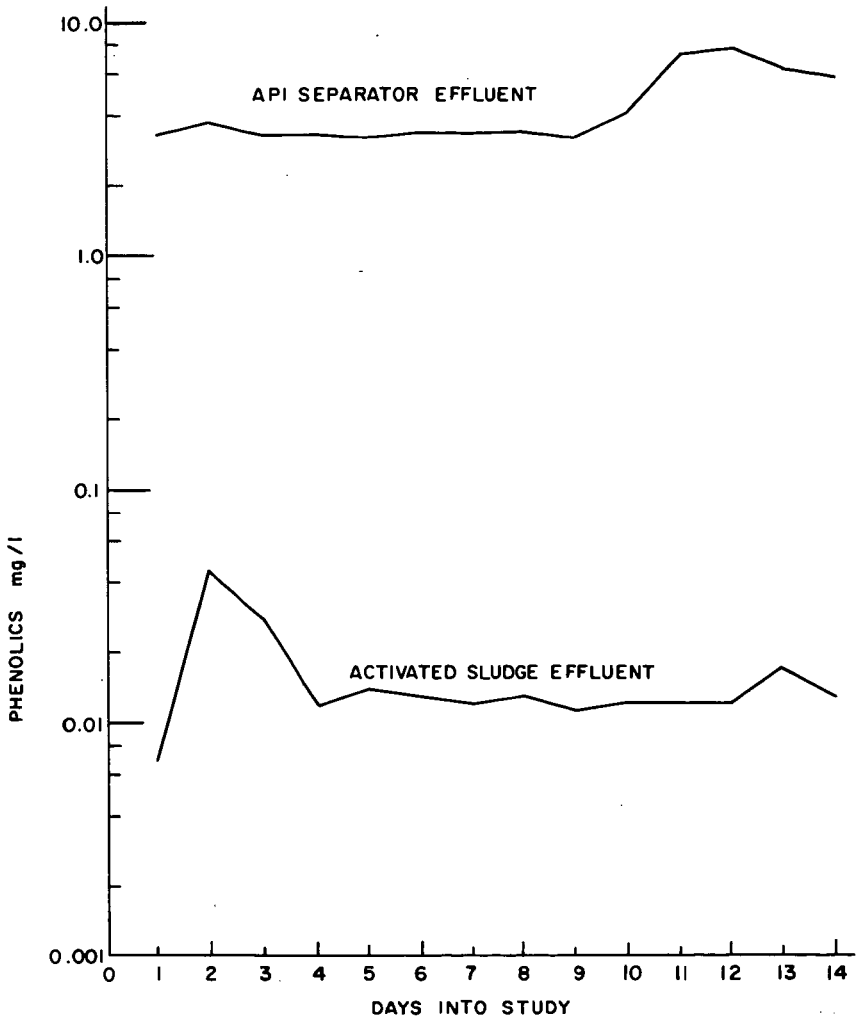

FIGURE 12 – ACTIVATED SLUDGE TREATMENT EFFICIENCY STUDY - REFINERY NO. 6693

Figure 13 is a graphical presentation of the daily phenolics content of the API separator effluent and the activated carbon effluent. During the 5th day into the study the carbon effluent showed a tremendous increase in phenolics. At about the same time a shift in the column feed pH from 6 to 9 was noted. During the remainder of the study, the pH remained on the alkaline side. It is very likely that a slug of caustic went through the column causing the carbon to release any adsorbed phenolics. This occurs under alkaline conditions because phenol shifts to the phenate form which is more water soluble and difficult to absorb. After the initial "upset" the column effluent showed a continuous increase in concentration to the point where at the end of the study the column effluent was approaching the feed concentration. This continuing increase was probably due to the fact that the column was operating under alkaline conditions, and its capacity for phenolics adsorption was significantly reduced. The increased phenolics content at the end of the study was probably attributable to column exhaustion (breakthrough).

Figure 14 contains a graphical presentation of the effluent of the activated carbon pilot plant which followed biological treatment. The activated sludge produced an effluent whose pH was consistently less than 7 (5 to 7). As a result of pH level being consistently below 7, the phenolic content from the carbon columns remained fairly constant at a very low level.

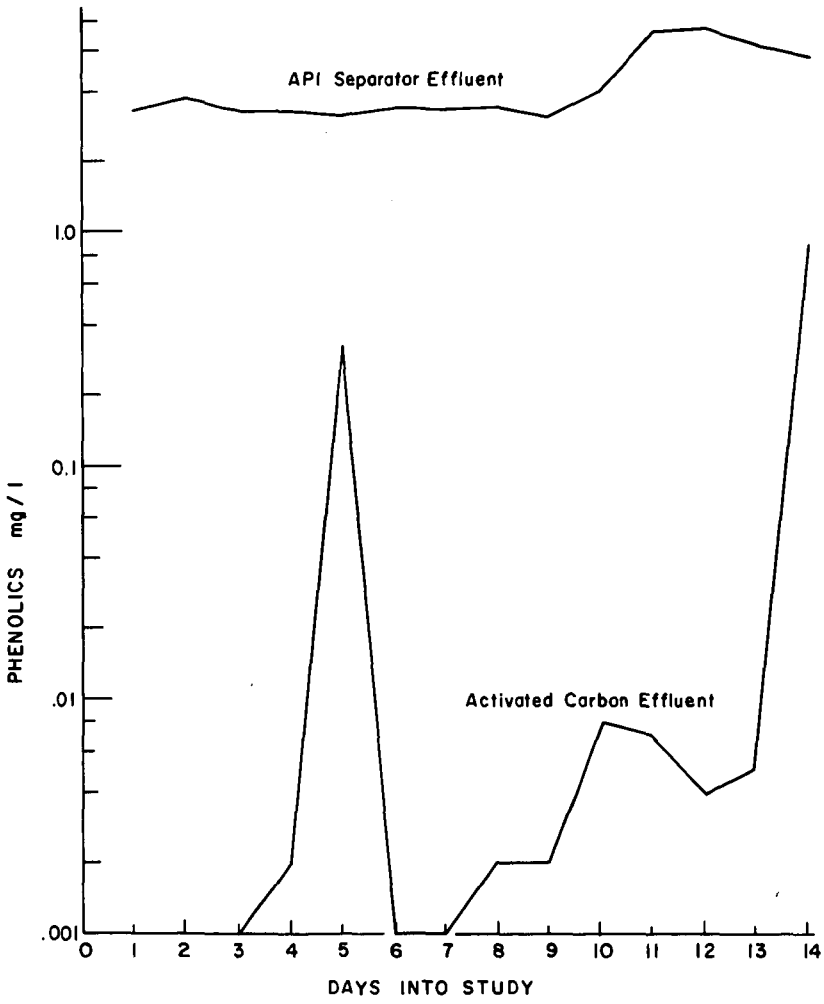

FIGURE 13 – ACTIVATED CARBON TREATMENT EFFICIENCY STUDY – REFINERY NO. 6693

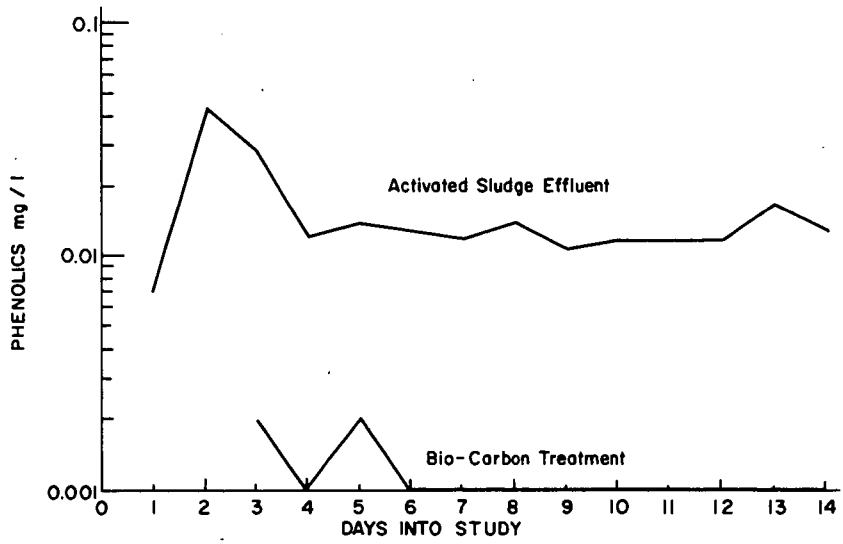

FIGURE 14 — BIO-CARBON TREATMENT EFFICIENCY STUDY
REFINERY NO. 6693

SUMMARY

1. Analytical variability of refinery wastewater data, as analyzed EPA methodology, was improved after a seminar on analytical procedures.

2. Both biological and activated carbon treatment systems showed high capacity for the removal of phenolics.

3. Biological systems appear to "upset" easily with changes in phenolics concentration. At times biological systems will "upset" with no apparent cause.

4. Activated carbon systems can provide excellent treatment capability if the hydrogen ion concentration of the waste streams is controlled. It is particularly important to avoid caustic conditions in the activated carbon columns.